Potassium Channels in Microglia as a Target for Ischemic Stroke

By

RUTH DIANA LEE

DISSERTATION

Submitted in partial satisfaction of the requirements for the degree of

DOCTOR OF PHILOSOPHY

in

Molecular, Cellular, and Integrative Physiology

in the

OFFICE OF GRADUATE STUDIES

of the

UNIVERSITY OF CALIFORNIA

DAVIS

Approved:

Heike Wulff, Chair

Fredric A. Gorin

Yi-Je (Jay) Chen

Committee in Charge

2023

DEDICATION

To me, the pursuit of a PhD is like a hero's journey, not because I think of grad students as the main protagonists of their individual stories, but because it shares so many similarities to the classic literature archetype riddled with lessons, friendships, failures, and successes. As I write this, I feel a mix of emotions as I reflect on my particular journey: humility, inspiration, a smidge of embarrassment, but overwhelmingly, gratitude.

First and foremost, I want to express my heartfelt appreciation to my advisor, Dr. Heike Wulff, for her unwavering guidance, encouragement, and mentorship throughout my journey. Like a moth to a flame, I knew I wanted to work with her even prior to the start of my PhD (and was heartbreakingly rejected as an MS student), and I was overjoyed when she accepted me into her lab the second time around as an MD/PhD student. I was, and still am, drawn to her frank desire for translating scientific discoveries into the real world. Since joining her lab, we have fostered such a special relationship, supporting each other inside the lab and out. You did not have to verbalize once that you were dedicated to my success because it was evident in everything that you did. Thank you for not only imparting knowledge, but also, instilling in me a commitment to excellence and precision. I truly appreciated how hard you pushed—not just me, but everyone in your lab—to conduct good experiments, to produce robust, reproducible data, and to tell meaningful, interesting stories. You modeled, by example, the work ethic and passion for your work that every scientist should have. I feel humbled to have been a part of your lab and research, and I cannot thank you enough.

I extend my immense gratitude to the members of my dissertation committee, Dr. Yi-Je (Jay) Chen and Dr. Fred Gorin. It has been a special experience working alongside Dr. Chen on the animal experiments in this dissertation, and I am grateful for his constructive feedback, troubleshooting skills, and scholarly expertise on animal stroke models. More broadly, thank you for sharing with me the tools (both physical and mental) needed for taking ideas from paper into reality. Dr. Gorin, thank you for accepting to be on my dissertation committee, even as a retired neurologist. Your scientific expertise and comments have deeply influenced the work in this dissertation. Your mentorship has been invaluable because you personally understood the unique challenges of pursuing a dual-degree; your honesty and stories you shared about your own MD/PhD path have enriched my own journey as an in-betweener straddling the basic science and clinical worlds.

Many of the clinical ideas within this dissertation came later for me, when I started working closely with patients during my clerkships. And even though I have admittingly spent much less time working with patients than with rodents, that time has unmistakably made a substantial impact on the work presented here. To Dr. Alan Yee, thank you for letting me onto your stroke service/clinic and giving me a window into your mind and into stroke patient care. That time spent with you has grounded me and my work. Each time I wrote about stroke symptoms or improving outcomes, I thought about the stroke patients on your service and about how hard you work to help them lead independent lives. To Drs. Adrienne Atencio, Craig Keenan, Mark Henderson,

thank you for reminding me that patients are “the why” behind my research—they are the reason behind our papers/grants, or our time spent (and in some cases, blood, sweat, and tears) in the lab developing novel therapeutics and rodent models. Watching you simply *care* so much about your patients and their well-being has refocused the ideas in this dissertation to reflect that: patients are at the center of my why. Your impact also extends far beyond the covers of this work because this sentiment will hold true through whatever life has to throw at me, steadily guiding me through my future forks-in-the-road and, more generally, how I fundamentally think about my own future research and patient care.

To my fellow previous and current lab mates, you have been my companions on this challenging yet rewarding voyage, getting your hands “dirty” with me on the ground-floor. Together, we have weathered qualifying exams, presentations, experiments gone awry, and moments of self-doubt. Your camaraderie, shared experiences, and intellectual discussions have made my journey all the more memorable. I am grateful for the relationships we have forged and for the support we have provided to one another.

Words cannot express my sincerest thanks to my parents and to my chosen family here in the Davis/Greater Sacramento area. I started my education at UC Davis in 2011 and haven’t left since (12 years as of writing this!), frankly because of the people here. To my parents, thank you not only for your unconditional love and support, but also, for your emphasis on academic rigor growing up; it has undoubtedly laid a solid foundation for me to get to where I am today. To my chosen family, I apologize in advance for being unable to name all of the people who have been instrumental to my journey here because it would fill another chapter in and of itself. Thank you to Dr. Chao-Yin Chen for believing I could do this even when I struggled to find my bearings as a nascent grad student. Thank you to Dr. Jeff Robin, Barbara Robin, David and Rebecca Graulich, and to my kind friends for their constant love, understanding, wise advice, unwavering support—and for just being there for me, showing up, and truly listening. Thank you for modeling how I should be treating people I care deeply about. Last, but not least, thank you to my fluffy, rapid-acting selective serotonin reuptake inhibitor, Zoloft (or Zoey for short), for her unbridled enthusiasm, toothy canine grins, and unrelentless tail wags.

As time progresses, I will inevitably forget a lot. I might not remember the nuances of every experiment I conducted for this work, but I will remember the people who helped make it possible, who were kinder and more generous to me than they ever needed to be. It’s not that I would not be here without them; I simply would not be without them. With a full heart, I thank you. It truly took a village, and this dissertation is for all of you.

ABSTRACT

The primary goal of stroke research is to improve outcomes and to reduce morbidity and mortality for stroke patients. Although stroke symptoms vary greatly from patient to patient, preclinical research has heavily relied on rodent models for mimicking the stroke condition, aiming to elucidate the mechanisms of stroke and to test potential interventions in a controlled setting. The first chapter discusses our current understanding of the pathophysiology of ischemic stroke, including processes like the formation of the ischemic penumbra, cerebral edema, and neuroinflammation, and explores the benefits and limitations of rodent stroke models. We also compare the temporal development of an infarct, and its associated functional outcomes, in rodent models to what is observed in human patients.

In chapters 2 and 3, we explore immunocytoprotective drug candidates for ischemic stroke. Despite advances in stroke treatment, there are currently only two treatment options available for ischemic stroke that have been shown to improve outcomes, both of which are usually administered within the “early” hours after stroke onset: thrombolysis at <4.5 hours and thrombectomy at <6 hours. In this dissertation, we explore K^+ channel blockers as drug candidates that, when used in conjunction with thrombectomy, target neuroinflammation at “later” time points in ischemic stroke, showing that both $K_V1.3$ blockers and $K_{Ca}3.1$ blockers reduce infarct size and improve neurological deficits 8 days post-stroke in rodent stroke models when administered at least 12 hours post-stroke.

In the last chapter, we examine the broader implications of ischemic stroke, its significant economic burden on the United States and its disproportionate effects on minority racial groups. Lastly, we close by discussing the future directions of stroke research, and the roles immunocytoprotective drugs like $K_V1.3$ and $K_{Ca}3.1$ blockers may play as adjunctive therapies for

enhancing the benefits of thrombectomy/reperfusion. Future preclinical research must incorporate and adapt to the technological advances, changes, and needs of the present stroke field so that we can maximize outcomes for all stroke patients.

TABLE OF CONTENTS

CHAPTER 1

INTRODUCTION

Ischemic Stroke and its Animal Models

Ischemic strokes can be subcategorized into embolic events (clots migrating from sources like the heart or distant vessels), thrombotic events (occlusion of large or small vessels), systemic cerebral hypoperfusion events (via watershed junctions, or borders between two arterial territories that are particularly vulnerable to ischemic injury) (Mangla, Kolar, Almast, & Ekholm, 2011), and in some rare cases, cerebral venous thromboses (occlusion of a venous sinus or of smaller cortical veins) (Kim, Martinez, & Sirotkin, 2017). Regardless of the cause, however, the underlying result is still the same—blocking a cerebral blood vessel leads to ischemia of brain tissue, triggering a cascade of dynamic changes in the brain that continues to evolve over time after the initial insult.

The time course with which infarct pathology develops is variable in patients because it is dependent on individual factors like the size and location of the vessel occluded, blood volume, presence and richness of collateral blood flow, in addition to underlying comorbidities like atherosclerosis, diabetes mellitus, and hypertension (Saver, 2006). This variability is one reason why the stroke research community has been focused on developing standardized, well-controlled animal stroke models over the last fifty years. Rigorous, reproducible animal stroke

models are essential for addressing the variability we see in patients because they help: (1) isolate the effect of individual factors, like the size/location of the vessel occluded, presence/absence of comorbidities, (2) test hypotheses about how these factors influence stroke outcomes by comparing and quantifying infarct size and motor and sensory deficits, and (3) all to test potential therapies in a controlled manner before translation into clinical studies.

Modeling ischemic stroke in rodents

Ischemic stroke has been modeled in animals since the late 1970's (Bacigaluppi, Comi, & Hermann, 2010). Since then, many different animal models of ischemic stroke have been developed, ranging from small animals like rodents and rabbits to large animals like pigs and non-human primates (Graham, McCullough, & Murphy, 2004; Taha et al., 2022). However, with the explosion of funding into rodent genomics and the expansion of institutions like Jackson Laboratories leading up to the 1990's, mice and rats became the most commonly used species in stroke studies because of: their convenient size, availability, cost, genetic/strain homogeneity, and relative similarity of their cerebral physiology to humans (Fluri, Schuhmann, & Kleinschnitz, 2015; Lyon, 2002). Of the two rodents, researchers initially used rats to model ischemic strokes because of their larger size but later increasingly used mice because of the possibility of using transgenics (Bacigaluppi et al., 2010).

In terms of technique, many methods modeling ischemic stroke have been used and described in detail in the literature (Sommer, 2017; Wang-Fischer, 2008). Occlusion of the middle cerebral artery (MCAO) with a filament is the most commonly used method because 70% of ischemic strokes in humans affect the middle cerebral artery (MCA) and its branches (Bogousslavsky, Van Melle, & Regli, 1988). In MCAO, the pattern of cerebral insult starts in the striatum/subcortical structures before radiating to cortical structures (Fluri et al., 2015), which

closely recapitulates the infarct size and structures seen in human MCA infarcts. In patients, MCA infarcts frequently affect the striatocapsular region of the brain, including the basal ganglia and internal capsule (Phan, Donnan, Wright, & Reutens, 2005), which are responsible for motor and sensory functions. Thus, many patients have clinical presentations exhibiting both cortical deficits, like aphasia and hemispatial neglect, and subcortical symptoms, like dysarthria and hemiparesis (Corbetta et al., 2015; Hillis et al., 2002).

Compared to humans, some “classic” stroke symptoms like dysarthria and aphasia are extremely difficult to assess in rodents. Another example is hand dominance, a factor usually assessed in stroke patients because it helps providers better understand the location and severity of the stroke, as well as the patient’s rehabilitation needs and potential for recovery (Harris & Eng, 2016; Waller & Whitall, 2016). Many of the functional tests in rodents have instead been focused on assessing motor, sensorimotor, and cognitive deficits for modeling the loss of limb function and learning and memory symptoms in stroke patients (Schaar, Brenneman, & Savitz, 2010). Although it is not possible for any rodent model to truly characterize the full scope of deficits that occur after stroke, it is still important to acknowledge both their advantages and limitations so that we can understand the extent in which they best serve us as a model. We are then left with the questions: what is the point at which we will need to transition into another species (Fisher et al., 2009)? Or, in other cases, for example when investigating a repurposed drug that has already demonstrated safety in other species and in humans (with other clinical indications), at what point can we transition into human stroke patients (Amantea & Bagetta, 2016; Y.-J. Chen et al., 2016; Fagan, 2010)?

With respect to the latter, minocycline is an example of such a drug. Minocycline is a second-generation tetracycline that is widely used in patients as an antibiotic, but has been shown to be neuroprotective in a variety of neurological disorders (M. Chen et al., 2000; Yong et al., 2004; Zhu et al., 2002), including ischemic stroke (Xu et al., 2004). It has demonstrated efficacy

as a stroke drug in animal studies, including reducing infarct size, reducing hemorrhagic transformation, and improving behavioral outcomes, without interfering with the fibrinolytic effects of tissue plasminogen activator (tPA) (Fan, Lo, & Wang, 2013; Kohler et al., 2013; Machado et al., 2009). Minocycline is a lipophilic compound that crosses the blood-brain-barrier (BBB), and while its mechanism of action is not completely understood, one of the key mechanisms by which minocycline may provide neuroprotection in stroke is by inhibiting the activation of microglia, which are immune cells in the brain that play a key role in the inflammatory response following ischemic injury (Lu et al., 2021). After extensive research on minocycline (including studies elucidating efficacy, interactions with tPA, functional outcomes, and even mechanism), the first human trial of minocycline in ischemic stroke was in 2007 (Lampl et al., 2007). What was the tipping point when it was considered "enough" to conduct studies in humans? With its history and relative safety as an antibiotic, in addition to general familiarity/acceptance as a drug by the public and medical community, could we have moved into human trials faster?

Chapter 2 of this thesis discusses one such repurposed drug, senicapoc, a $K_{Ca}3.1$ blocker that failed clinical trials in Phase III for sickle cell anemia in 2011 (Ataga et al., 2011). Senicapoc has already been shown to be clinically safe in humans, and we demonstrate that it could be used as an immunocytoprotective drug for ischemic stroke (R. D. Lee, Chen, Nguyen, et al., 2023). Chapter 3 discusses another drug, PAP-1, a brain-penetrant $K_v1.3$ blocker with a track-record of rodent data demonstrating that it reduces neuroinflammation in a wide range of disorders (Kundu-Raychaudhuri, Chen, Wulff, & Raychaudhuri, 2014; Maezawa et al., 2018; Schmitz et al., 2005). In ischemic stroke, we previously showed that it is effective at reducing infarct size and improving neurological deficits in multiple rodent models, including MCAO rats and young (16-week-old) and senescent (80-week-old) MCAO mice of both sexes (Y. J. Chen, Cui, Singh, & Wulff, 2021). We also already showed that PAP-1 is beneficial when given at 12 hours post-MCAO in rats (Y. Chen, Nguyen, Maezawa, Jin, & Wulff, 2018); in Chapter 3, we further explore its treatment time-window

and compare its therapeutic effects 2 hours and 3 days post-MCAO. We also investigate if it is necessary for a $K_V1.3$ blocker to penetrate the brain in order to exhibit beneficial effects in ischemic stroke by comparing the effects of a brain-penetrant $K_V1.3$ blocker, like PAP-1, to a non-brain-penetrant peptidic $K_V1.3$ blocker (R. D. Lee, Chen, Singh, Nguyen, & Wulff, 2023).

In an attempt to define the boundaries of where rodent stroke models can be most useful in preclinical research, this introductory chapter will discuss the temporal evolution of an infarct, comparing the pathophysiology, histopathology, and the associated functional outcomes we see in rodents to what we observe clinically in patients.

Pathophysiological changes in ischemic stroke

In ischemic stroke patients, the initial occlusion of a cerebral blood vessel leads to changes in the surrounding brain parenchyma in the first few hours. Within minutes, the sharp decline in blood flow cannot support the metabolic needs of cells in the immediate surrounding tissue, leading to irreversible ischemia-induced cell death, termed the ischemic core (Liu, Levine, & Winn, 2010). Outside of this core is the ischemic penumbra, injured but still salvageable brain tissue that has potential to become recruited into the ischemic core. In patients with large vessel ischemic strokes, some PET imaging studies have shown that this change can range from 5 to 18 hours (Baron, 1999); in other magnetic resonance (MR) diffusion-perfusion mismatch and positron emission tomography (PET) imaging studies, there has been evidence that this penumbra persists for at least between 8 to 12 hours (Saver, 2006). This is pertinent because the concept of the ischemic penumbra infers that there is a critical time frame for salvaging at-risk brain tissue from irreversible damage, known in the literature as “time is brain” (Saver, 2006).

The idea of the ischemic penumbra originated from animal experiments showing the relationship between the cessation of cerebral blood flow in specific areas of the brain and decline in neuronal electrical activity (i.e., baboons in the 1970's, and cats in the 1990's) (Astrup, Siesjö, & Symon, 1981; Heiss et al., 1994; Symon, Branston, Strong, & Hope, 1977). As stroke research progressed into rodent models, histopathology became one common way of assessing stroke burden, and thus, the time course of ischemic core and penumbra development. In contrast to other larger animals and humans, the histopathology of brain tissue in rodents is arguably much easier to assess with open-access resources like the Allen Mouse Brain Atlas ("Allen Reference Atlas – Mouse Brain [brain atlas]," 2004). One classic, almost cornerstone method of assessing infarct volume in rodent stroke models is performing serial coronal sections of a whole brain and staining with 2,3,5-triphenyltetrazolium chloride (TTC), which allows researchers to visualize and quantify the spatial distribution of an infarct through the whole brain (Joshi, Jain, & Murthy, 2004; Santo et al., 2023).

In MCAO in rats, Memezawa and colleagues showed that the size of ischemic tissue salvageable by reperfusion is directly related to occlusion time: 15 minutes of MCAO induced neuronal necrosis in the caudoputamen; 30 minutes of occlusion led to neuronal necrosis in the caudoputamen and selectively in the neocortex; 60 minutes yielded cortical infarcts; 120 to 180 minutes of occlusion led to infarct sizes similar to those following 24 hours of permanent MCAO. This suggests that the time window for salvaging parts of the brain like the neocortex and cortex is ~60 minutes, and possibly ~120 minutes in some cases (Memezawa, Smith, & Siesjö, 1992). Other rat studies have equated salvageable area as a function of ^{18}F-fluoromisonidazole (^{18}F-FMISO) binding, a PET marker for active cellular metabolism, and have shown that this potential for salvage peaks at 0.5 to 1 hour after MCAO, is still existent at 2 to 3 hours, and is negligible by 22 hours (Saita et al., 2004).

In MCAO mouse models, metabolic studies have demonstrated that penumbral tissue can be seen as early as 20-30 minutes (Kiewert, Mdzinarishvili, Hartmann, Bickel, & Klein, 2010), while on MRI, the penumbra can be visualized at 1 hour after occlusion, with lesions reaching a maximum volume at 12 hours (Yang et al., 2016). Other studies using mass spectrometry of lipid changes between the infarct penumbra and core have shown that the penumbra becomes clearly distinguishable from the core at 8 hours after MCAO (Mulder et al., 2019). Gene analyses comparing rats to mice have suggested that mice might be more sensitive to ischemia than rats at earlier hours, with an earlier activation in MAPK and toll-like receptor signaling, and that between the two rodents, rats might be more similar to humans with regards to gene responses to ischemic insults (Wu, Sun, Teves, Mayor, & Tymianski, 2021).

Overall, while rodents and humans share some similarities in the physiological development of the ischemic core and penumbra, the temporal evolution of ischemic insults seems to happen more rapidly in rodents than in humans. As a rough estimate based on the far ends of the time ranges in the given studies above (18 hours in humans, 12 hours in rodents), rodents may develop stroke volumes about 1.5x faster than humans.

Development of edema and inflammation after an infarct

Secondary to the primary development of the ischemic core and penumbra are parallel processes like cerebral edema and inflammation, each with their own time courses.

The time course of cerebral edema is similar in both rodents and humans, progressing over minutes to days and occurring in three phases, cytotoxic edema, interstitial or ionic edema, and lastly, vasogenic edema (Clément, Rodriguez-Grande, & Badaut, 2020; Klatzo, 1987; Stokum, Gerzanich, & Simard, 2015). Both in humans (J. Fiebach et al., 2014) and in rodents

(Liang, Bhatta, Gerzanich, & Simard, 2007), cytotoxic edema begins minutes after the onset of stroke and is characterized by a decrease in Na^+/K^+-ATPase activity and subsequent accumulation of fluid within astrocytes and neurons, but generally without tissue swelling (S. Chen, Shao, & Ma, 2021; Liang et al., 2007). Diffusion-weighted MRI is especially sensitive for rapidly detecting this reduction in water diffusion (J. Fiebach et al., 2014), which is why it is commonly used in clinical practice for diagnosing hyperacute stroke patients (<6 hours) (J. B. Fiebach et al., 2002). Tissue swelling occurs in 4 to 6 hours, when there is a large enough ionic gradient between the vasculature and the interstitium to drive water osmotically into the tissue, termed interstitial or ionic edema (S. Chen et al., 2021; Hatashita & Hoff, 1990). This is followed by vasogenic edema, characterized by breakdown of the BBB, which allows water and proteins (i.e., IgG, albumin) to leak from the blood vessels into the brain tissue (Loftspring, Beiler, Beiler, & Wagner, 2006). In humans and rats, vasogenic edema peaks at 1 to 2 days and tapers by 6 days after the onset of stroke and can result in a rapid increase in brain volume, elevation in intracranial pressure, and further damage of brain tissue (Dostovic, Dostovic, Smajlovic, & Avdic, 2016; Schwamm et al., 1998; Slivka, Murphy, & Horrocks, 1995). This type of edema is one of the primary mediators of malignant cerebral edema in a large subset of patients (more than 50% of patients with large hemispheric infarcts), who also experience severe functional decline within 2 to 3 days from stroke onset (Liebeskind et al., 2019). Since cerebral edema is one of the biggest contributors of infarct volume growth, imaging at these early time points may show misleadingly larger lesion volumes due to edema (Schwamm et al., 1998).

Edema and neuroinflammation are closely intertwined in the pathophysiology of stroke. The occlusion of a blood vessel immediately triggers an inflammatory cascade of events, eventually leading to the breakdown of the BBB and the subsequent leakage of leukocytes and water into the brain from the periphery (Jurcau & Simion, 2021). One key player in this inflammatory cascade are microglia, the resident immune cells of the brain. Activated microglia

contribute to BBB breakdown and increased permeability by several mechanisms, including: the release of pro-inflammatory mediators like tumor necrosis factor-alpha (TNF-α) which directly damage the BBB and recruit other immune cells to the site of injury, exasperating inflammation (A.-Q. Chen et al., 2019); the production of metalloproteinases, which degrade tight junction complexes and cause structural changes in the BBB (da Fonseca et al., 2014); and upregulation of adhesion molecules on the endothelial cells of the BBB, facilitating invasion by circulating immune cells (Haruwaka et al., 2019). Even though these are examples of how microglia contribute to tissue damage in a pro-inflammatory neurodegenerative manner, microglia are much more complex and are responsible for playing anti-inflammatory roles as well: phagocytosing damaged cells and debris (Jia et al., 2022), and releasing neurotrophic mediators like growth factors and anti-inflammatory cytokines (Wang, Leak, & Cao, 2022). As another layer of complexity, there have been recent studies showing that microglial activation does not necessarily fall into pro-inflammatory and anti-inflammatory discrete categories, but rather, presents as a spectrum of intermediate phenotypes (Guo, Wang, & Yin, 2022). In this paper, however, we will be referring to pro-inflammatory microglia as “M1-like” and anti-inflammatory microglia as “M2-like”, in line with the historic literature.

Immediately after reperfusion in a transient MCAO rodent model, macrophages/microglia can be seen at the peri-ischemic areas of the brain as early as 3.5 hours after reperfusion, in the ischemic penumbra starting 6 hours, extending to both the infarct core and penumbra between 12 and 24 hours (Weinstein, Koerner, & Möller, 2010; Zhang et al., 2022). The peak number of macrophages/microglia at the infarcted area was between day 4 and 7 post-stroke, decreasing by day 14 to 21 after MCAO (Ito, Tanaka, Suzuki, Dembo, & Fukuuchi, 2001; Schroeter, Jander, Huitinga, Witte, & Stoll, 1997). Of note, many of these experiments assessed macrophages/microglia with Iba1 (a marker found on both blood-borne macrophages and on microglia), making it difficult to distinguish if these cells originated from the blood or from the brain

(Ito et al., 2001). Hu *et al.* (2012) showed that M2-like microglia are the first to infiltrate into infarcted areas after an ischemic injury, perhaps as an effort to clear necrotic debris and restrict the damage. The number of these M2-like microglia taper off by day 7 after the stroke (Hu et al., 2012). On day 3 after MCAO, “M1-like” microglia begin increasing in number and continue to rise even 14 days after stroke; day 7 after MCAO marks a time-point when “M1-like” microglia predominate over “M2-like” microglia and was hypothesized to be responsible for expanding neuronal injury (Hu et al., 2012). Targeting this pro-inflammatory M1-like microglial activation has been a strategy for reducing the secondary inflammatory damage seen in stroke (Y. Chen et al., 2018; Y.-J. Chen et al., 2016; Y.-J. Chen, Raman, Bodendiek, O'Donnell, & Wulff, 2011; Y. J. Chen et al., 2021).

There have been much fewer histological studies investigating microglia in humans than in rodents, but activated macrophages/microglia have still been seen in the ischemic core 1 to 2 days post-stroke in patients (Weinstein et al., 2010). Instead, there are many more studies investigating the role of microglia in human stroke patients using advanced imaging techniques, like PET and MRI.

PET has been used to visualize microglia activation in humans by targeting the translocator protein (TSPO), which is upregulated in activated microglia. TSPO is a transporter protein located at the outer mitochondrial membrane and is involved in steroidogenesis. Expression of TSPO is increased in pro-inflammatory microglia (Beckers et al., 2017), so increased binding of TSPO ligands like ^{11}C-PK11195, an isoquinoline, and Ro5-4864, a benzodiazepine, have been used as a marker of neuroinflammation (Benavides, Fage, Carter, & Scatton, 1987; Y. Lee, Park, Nam, Lee, & Yu, 2020).

In 1992, Ramsay *et al.* assessed ^{11}C-PK11195 retention in one patient 6, 13, and 20 days after an ischemic stroke. In this time course study, the investigators found an increase in ^{11}C-

PK11195 at the borders of the infarct on day 6, significant extension throughout the infarct by day 13, which still persisted through day 20 (Ramsay et al., 1992). In 2006, Price *et al.* expanded on this time course with a ^{11}C-PK11195 temporal study on four ischemic stroke patients and found that there is minimal binding within 72 hours of stroke onset, the largest increase in the first week after stroke, declining by weeks 3 to 4. The study also showed that ^{11}C-PK11195 binding was highest at the core during that first week, only extending to peri-infarct zones by days 7-10 (Price et al., 2006).

In general, rodent models are useful for modeling the pathophysiology of strokes in humans because they share many similarities in the molecular and cellular mechanisms underlying the pathological events after stroke, like breakdown of the BBB, cerebral edema, and neuroinflammation following stroke. However, comparing these animal and patient studies does highlight one significant difference between the two: the time course of stroke progression in rodents is generally much faster than in humans. One reasonable estimate for *how* much faster is: ischemic events in rodents may present about 1 week earlier than in humans, at least comparing an adult rodent with an adult human within the first month after MCAO.

Measuring functional outcomes in rodents and humans with ischemic stroke

There are several behavioral tests used in rodent models of MCAO to assess functional deficits resulting from ischemic stroke, which has been reviewed many times in the literature (Ruan & Yao, 2020; Schaar et al., 2010). High variability has been a reported issue with behavioral testing in rodent models of ischemic stroke (Encarnacion et al., 2011), which is why some stroke researchers opt to use composite scoring systems that comprehensively evaluate multiple neurological functions as a way to assess deficits over time. Neurological scoring has the benefit of broadly (and efficiently) assessing a wide range of neurological functions, including

sensorimotor function, cognition, brainstem reflexes, and vision, with one scoring system (Ruan & Yao, 2020). Each of the most common neurological tests in rodent MCAO models, the Bederson score, the Garcia score, the Longa score, and the modified neurological severity score (mNSS), have an optimal time window when they can still detect neurological impairments after an ischemic insult, which is summarized in Table 1 (Ruan & Yao, 2020). Of these composite tests, mNSS has the largest time window when deficits can still be sensitively assessed, at least until 28 days after MCAO. This has been demonstrated with multiple studies, including one investigating 60- and 90-minute transient MCAO mouse models (Park et al., 2014), and another with a 2 hour MCAO rat model (Shen et al., 2006).

By contrast, in human stroke patients, functional outcomes are typically measured using standardized scales such as the National Institutes of Health Stroke Scale (NIHSS) and the modified Rankin Scale (mRS). These are important tools because they help clinicians use stroke severity and a patient's clinical symptoms to predict outcomes (König et al., 2008; Wityk, Pessin, Kaplan, & Caplan, 1994), like likelihood of a patient's recovery after stroke (Adams et al., 1999) and mortality (Smith et al., 2010). More broadly, when these functional assessments are pooled with other variables, they can be used to accurately predict the outcome of a clinical trial (Mandava & Kent, 2009).

The NIHSS is a 15-item measure of stroke severity that evaluates several neurological domains, including consciousness, language, motor function, and vision. This scale ranges from 0 to 42 points, with higher scores indicating more severe neurological deficits. Saver *et al.* (2012) showed that for the first few hours after stroke onset, stroke symptom severity is highly labile, and this is reflected in the variance of the NIHSS score at 1 to 3 hours after onset. The authors also showed that the NIHSS score obtained at 24 hours after the ischemic stroke best predicted final outcomes (Saver & Altman, 2012). In a separate study of 29 acute ischemic stroke patients, more than 50% of the stroke patients had showed dramatic improvement by 6 hours after the onset of

symptoms, defined as a 2+ point decrease from baseline modified NIHSS score (Biller et al., 1990). Because NIHSS scores change based on the time in which it was assessed, investigations on a new stroke drug should also include time from stroke onset as a variable when assessing and comparing drug effects (Saver & Altman, 2012).

Unlike the NIHSS, the mRS is a 6-point patient-centered outcome measure of disability that assesses a patient's ability to walk, to carry out activities of daily living and takes into account the patient's perspective on their own recovery and quality of life. It assesses not only physical disability but also the patient's ability to carry out activities of daily living, participate in social and leisure activities, and their overall sense of well-being. Studies have shown that there is a direct relationship between infarct volume and mRS functional prognosis; the larger the infarct, the higher the chance of dependency (Beloosesky, Streifler, Burstin, & Grinblat, 1995; Schiemanck, Post, Kwakkel, et al., 2005; Schiemanck, Post, Witkamp, Kappelle, & Prevo, 2005). Although there has been some contention as to the reliability of the mRS as an intrinsically subjective measure (Banks & Marotta, 2007; Quinn, Dawson, Walters, & Lees, 2009), most stroke clinical trials complete follow-up with a mRS assessment at 90 days post-stroke and is one of the most used primary endpoints for stroke randomized clinical trials (Sulter, Steen, & Jacques De, 1999). 90 days is chosen because, if a treatment is truly effective, we can expect to detect its effect (on functional recovery) on a population level by the 3 month time point (Lees, Selim, Molina, & Broderick, 2016). Some have argued that later primary outcome measures at 6 to 12 months post-stroke should be used instead, especially for indications where differences in outcomes manifest outside of this traditional 3 month time frame, or for testing a therapy’s sustainability over a longer period of time (Lees et al., 2016).

How well do rodent functional outcomes translate into humans in terms of symptoms and time course? Ischemic stroke is difficult to model because no two ischemic stroke patients are exactly the same. Stroke patients exhibit a broad range of symptoms that span multiple system—

from vision to motor function—which is why the effects of stroke on an individual can be so debilitating (Chohan, Venkatesh, & How, 2019). Rodents have been used to model a subset of specific stroke phenotypes, like sensorimotor functions and brainstem reflexes, but realistically, no disease model will ever fully capture the human stroke condition. As we have discussed above, for many rodent studies, the latest timepoint for assessing stroke deficits with neurological scoring in a rodent model is around 28 days post-stroke. If this was an adult wild-type (WT) mouse, using an estimate of 2.6 mice days ≈ one human year as suggested by some researchers (Dutta & Sengupta, 2016), this is equivalent to ~10.7 years in a human. If this was a senescent mouse (more than 15 months old), 28 senescent mouse days is roughly equivalent to ~3.2 human years, approximating 8.82 senescent mouse days with one human year (Dutta & Sengupta, 2016). Both these estimates are far later than the 90-day clinical endpoint many stroke trials define when comparing outcomes of different interventions. Thus, the time point when we measure outcomes in rodents cannot be the same time point when we measure outcomes in human patients.

Conclusion

Overall, while rodent models have been valuable in advancing our understanding of stroke pathophysiology and testing potential treatments, it is important to acknowledge their limitations (Gennaro, Mattiello, & Pizzorusso, 2019; Kwiecien, Sy, & Ding, 2014; Macrae, 2011; Wiebers, Adams, & Whisnant, 1990). We show here that the time course of events in ischemic stroke can drastically differ between rodents and humans, depending on what lens is worn (i.e., whether scrutinization occurs with the “cerebral edema” lens or “microglia activation” lens). In general, however, the time course of events in rodent models of ischemic stroke are more compressed than in human stroke. As a result, outcomes measured at a specific time point in humans are not equivalent to the same time point in rodents. We suggest that alternatively, a

shorter, more compressed time-course will better reflect the more rapid progression of events in rodent models of ischemic stroke, when compared to humans. Understanding the translational relevance of findings from rodent models can help facilitate the transition of highly effective preclinical therapies into the clinical world.

Our overarching goal is to translate $K_V1.3$ and $K_{Ca}3.1$ into therapeutic targets of ischemic stroke because of their relative safety (Schmitz et al., 2005; Wulff & Castle, 2014), specificity in targeting immune cells (i.e., microglia in the central nervous system, and T-cells in the periphery) (DeCoursey, Chandy, Gupta, & Cahalan, 1984; Feske, Wulff, & Skolnik, 2015; Matteson & Deutsch, 1984), and their demonstrated effects on reducing infarct size and improving neurological deficits 1 week after MCAO, when administered at 12 hours post-stroke (Y.-J. Chen et al., 2016; Y.-J. Chen et al., 2011; Y. J. Chen et al., 2021; R. D. Lee, Chen, Nguyen, et al., 2023; R. D. Lee, Chen, Singh, et al., 2023). We also discuss why immunomodulating drug targets have been particularly attractive for a range of autoimmune and neurological disorders in the past (Beeton et al., 2006; Jin et al., 2019; Mauler et al., 2004; Ramesha et al., 2021; Reich et al., 2005) and why they hold potential as adjunctive treatments for ischemic stroke to tPA and EVT. Specifically, with $K_V1.3$, we show that PAP-1 has effects when administered as early as 2 hours and as late as 3 days after reperfusion. Lastly, we explore if it is necessary for an immunomodulating stroke therapeutic to cross the BBB in order to mitigate the damage seen in ischemic stroke.

References

Adams, H. P., Davis, P. H., Leira, E. C., Chang, K. C., Bendixen, B. H., Clarke, W. R., Woolson, R. F., & Hansen, M. D. (1999). Baseline NIH Stroke Scale score strongly predicts outcome after stroke: A report of the Trial of Org 10172 in Acute Stroke Treatment (TOAST). *Neurology, 53*(1), 126-126. doi:10.1212/wnl.53.1.126

Allen Reference Atlas – Mouse Brain [brain atlas]. (2004). *Allen Institute for Brain Science.* Retrieved from atlas.brain-map.org

Amantea, D., & Bagetta, G. (2016). Drug repurposing for immune modulation in acute ischemic stroke. *Current Opinion in Pharmacology, 26*, 124-130. doi:10.1016/j.coph.2015.11.006

Astrup, J., Siesjö, B. K., & Symon, L. (1981). Thresholds in cerebral ischemia - the ischemic penumbra. *Stroke, 12*(6), 723-725. doi:10.1161/01.Str.12.6.723

Ataga, K. I., Reid, M., Ballas, S. K., Yasin, Z., Bigelow, C., James, L. S., Smith, W. R., Galacteros, F., Kutlar, A., Hull, J. H., Stocker, J. W., & Investigators, I.-.-S. (2011). Improvements in haemolysis and indicators of erythrocyte survival do not correlate with acute vaso-occlusive crises in patients with sickle cell disease: a phase III randomized, placebo-controlled, double-blind study of the Gardos channel blocker senicapoc (ICA-17043). *British Journal of Haematology, 153*(1), 92-104. doi:doi: 10.1111/j.1365-2141.2010.08520.x.

Bacigaluppi, M., Comi, G., & Hermann, D. M. (2010). Animal Models of Ischemic Stroke. Part Two: Modeling Cerebral Ischemia~!2009-05-11~!2009-12-22~!2010-06-14~! *The Open Neurology Journal, 4*(2), 34-38. doi:10.2174/1874205x01004020034

Banks, J. L., & Marotta, C. A. (2007). Outcomes Validity and Reliability of the Modified Rankin Scale: Implications for Stroke Clinical Trials. *Stroke, 38*(3), 1091-1096. doi:10.1161/01.STR.0000258355.23810.c6

Baron, J.-C. (1999). Mapping the Ischaemic Penumbra with PET: Implications for Acute Stroke Treatment. *Cerebrovascular Diseases, 9*(4), 193-201. doi:10.1159/000015955

Beckers, L., Ory, D., Geric, I., Declercq, L., Koole, M., Kassiou, M., Bormans, G., & Baes, M. (2017). Increased Expression of Translocator Protein (TSPO) Marks Pro-inflammatory Microglia but Does Not Predict Neurodegeneration. *Molecular Imaging and Biology, 20*(1), 94-102. doi:10.1007/s11307-017-1099-1

Beeton, C., Wulff, H., Standifer, N. E., Azam, P., Mullen, K. M., Pennington, M. W., Kolski-Andreaco, A., Wei, E., Grino, A., Counts, D. R., Wang, P. H., LeeHealey, C. J., S. Andrews, B., Sankaranarayanan, A., Homerick, D., Roeck, W. W., Tehranzadeh, J., Stanhope, K. L., Zimin, P., Havel, P. J., Griffey, S., Knaus, H.-G., Nepom, G. T., Gutman, G. A., Calabresi, P. A., & Chandy, K. G. (2006). Kv1.3 channels are a therapeutic target for T cell-mediated autoimmune diseases. *Proceedings of the National Academy of Sciences, 103*(46), 17414-17419. doi:10.1073/pnas.0605136103

Beloosesky, Y., Streifler, J. Y., Burstin, A., & Grinblat, J. (1995). The Importance of Brain Infarct Size and Location in Predicting Outcome after Stroke. *Age and Ageing, 24*(6), 515-518. doi:10.1093/ageing/24.6.515

Benavides, J., Fage, D., Carter, C., & Scatton, B. (1987). Peripheral type benzodiazepine binding sites are a sensitive indirect index of neuronal damage. *Brain Research, 421*(1-2), 167-172. doi:10.1016/0006-8993(87)91287-x

Biller, J., Love, B. B., Marsh, E. E., Jones, M. P., Knepper, L. E., Jiang, D., Adams, H. P., & Gordon, D. L. (1990). Spontaneous improvement after acute ischemic stroke. A pilot study. *Stroke, 21*(7), 1008-1012. doi:10.1161/01.Str.21.7.1008

Bogousslavsky, J., Van Melle, G., & Regli, F. (1988). The Lausanne Stroke Registry: analysis of 1,000 consecutive patients with first stroke. *Stroke, 19*(9), 1083-1092. doi:10.1161/01.Str.19.9.1083

Chen, A.-Q., Fang, Z., Chen, X.-L., Yang, S., Zhou, Y.-F., Mao, L., Xia, Y.-P., Jin, H.-J., Li, Y.-N., You, M.-F., Wang, X.-X., Lei, H., He, Q.-W., & Hu, B. (2019). Microglia-derived TNF-α mediates endothelial necroptosis aggravating blood brain–barrier disruption after ischemic stroke. *Cell Death & Disease, 10*(7). doi:10.1038/s41419-019-1716-9

Chen, M., Ona, V. O., Li, M., Ferrante, R. J., Fink, K. B., Zhu, S., Bian, J., Guo, L., Farrell, L. A., Hersch, S. M., Hobbs, W., Vonsattel, J.-P., Cha, J.-H. J., & Friedlander, R. M. (2000). Minocycline inhibits caspase-1 and caspase-3 expression and delays mortality in a transgenic mouse model of Huntington disease. *Nature Medicine, 6*(7), 797-801. doi:10.1038/77528

Chen, S., Shao, L., & Ma, L. (2021). Cerebral Edema Formation After Stroke: Emphasis on Blood–Brain Barrier and the Lymphatic Drainage System of the Brain. *Frontiers in Cellular Neuroscience, 15*. doi:10.3389/fncel.2021.716825

Chen, Y., Nguyen, H., Maezawa, I., Jin, L., & Wulff, H. (2018). Inhibition of the potassium channel Kv1.3 reduces infarction and inflammation in ischemic stroke. *Ann Clin Transl Neurol, 5*, 147-161.

Chen, Y.-J., Nguyen, H. M., Maezawa, I., Grössinger, E. M., Garing, A. L., Köhler, R., Jin, L.-W., & Wulff, H. (2016). The potassium channel KCa3.1 constitutes a pharmacological target for neuroinflammation associated with ischemia/reperfusion stroke. *Journal of cerebral blood flow and metabolism : official journal of the International Society of Cerebral Blood Flow and Metabolism, 36*(12), 2146-2161. doi:doi: 10.1177/0271678X15611434

Chen, Y.-J., Raman, G., Bodendiek, S., O'Donnell, M. E., & Wulff, H. (2011). The KCa3.1 blocker TRAM-34 reduces infarction and neurological deficit in a rat model of ischemia/reperfusion stroke. *Journal of cerebral blood flow and metabolism : official journal of the International Society of Cerebral Blood Flow and Metabolism, 31*(12), 2363-2374. doi:doi: 10.1038/jcbfm.2011.101

Chen, Y. J., Cui, Y., Singh, L., & Wulff, H. (2021). The potassium channel Kv1.3 as a therapeutic target for immunocytoprotection after reperfusion. *Annals of Clinical and Translational Neurology, 8*(10), 2070-2082. doi:10.1002/acn3.51456

Chohan, S. A., Venkatesh, P. K., & How, C. H. (2019). Long-term complications of stroke and secondary prevention: an overview for primary care physicians. *Singapore Medical Journal, 60*(12), 616-620. doi:10.11622/smedj.2019158

Clément, T., Rodriguez-Grande, B., & Badaut, J. (2020). Aquaporins in brain edema. *Journal of Neuroscience Research, 98*(1), 9-18. doi:10.1002/jnr.24354

Corbetta, M., Ramsey, L., Callejas, A., Baldassarre, A., Hacker, Carl D., Siegel, Joshua S., Astafiev, Serguei V., Rengachary, J., Zinn, K., Lang, Catherine E., Connor, Lisa T., Fucetola, R., Strube, M., Carter, Alex R., & Shulman, Gordon L. (2015). Common Behavioral Clusters and Subcortical Anatomy in Stroke. *Neuron, 85*(5), 927-941. doi:10.1016/j.neuron.2015.02.027

da Fonseca, A. C. C., Matias, D., Garcia, C., Amaral, R., Geraldo, L. H., Freitas, C., & Lima, F. R. S. (2014). The impact of microglial activation on blood-brain barrier in brain diseases. *Frontiers in Cellular Neuroscience, 8*. doi:10.3389/fncel.2014.00362

DeCoursey, T. E., Chandy, K. G., Gupta, S., & Cahalan, M. D. (1984). Voltage-gated K+ channels in human T lymphocytes: a role in mitogenesis? *Nature, 307*(5950), 465-468. doi:10.1038/307465a0

Dostovic, Z., Dostovic, E., Smajlovic, D., & Avdic, O. (2016). Brain Edema After Ischaemic Stroke. *Medical Archives, 70*(5). doi:10.5455/medarh.2016.70.339-341

Dutta, S., & Sengupta, P. (2016). Men and mice: Relating their ages. *Life Sciences, 152*, 244-248. doi:10.1016/j.lfs.2015.10.025

Encarnacion, A., Horie, N., Keren-Gill, H., Bliss, T. M., Steinberg, G. K., & Shamloo, M. (2011). Long-term behavioral assessment of function in an experimental model for ischemic stroke. *Journal of Neuroscience Methods, 196*(2), 247-257. doi:10.1016/j.jneumeth.2011.01.010

Fagan, S. C. (2010). Drug Repurposing for Drug Development in Stroke. *Pharmacotherapy, 30*(7, part 2), 51S-54S. doi:10.1592/phco.30.pt2.51S

Fan, X., Lo, E. H., & Wang, X. (2013). Effects of Minocycline Plus Tissue Plasminogen Activator Combination Therapy After Focal Embolic Stroke in Type 1 Diabetic Rats. *Stroke, 44*(3), 745-752. doi:10.1161/strokeaha.111.000309

Feske, S., Wulff, H., & Skolnik, E. Y. (2015). Ion Channels in Innate and Adaptive Immunity. *Annual Review of Immunology, 33*(1), 291-353. doi:10.1146/annurev-immunol-032414-112212

Fiebach, J., Jansen, O., Schellinger, P., Heiland, S., Hacke, W., & Sartor, K. (2014). Serial analysis of the apparent diffusion coefficient time course in human stroke. *Neuroradiology, 44*(4), 294-298. doi:10.1007/s00234-001-0720-8

Fiebach, J. B., Schellinger, P. D., Jansen, O., Meyer, M., Wilde, P., Bender, J., Schramm, P., Jüttler, E., Oehler, J., Hartmann, M., Hähnel, S., Knauth, M., Hacke, W., & Sartor, K. (2002). CT and Diffusion-Weighted MR Imaging in Randomized Order. *Stroke, 33*(9), 2206-2210. doi:10.1161/01.Str.0000026864.20339.Cb

Fisher, M., Feuerstein, G., Howells, D. W., Hurn, P. D., Kent, T. A., Savitz, S. I., & Lo, E. H. (2009). Update of the Stroke Therapy Academic Industry Roundtable Preclinical Recommendations. *Stroke, 40*(6), 2244-2250. doi:10.1161/strokeaha.108.541128

Fluri, F., Schuhmann, M., & Kleinschnitz, C. (2015). Animal models of ischemic stroke and their application in clinical research. *Drug Design, Development and Therapy*. doi:10.2147/dddt.S56071

Gennaro, M., Mattiello, A., & Pizzorusso, T. (2019). Rodent Models of Developmental Ischemic Stroke for Translational Research: Strengths and Weaknesses. *Neural Plasticity, 2019*, 1-16. doi:10.1155/2019/5089321

Graham, S. M., McCullough, L. D., & Murphy, S. J. (2004). Animal models of ischemic stroke: balancing experimental aims and animal care. *Comp Med, 54*(5), 486-496.

Guo, S., Wang, H., & Yin, Y. (2022). Microglia Polarization From M1 to M2 in Neurodegenerative Diseases. *Frontiers in Aging Neuroscience, 14*. doi:10.3389/fnagi.2022.815347

Harris, J. E., & Eng, J. J. (2016). Individuals with the Dominant Hand Affected following Stroke Demonstrate Less Impairment Than Those with the Nondominant Hand Affected. *Neurorehabilitation and Neural Repair, 20*(3), 380-389. doi:10.1177/1545968305284528

Haruwaka, K., Ikegami, A., Tachibana, Y., Ohno, N., Konishi, H., Hashimoto, A., Matsumoto, M., Kato, D., Ono, R., Kiyama, H., Moorhouse, A. J., Nabekura, J., & Wake, H. (2019). Dual microglia effects on blood brain barrier permeability induced by systemic inflammation. *Nature Communications, 10*(1). doi:10.1038/s41467-019-13812-z

Hatashita, S., & Hoff, J. T. (1990). Brain edema and cerebrovascular permeability during cerebral ischemia in rats. *Stroke, 21*(4), 582-588. doi:10.1161/01.Str.21.4.582

Heiss, W. D., Graf, R., Wienhard, K., Lottgen, J., Saito, R., Fujita, T., Rosner, G., & Wagner, R. (1994). Dynamic penumbra demonstrated by sequential multitracer PET after middle cerebral artery occlusion in cats. *J Cereb Blood Flow Metab, 14*(6), 892-902. doi:10.1038/jcbfm.1994.120

Hillis, A. E., Wityk, R. J., Barker, P. B., Beauchamp, N. J., Gailloud, P., Murphy, K., Cooper, O., & Metter, E. J. (2002). Subcortical aphasia and neglect in acute stroke: the role of cortical hypoperfusion. *Brain, 125*(5), 1094-1104. doi:10.1093/brain/awf113

Hu, X., Li, P., Guo, Y., Wang, H., Leak, R. K., Chen, S., Gao, Y., & Chen, J. (2012). Microglia/Macrophage Polarization Dynamics Reveal Novel Mechanism of Injury Expansion After Focal Cerebral Ischemia. *Stroke, 43*(11), 3063-3070. doi:10.1161/strokeaha.112.659656

Ito, D., Tanaka, K., Suzuki, S., Dembo, T., & Fukuuchi, Y. (2001). Enhanced Expression of Iba1, Ionized Calcium-Binding Adapter Molecule 1, After Transient Focal Cerebral Ischemia In Rat Brain. *Stroke, 32*(5), 1208-1215. doi:10.1161/01.Str.32.5.1208

Jia, J., Yang, L., Chen, Y., Zheng, L., Chen, Y., Xu, Y., & Zhang, M. (2022). The Role of Microglial Phagocytosis in Ischemic Stroke. *Frontiers in Immunology, 12*. doi:10.3389/fimmu.2021.790201

Jin, L.-W., Lucente, J. D., Nguyen, H. M., Singh, V., Singh, L., Chavez, M., Bushong, T., Wulff, H., & Maezawa, I. (2019). Repurposing the KCa3.1 inhibitor senicapoc for Alzheimer's disease. *Annals of Clinical Translational Neurology, 6*(4), 723-738. doi:doi: 10.1002/acn3.754

Joshi, C. N., Jain, S. K., & Murthy, P. S. R. (2004). An optimized triphenyltetrazolium chloride method for identification of cerebral infarcts. *Brain Research Protocols, 13*(1), 11-17. doi:10.1016/j.brainresprot.2003.12.001

Jurcau, A., & Simion, A. (2021). Neuroinflammation in Cerebral Ischemia and Ischemia/Reperfusion Injuries: From Pathophysiology to Therapeutic Strategies. *International Journal of Molecular Sciences, 23*(1). doi:10.3390/ijms23010014

Kiewert, C., Mdzinarishvili, A., Hartmann, J., Bickel, U., & Klein, J. (2010). Metabolic and transmitter changes in core and penumbra after middle cerebral artery occlusion in mice. *Brain Research, 1312*, 101-107. doi:10.1016/j.brainres.2009.11.068

Kim, J., Martinez, C., & Sirotkin, I. (2017). Cerebral Venous Thrombosis. *Fed Pract, 34*(7), 33-37.

Klatzo, I. (1987). Pathophysiological aspects of brain edema. *Acta Neuropathologica, 72*(3), 236-239. doi:10.1007/bf00691095

Kohler, E., Prentice, D. A., Bates, T. R., Hankey, G. J., Claxton, A., van Heerden, J., & Blacker, D. (2013). Intravenous Minocycline in Acute Stroke. *Stroke, 44*(9), 2493-2499. doi:10.1161/strokeaha.113.000780

König, I. R., Ziegler, A., Bluhmki, E., Hacke, W., Bath, P. M. W., Sacco, R. L., Diener, H. C., & Weimar, C. (2008). Predicting Long-Term Outcome After Acute Ischemic Stroke. *Stroke, 39*(6), 1821-1826. doi:10.1161/strokeaha.107.505867

Kundu-Raychaudhuri, S., Chen, Y.-J., Wulff, H., & Raychaudhuri, S. P. (2014). Kv1.3 in psoriatic disease: PAP-1, a small molecule inhibitor of Kv1.3 is effective in the SCID mouse psoriasis – Xenograft model. *Journal of Autoimmunity, 55*, 63-72. doi:10.1016/j.jaut.2014.07.003

Kwiecien, T. D., Sy, C., & Ding, Y. (2014). Rodent models of ischemic stroke lack translational relevance… are baboon models the answer? *Neurological Research, 36*(5), 417-422. doi:10.1179/1743132814y.0000000358

Lampl, Y., Boaz, M., Gilad, R., Lorberboym, M., Dabby, R., Rapoport, A., Anca-Hershkowitz, M., & Sadeh, M. (2007). Minocycline treatment in acute stroke: An open-label, evaluator-blinded study. *Neurology, 69*(14), 1404-1410. doi:10.1212/01.wnl.0000277487.04281.db

Lee, R. D., Chen, Y.-J., Nguyen, H. M., Singh, L., Dietrich, C. J., Pyles, B. R., Cui, Y., Weinstein, J. R., & Wulff, H. (2023). Repurposing the KCa3.1 Blocker Senicapoc for Ischemic Stroke. *Translational Stroke Research*. doi:10.1007/s12975-023-01152-6

Lee, R. D., Chen, Y.-J., Singh, L., Nguyen, H. M., & Wulff, H. (2023). Immunocytoprotection after reperfusion with Kv1.3 inhibitors has an extended treatment window for ischemic stroke. *Frontiers in Pharmacology, 14*. doi:10.3389/fphar.2023.1190476

Lee, Y., Park, Y., Nam, H., Lee, J.-W., & Yu, S.-W. (2020). Translocator protein (TSPO): the new story of the old protein in neuroinflammation. *BMB Reports, 53*(1), 20-27. doi:10.5483/BMBRep.2020.53.1.273

Lees, K. R., Selim, M. H., Molina, C. A., & Broderick, J. P. (2016). Early Versus Late Assessment of Stroke Outcome. *Stroke, 47*(5), 1416-1419. doi:10.1161/strokeaha.115.011153

Liang, D., Bhatta, S., Gerzanich, V., & Simard, J. M. (2007). Cytotoxic edema: mechanisms of pathological cell swelling. *Neurosurgical Focus, 22*(5), 1-9. doi:10.3171/foc.2007.22.5.3

Liebeskind, D. S., Jüttler, E., Shapovalov, Y., Yegin, A., Landen, J., & Jauch, E. C. (2019). Cerebral Edema Associated With Large Hemispheric Infarction. *Stroke, 50*(9), 2619-2625. doi:10.1161/strokeaha.118.024766

Liu, S., Levine, S. R., & Winn, H. R. (2010). Targeting ischemic penumbra Part I: from pathophysiology to therapeutic strategy. *Journal of Experimental Stroke and Translational Medicine, 3*(1), 47-55. doi:10.6030/1939-067x-3.1.47

Loftspring, M. C., Beiler, S., Beiler, C., & Wagner, K. R. (2006). Plasma Proteins in Edematous White Matter after Intracerebral Hemorrhage Confound Immunoblots: An ELISA to Quantify Contamination. *Journal of Neurotrauma, 23*(12), 1904-1911. doi:10.1089/neu.2006.23.1904

Lu, Y., Zhou, M., Li, Y., Li, Y., Hua, Y., & Fan, Y. (2021). Minocycline promotes functional recovery in ischemic stroke by modulating microglia polarization through STAT1/STAT6 pathways. *Biochemical Pharmacology, 186*. doi:10.1016/j.bcp.2021.114464

Lyon, M. F. (2002). A Personal History of the Mouse Genome. *Annual Review of Genomics and Human Genetics, 3*(1), 1-16. doi:10.1146/annurev.genom.3.021202.150353

Machado, L. S., Sazonova, I. Y., Kozak, A., Wiley, D. C., El-Remessy, A. B., Ergul, A., Hess, D. C., Waller, J. L., & Fagan, S. C. (2009). Minocycline and Tissue-Type Plasminogen Activator for Stroke. *Stroke, 40*(9), 3028-3033. doi:10.1161/strokeaha.109.556852

Macrae, I. M. (2011). Preclinical stroke research - advantages and disadvantages of the most common rodent models of focal ischaemia. *British Journal of Pharmacology, 164*(4), 1062-1078. doi:10.1111/j.1476-5381.2011.01398.x

Maezawa, I., Nguyen, H. M., Di Lucente, J., Jenkins, D. P., Singh, V., Hilt, S., Kim, K., Rangaraju, S., Levey, A. I., Wulff, H., & Jin, L.-W. (2018). Kv1.3 inhibition as a potential microglia-targeted therapy for Alzheimer's disease: preclinical proof of concept. *Brain, 141*(2), 596-612. doi:10.1093/brain/awx346

Mandava, P., & Kent, T. A. (2009). A Method to Determine Stroke Trial Success Using Multidimensional Pooled Control Functions. *Stroke, 40*(5), 1803-1810. doi:10.1161/strokeaha.108.532820

Mangla, R., Kolar, B., Almast, J., & Ekholm, S. E. (2011). Border Zone Infarcts: Pathophysiologic and Imaging Characteristics. *RadioGraphics, 31*(5), 1201-1214. doi:10.1148/rg.315105014

Matteson, D. R., & Deutsch, C. (1984). K channels in T lymphocytes: a patch clamp study using monoclonal antibody adhesion. *Nature, 307*(5950), 468-471. doi:10.1038/307468a0

Mauler, F., Hinz, V., Horvath, E., Schuhmacher, J., Hofmann, H. A., Wirtz, S., Hahn, M. G., & Urbahns, K. (2004). Selective intermediate-/small-conductance calcium-activated potassium channel (KCNN4) blockers are potent and effective therapeutics in experimental brain oedema and traumatic brain injury caused by acute subdural haematoma. *European Journal of Neuroscience, 20*(7), 1761-1768. doi:10.1111/j.1460-9568.2004.03615.x

Memezawa, H., Smith, M. L., & Siesjö, B. K. (1992). Penumbral tissues salvaged by reperfusion following middle cerebral artery occlusion in rats. *Stroke, 23*(4), 552-559. doi:10.1161/01.Str.23.4.552

Mulder, I. A., Ogrinc Potočnik, N., Broos, L. A. M., Prop, A., Wermer, M. J. H., Heeren, R. M. A., & van den Maagdenberg, A. M. J. M. (2019). Distinguishing core from penumbra by lipid profiles using Mass Spectrometry Imaging in a transgenic mouse model of ischemic stroke. *Scientific Reports, 9*(1). doi:10.1038/s41598-018-37612-5

Park, S.-Y., Marasini, S., Kim, G.-H., Ku, T., Choi, C., Park, M.-Y., Kim, E.-H., Lee, Y.-D., Suh-Kim, H., & Kim, S.-S. (2014). A Method for Generate a Mouse Model of Stroke: Evaluation of Parameters for Blood Flow, Behavior, and Survival. *Experimental Neurobiology, 23*(1), 104-114. doi:10.5607/en.2014.23.1.104

Phan, T. G., Donnan, G. A., Wright, P. M., & Reutens, D. C. (2005). A Digital Map of Middle Cerebral Artery Infarcts Associated With Middle Cerebral Artery Trunk and Branch Occlusion. *Stroke, 36*(5), 986-991. doi:10.1161/01.STR.0000163087.66828.e9

Price, C. J. S., Wang, D., Menon, D. K., Guadagno, J. V., Cleij, M., Fryer, T., Aigbirhio, F., Baron, J.-C., & Warburton, E. A. (2006). Intrinsic Activated Microglia Map to the Peri-infarct Zone in the Subacute Phase of Ischemic Stroke. *Stroke, 37*(7), 1749-1753. doi:10.1161/01.STR.0000226980.95389.0b

Quinn, T. J., Dawson, J., Walters, M. R., & Lees, K. R. (2009). Reliability of the Modified Rankin Scale. *Stroke, 40*(10), 3393-3395. doi:10.1161/strokeaha.109.557256

Ramesha, S., Rayaprolu, S., Bowen, C. A., Giver, C. R., Bitarafan, S., Nguyen, H. M., Chen, T. G. M. J., Nwabueze, N., Engstrom, E. B. D. A. K., Xiao, H., Pennati, A., Seyfried, N. T., Katz, D. J., Galipeau, J., Wulff, H., Waller, E. K., Wood, L. B., Levey, A. I., & Rangaraju, S. (2021). Unique molecular characteristics and microglial origin of Kv1.3 channel–positive brain myeloid cells in Alzheimer's disease. *Proceedings of the National Academy of Sciences of the United States of America, 118*(11), e2013545118.

Ramsay, S. C., Weiller, C., Myers, R., Cremer, J. E., Luthra, S. K., Lammertsma, A. A., & Frackowiak, R. S. J. (1992). Monitoring by PET of macrophage accumulation in brain after ischaemic stroke. *The Lancet, 339*(8800), 1054-1055. doi:10.1016/0140-6736(92)90576-o

Reich, E.-P., Cui, L., Yang, L., Pugliese-Sivo, C., Golovko, A., Petro, M., Vassileva, G., Chu, I., Nomeir, A. A., Zhang, L.-K., Liang, X., Kozlowski, J. A., Narula, S. K., Zavodny, P. J., & Chou, C.-C. (2005). Blocking ion channel KCNN4 alleviates the symptoms of experimental autoimmune encephalomyelitis in mice. *European Journal of Immunology, 35*(4), 1027-1036. doi:10.1002/eji.200425954

Ruan, J., & Yao, Y. (2020). Behavioral tests in rodent models of stroke. *Brain Hemorrhages, 1*(4), 171-184. doi:10.1016/j.hest.2020.09.001

Saita, K., Chen, M., Spratt, N. J., Porritt, M. J., Liberatore, G. T., Read, S. J., Levi, C. R., Donnan, G. A., Ackermann, U., Tochon-Danguy, H. J., Sachinidis, J. I., & Howells, D. W. (2004). Imaging the Ischemic Penumbra with 18F-Fluoromisonidazole in a Rat Model of Ischemic Stroke. *Stroke, 35*(4), 975-980. doi:10.1161/01.STR.0000121647.01941.ba

Santo, B. A., Ciecierska, S.-S. K., Mousavi Janbeh Sarayi, S. M., Jenkins, T. D., Baig, A. A., Monteiro, A., Koenigsknecht, C., Pionessa, D., Gutierrez, L., King, R. M., Gounis, M., Siddiqui, A. H., & Tutino, V. M. (2023). Tectonic infarct analysis: A computational tool for automated whole-brain infarct analysis from TTC-stained tissue. *Heliyon, 9*(4). doi:10.1016/j.heliyon.2023.e14837

Saver, J. L. (2006). Time Is Brain—Quantified. *Stroke, 37*(1), 263-266. doi:10.1161/01.STR.0000196957.55928.ab

Saver, J. L., & Altman, H. (2012). Relationship Between Neurologic Deficit Severity and Final Functional Outcome Shifts and Strengthens During First Hours After Onset. *Stroke, 43*(6), 1537-1541. doi:10.1161/strokeaha.111.636928

Schaar, K. L., Brenneman, M. M., & Savitz, S. I. (2010). Functional assessments in the rodent stroke model. *Experimental & Translational Stroke Medicine, 2*(1). doi:10.1186/2040-7378-2-13

Schiemanck, S. K., Post, M. W., Kwakkel, G., Witkamp, T. D., Kappelle, L. J., & Prevo, A. J. (2005). Ischemic lesion volume correlates with long-term functional outcome and quality of life of middle cerebral artery stroke survivors. *Restor Neurol Neurosci, 23*(3-4), 257-263.

Schiemanck, S. K., Post, M. W., Witkamp, T. D., Kappelle, L. J., & Prevo, A. J. (2005). Relationship between ischemic lesion volume and functional status in the 2nd week after middle cerebral artery stroke. *Neurorehabil Neural Repair, 19*(2), 133-138. doi:10.1177/154596830501900207

Schmitz, A., Sankaranarayanan, A., Azam, P., Schmidt-Lassen, K., Homerick, D., Hänsel, W., & Wulff, H. (2005). Design of PAP-1, a Selective Small Molecule Kv1.3 Blocker, for the Suppression of Effector Memory T Cells in Autoimmune Diseases. *Molecular Pharmacology, 68*(5), 1254-1270. doi:10.1124/mol.105.015669

Schroeter, M., Jander, S., Huitinga, I., Witte, O. W., & Stoll, G. (1997). Phagocytic Response in Photochemically Induced Infarction of Rat Cerebral Cortex. *Stroke, 28*(2), 382-386. doi:10.1161/01.Str.28.2.382

Schwamm, L. H., Koroshetz, W. J., Sorensen, A. G., Wang, B., Copen, W. A., Budzik, R., Rordorf, G., Buonanno, F. S., Schaefer, P. W., & Gonzalez, R. G. (1998). Time Course of Lesion Development in Patients With Acute Stroke. *Stroke, 29*(11), 2268-2276. doi:10.1161/01.Str.29.11.2268

Shen, L. H., Li, Y., Chen, J., Zhang, J., Vanguri, P., Borneman, J., & Chopp, M. (2006). Intracarotid transplantation of bone marrow stromal cells increases axon-myelin remodeling after stroke. *Neuroscience, 137*(2), 393-399. doi:10.1016/j.neuroscience.2005.08.092

Slivka, A., Murphy, E., & Horrocks, L. (1995). Cerebral Edema After Temporary and Permanent Middle Cerebral Artery Occlusion in the Rat. *Stroke, 26*(6), 1061-1066. doi:10.1161/01.Str.26.6.1061

Smith, E. E., Shobha, N., Dai, D., Olson, D. M., Reeves, M. J., Saver, J. L., Hernandez, A. F., Peterson, E. D., Fonarow, G. C., & Schwamm, L. H. (2010). Risk Score for In-Hospital Ischemic Stroke Mortality Derived and Validated Within the Get With The Guidelines–Stroke Program. *Circulation, 122*(15), 1496-1504. doi:10.1161/circulationaha.109.932822

Sommer, C. J. (2017). Ischemic stroke: experimental models and reality. *Acta Neuropathologica, 133*(2), 245-261. doi:10.1007/s00401-017-1667-0

Stokum, J. A., Gerzanich, V., & Simard, J. M. (2015). Molecular pathophysiology of cerebral edema. *Journal of Cerebral Blood Flow & Metabolism, 36*(3), 513-538. doi:10.1177/0271678x15617172

Sulter, G., Steen, C., & Jacques De, K. (1999). Use of the Barthel Index and Modified Rankin Scale in Acute Stroke Trials. *Stroke, 30*(8), 1538-1541. doi:10.1161/01.Str.30.8.1538

Symon, L., Branston, N. M., Strong, A. J., & Hope, T. D. (1977). The concepts of thresholds of ischaemia in relation to brain structure and function. *Journal of Clinical Pathology, s3-11*(1), 149-154. doi:10.1136/jcp.s3-11.1.149

Taha, A., Bobi, J., Dammers, R., Dijkhuizen, R. M., Dreyer, A. Y., van Es, A. C. G. M., Ferrara, F., Gounis, M. J., Nitzsche, B., Platt, S., Stoffel, M. H., Volovici, V., del Zoppo, G. J., Duncker, D. J., Dippel, D. W. J., Boltze, J., & van Beusekom, H. M. M. (2022). Comparison of Large Animal Models for Acute Ischemic Stroke: Which Model to Use? *Stroke, 53*(4), 1411-1422. doi:10.1161/strokeaha.121.036050

Waller, S. M., & Whitall, J. (2016). Hand dominance and side of stroke affect rehabilitation in chronic stroke. *Clinical Rehabilitation, 19*(5), 544-551. doi:10.1191/0269215505cr829oa

Wang, Y., Leak, R. K., & Cao, G. (2022). Microglia-mediated neuroinflammation and neuroplasticity after stroke. *Frontiers in Cellular Neuroscience, 16*. doi:10.3389/fncel.2022.980722

Wang-Fischer, Y. (2008). *Manual of Stroke Models in Rats*.

Weinstein, J. R., Koerner, I. P., & Möller, T. (2010). Microglia in ischemic brain injury. *Future Neurology, 5*(2), 227-246. doi:10.2217/fnl.10.1

Wiebers, D. O., Adams, H. P., & Whisnant, J. P. (1990). Animal models of stroke: are they relevant to human disease? *Stroke, 21*(1), 1-3. doi:10.1161/01.Str.21.1.1

Wityk, R. J., Pessin, M. S., Kaplan, R. F., & Caplan, L. R. (1994). Serial assessment of acute stroke using the NIH Stroke Scale. *Stroke, 25*(2), 362-365. doi:10.1161/01.Str.25.2.362

Wu, Q. J., Sun, X., Teves, L., Mayor, D., & Tymianski, M. (2021). Mice and Rats Exhibit Striking Inter-species Differences in Gene Response to Acute Stroke. *Cellular and Molecular Neurobiology, 42*(8), 2773-2789. doi:10.1007/s10571-021-01138-8

Wulff, H., & Castle, N. A. (2014). Therapeutic potential of KCa3.1 blockers: recent advances and promising trends. *Expert Review of Clinical Pharmacology, 3*(3), 385-396. doi:10.1586/ecp.10.11

Xu, L., Fagan, S. C., Waller, J. L., Edwards, D., Borlongan, C. V., Zheng, J., Hill, W. D., Feuerstein, G., & Hess, D. C. (2004). Low dose intravenous minocycline is neuroprotective after middle cerebral artery occlusion-reperfusion in rats. *BMC Neurology, 4*(1). doi:10.1186/1471-2377-4-7

Yang, Y., Qian, C., Li, P.-C., Jiao, Y., Yao, H.-H., Chen, Y.-C., Yang, J., Ding, J., Yang, X.-Y., & Teng, G.-J. (2016). Precise Characterization of the Penumbra Revealed by MRI: A Modified Photothrombotic Stroke Model Study. *PLoS ONE, 11*(4). doi:10.1371/journal.pone.0153756

Yong, V. W., Wells, J., Giuliani, F., Casha, S., Power, C., & Metz, L. M. (2004). The promise of minocycline in neurology. *The Lancet Neurology, 3*(12), 744-751. doi:10.1016/s1474-4422(04)00937-8

Zhang, Y., Lian, L., Fu, R., Liu, J., Shan, X., Jin, Y., & Xu, S. (2022). Microglia: The Hub of Intercellular Communication in Ischemic Stroke. *Frontiers in Cellular Neuroscience, 16*. doi:10.3389/fncel.2022.889442

Zhu, S., Stavrovskaya, I. G., Drozda, M., Kim, B. Y. S., Ona, V., Li, M., Sarang, S., Liu, A. S., Hartley, D. M., Wu, D. C., Gullans, S., Ferrante, R. J., Przedborski, S., Kristal, B. S., & Friedlander, R. M. (2002). Minocycline inhibits cytochrome c release and delays progression of amyotrophic lateral sclerosis in mice. *Nature, 417*(6884), 74-78. doi:10.1038/417074a

CHAPTER 2

Repurposing the $K_{Ca}3.1$ Blocker Senicapoc for Ischemic Stroke

Ruth D. Lee, MS[1]*, Yi-Je Chen, DVM, PhD[1,2]*, Hai M. Nguyen, PhD[1], Latika Singh, PhD[1], Connor J. Dietrich, BS[1], Benjamin R. Pyles, MS[1], Yanjun Cui, MS[1], Jonathan R. Weinstein, MD, PhD[3], Heike Wulff, PhD[1]

* These authors contributed equally.

[1]Department of Pharmacology, School of Medicine, University of California, Davis, CA 95616, USA; [2]Animal Models Core, Department of Pharmacology, School of Medicine, University of California, Davis, CA 95616, USA; [3]Department of Neurology, School of Medicine, University of Washington, Seattle, WA 98195, USA

Address Correspondence to Heike Wulff, PhD, Department of Pharmacology, School of Medicine, University of California, Davis; 451 Health Sciences Drive, GBSF 3502, Davis, CA 95616. Email: hwulff@ucdavis.edu

Abstract

Senicapoc, a small molecule inhibitor of the calcium-activated potassium channel $K_{Ca}3.1$, was safe and well-tolerated in clinical trials for sickle cell anemia. We previously reported proof-of-concept data suggesting that both pharmacological inhibition and genetic deletion of $K_{Ca}3.1$ reduces infarction and improves neurologic recovery in rodents by attenuating neuroinflammation. Here we evaluated the potential of repurposing senicapoc for ischemic stroke. In cultured microglia senicapoc inhibited $K_{Ca}3.1$ currents with an IC_{50} of 7 nM, reduced Ca^{2+} signaling induced by the purinergic agonist ATP, suppressed expression of pro-inflammatory cytokines and enzymes (iNOS and COX-2), and prevented induction of the inflammasome component NLRP3. When transient middle cerebral artery occlusion (tMCAO, 60-min) was induced in male C57BL/6J mice, twice daily administration of senicapoc at 10 and 40 mg/kg starting 12 h after reperfusion, dose-dependently reduced infarct area determined by T2-weighted magnetic resonance imaging (MRI) and improved neurological deficit on day-8. Ultra-high-performance liquid chromatography/mass spectrometry analysis of total and free brain concentrations demonstrated sufficient $K_{Ca}3.1$ target engagement. Senicapoc treatment significantly reduced microglia/macrophage and T cell infiltration and activation and attenuated neuronal death. A different treatment paradigm with senicapoc started at 3 hours and MRI on day-3 and day-8 revealed that senicapoc reduces secondary infarct growth and suppresses expression of inflammation markers, including T cell cytokines in the brain. Lastly, we demonstrated that senicapoc does not impair the proteolytic activity of tissue plasminogen activator (tPA) *in-vitro*. We suggest that senicapoc could be repurposed as an adjunctive immunocytoprotective agent for combination with reperfusion therapy for ischemic stroke.

Keywords: Neuroinflammation, microglia activation, ischemic stroke, middle cerebral artery occlusion, senicapoc, $K_{Ca}3.1$

Introduction

Stroke is the leading cause of serious long-term disability and the fifth most common cause of death in the United States (Virani et al., 2020). Treatment options for stroke are few, of limited efficacy (Prabhakaran, Ruff, & Bernstein, 2015), and are greatly dependent on implementation within a narrow temporal window. Tissue plasminogen activator (tPA) remains the only FDA-approved drug for selected stroke patients who present no later than 3 hours of symptom onset (National Institute of Neurological & Stroke rt, 1995). In clinical practice, tPA is used up to 4.5 hours or sometimes longer when appropriate based on imaging (Prabhakaran et al., 2015). However, tPA carries a risk of hemorrhagic transformation and has a low success rate in lysing large clots. For stroke patients with large vessel occlusion (LVO), endovascular thrombectomy (EVT) with associated rapid (and often complete) cerebral reperfusion, has been proven effective in multiple large randomized controlled trials (Lin, Liang, & Lin, 2020; Palaniswami & Yan, 2015). However, every additional hour from stroke onset to reperfusion is associated with an increase in mortality (Mulder et al., 2018), and EVT is only recommended for eligible patients up to 24 hours after symptom onset. Therefore, there remains an unmet need for additional stroke therapeutics, especially for patients who do not fulfill the strict eligibility criteria for tPA or EVT. In addition, there is a need to develop novel pharmacotherapies as adjunctive immunocytoprotective agents that could be used in combination with the existing reperfusion-focused therapies (Savitz, Baron, Fisher, & Consortium, 2019) in order to reduce reperfusion injury, which is increasingly being recognized to occur with a relatively high frequency following recanalization in patients with acute ischemic stroke (Zhou et al., 2023).

We previously demonstrated in proof-of-concept animal experiments that inhibition of the calcium-activated potassium channel $K_{Ca}3.1$ may be a potential therapeutic approach for reducing stroke associated neuroinflammation and reperfusion damage (Chen et al., 2016; Chen, Raman, Bodendiek, O'Donnell, & Wulff, 2011) and are therefore proposing $K_{Ca}3.1$ as a target for

immunocytoprotection. $K_{Ca}3.1$ is expressed in erythrocytes and multiple cell types of the immune system such as macrophages, B cells and T cells, where the channel is involved in volume regulation and cellular activation processes (Brown, Shim, Christophersen, & Wulff, 2020; Feske, Wulff, & Skolnik, 2015). $K_{Ca}3.1$ expression has been described in cultured neonatal and acutely isolated adult microglia from a range of species including mice, rats, and humans (Blomster et al., 2016; Maezawa, Zimin, Wulff, & Jin, 2011; Nguyen, Blomster, Christophersen, & Wulff, 2017; Nguyen, Grossinger, et al., 2017). The channel regulates calcium signaling and cellular activation and expression therefore typically increases following microglia stimulation. $K_{Ca}3.1$ deletion or pharmacological inhibition reduces microglia activation and inflammatory cytokine production (Blomster et al., 2016; Maezawa et al., 2011; Nguyen, Blomster, et al., 2017; Nguyen, Grossinger, et al., 2017). Rats or mice treated with our $K_{Ca}3.1$ blocker, TRAM-34 (Wulff et al., 2000), had significantly smaller infarct areas, decreased markers of neuroinflammation, and improved fine-motor performance and proprioception eight days after transient middle cerebral artery occlusion (tMCAO) with reperfusion (Chen et al., 2016; Chen et al., 2011). Similar beneficial effects were observed in $K_{Ca}3.1^{-/-}$ mice (Chen et al., 2016). However, TRAM-34 has some significant limitations: it is out of patent life, not orally available, shows metabolic instability and has a short half-life (~2 hours in rats and primates) complicating chronic dosing (Maezawa, Jenkins, Jin, & Wulff, 2012). Thus, although TRAM-34 is a valuable experimental tool compound, it is not suitable for development as a drug.

In this study, we explore the use of another $K_{Ca}3.1$ blocker, senicapoc (McNaughton-Smith et al., 2008), for treating ischemic stroke. Senicapoc is a more drug-like molecule than TRAM-34 and entered development with clinical trials for the treatment of sickle cell anemia (Ataga & Stocker, 2009). The drug was well tolerated in dose escalating Phase I clinical trials in both healthy volunteers and in patients with sickle cell disease (Ataga et al., 2006). In a subsequent double-blind placebo-controlled Phase II study, senicapoc (at 10 mg/day) reduced hemolysis and

significantly increased hematocrit and hemoglobin levels (Ataga et al., 2008). However, Senicapoc failed in Phase III trials in 2011 because it did not meet the set clinical endpoint of reduction in the number of vaso-occlusive pain crises (Ataga et al., 2011), even though patients showed decreased hemolysis and improved anemia demonstrating engagement of erythrocyte $K_{Ca}3.1$ channels by the drug (Ataga, Staffa, Brugnara, & Stocker, 2021). Across its clinical trial lifespan, senicapoc was given to hundreds of patients from 19 medical centers across the USA and has been shown to be an orally available, metabolically stable, safe, and well-tolerated drug.

We hypothesized that senicapoc could be repurposed as an adjunctive immunocytoprotective agents for the treatment of ischemic stroke, and here evaluated whether senicapoc would decrease infarction, dampen neuroinflammation, and improve neurobehavioral outcomes in tMCAO in mice, a model that simulates both the ischemic and the reperfusion injury and inflammation associated with LVO strokes and subsequent EVT by its similarly rapid cerebral blood flow restoration (Sutherland et al., 2016). We here demonstrate that senicapoc is efficacious (1) *in-vitro* by blocking $K_{Ca}3.1$ in activated microglia, and (2) *in-vivo* by reducing infarction, attenuating stroke-induced microglia activation, T-cell infiltration, and inflammatory marker expression, and by improving neurologic recovery. Lastly, we demonstrate that senicapoc does not impair the proteolytic activity of tPA *in-vitro* suggesting that senicapoc could be combined with tPA without affecting its efficacy.

Material and Methods

Mouse microglia cell culture

An immortalized mouse microglial cell (MMC) line was kindly provided by Dr. D.T. Golenbock (University of Massachusetts Medical School, Worcester, MA) and previously used by our laboratory (Ramesha et al., 2021; Sarkar et al., 2020). Cells were cultured in Gibco's Dulbecco's modified Eagle's Medium (DMEM, high glucose, L-glutamine, high pyruvate) with 5% CO_2 at 37° with 1% penicillin/streptomycin and 10% fetal bovine serum. For the qPCR experiments, cells were seeded at 200,000 cells/mL; 24 hours later, medium was changed to DMEM with 2% FBS and cells were stimulated with 100 ng/mL LPS, in the presence or absence of senicapoc, or a 0.2% DMSO control. Cells were pre-incubated with senicapoc for 1 h prior to stimulation and harvested 24 hours after stimulation.

Electrophysiology

MMCs were plated on poly-Lysine-coated glass coverslips and $K_{Ca}3.1$ currents recorded in the whole-cell mode of the patch-clamp technique with an EPC-10 HEKA amplifier and 1 μM of free Ca^{2+} in the pipette solution as previously described (Nguyen, Grossinger, et al., 2017).

Calcium Imaging

Real-time changes of $[Ca^{2+}]_i$ in MMCs seeded on glass coverslips at a density of 10,000 cells/ cm^2 were measured using the time-lapse imaging module on a BZ-X780 fluorescence microscopy (Keyence LLC, Campbell, CA) and the fluorescent calcium indicator Fluo-4/AM from Invitrogen (ThermoFisher, Waltham, MA) as previously described (Nguyen et al., 2020). For

testing the effect of $K_{Ca}3.1$ inhibition on intracellular calcium changes, cells were pre-incubated with senicapoc during the de-esterification step and throughout the course of the experiment. All fluorescence measurements were made at 2-sec intervals at room temperature from subconfluent areas of the coverslips to ensure that only individual microglia were measured. Image data were analyzed off-line with Fiji using the ROI-1 click tool (Schindelin et al., 2012; Thomas & Gehrig, 2020) and the change in microglial $[Ca^{2+}]_i$ was represented as $\Delta F/F$ (change in fluorescence after baseline-subtraction).

Animals and Housing

This study was approved by the University of California, Davis Institutional Animal Care and Use Committee and conduced in accordance with the IMPROVE guidelines for ischemic stroke in rodents (Percie du Sert et al., 2017). Adult male C57BL/6J mice were purchased from Jackson Laboratory (stock number: 000664) at 14 weeks of age and used for surgery when they were 16 weeks old. Mice were group-housed in filtertop cages with an enriched environment (shredded paper) under a 12-hour light/dark cycle before and after surgery. Animals had ad libitum access to standard chow and water. Room temperature and humidity were monitored and kept at 22±1°C and 50±10%. After surgeries, soft water-soaked chow was provided in the cages.

Filament-Induced Transient Middle Cerebral Artery Occlusion

Reversible focal cerebral ischemia was induced by occlusion of the left middle cerebral artery (MCA) according to the classic filament method of Zea Longa (Longa, Weinstein, Carlson, & Cummins, 1989) as previously described for mice by our laboratory (Chen, Cui, Singh, & Wulff, 2021; Chen, Nguyen, Maezawa, Jin, & Wulff, 2018). All surgeries were performed in the

MicroSurgery Core of the UC Davis School of Medicine by a microsurgeon with 20 years of surgical experience using a silicone rubber-coated nylon monofilament with a tip diameter of 0.21 ± 0.02 mm (No. 702112PK5Re, Doccol Corporation). Anesthesia was induced with 5% isoflurane and then maintained with 0.5 to 1.5% isoflurane in medical pure oxygen administered through a facemask. To assure consistent and continuous reduction of cerebral blood flow (CBF), a Laser Doppler (Moor Instruments: MOORVMS-LDF) probe adapter was affixed to the surface of the skull over the brain area supplied by the MCA using dental cement. The probe remained in place throughout the MCAO surgery and CBF was measured continuously to confirm occlusion and later establishment of reperfusion. Animals were kept under anesthesia and body temperature was monitored throughout the whole procedure and maintained at >36.5°C using a feedback-controlled heating pad. Following 60 min of MCAO, the filament was withdrawn to allow reperfusion. Blood flow measurements were continued for another 15 min before removing the adapter and the laser Doppler probe. Animals received subcutaneous Buprenex at 0.02 mg/kg every 12 h to limit post-surgical pain for 24 hours after surgery. The survival rate was 93%. Animals where CBF was not reduced by at least 70% and which did not display any obvious neurological deficit with a neuroscore of 1-2 out of 14 at 12 h after reperfusion were excluded. In this study, out of the animals surviving to day-8 (45 out of 48), two animals were excluded because they lacked an obvious neurological deficit score at 12 hours. Animals that met inclusion criteria were assigned to the 3 groups (low and high dose senicapoc or vehicle) based on a computer-generated randomization scheme. Six sham animals, where the filament was placed into the external carotid artery but not advanced, were used as controls for the qPCR experiments.

Drug Treatment

Starting at 12 h after tMCAO, and following the first neurological scoring, animals received either the vehicle, Miglyol 812 neutral oil (Medium chain triglycerides, Spectrum Chemicals), a low dose of senicapoc at 10 mg/kg, or a high dose of senicapoc at 40 mg/kg via intraperitoneal (IP) injection. Mice then received the same dosage of senicapoc (or vehicle) IP every 12 hours for a total of 14 doses. In the experiment in Fig. 7 drug administration was started 3 h after reperfusion. Senicapoc was synthesized in our laboratory as described (Jin et al., 2019; McNaughton-Smith et al., 2008). Chemical identity and purity (>98%) were tested by ^{1}H and ^{13}C-NMR and HPLC.

Determination of Plasma and Brain Concentrations

In order to determine whether senicapoc sufficiently engages its target, additional mice were subjected to 60 min of MCAO, treated with 40 mg/kg senicapoc IP 12 h after reperfusion and then sacrificed 1 h, 4 h and 12 h later. Mice were deeply anesthetized with isoflurane, blood was collected from the vena cava into EDTA tubes, and then transcardially perfused with 30 mL of saline. The brain was removed, and the forebrain divided into ipsi- and contralateral side. Brain and plasma samples were stored at -80°C pending analysis and then prepared and analyzed as previously described (Jin et al., 2019) using a Waters Acquity UPLC (Waters, NY) equipped with a Acquity UPLC BEH 1.7 µm C-18 column interfaced to a TSQ Quantum Access Max mass spectrometer (Thermo Fisher Scientific, MA). Senicapoc was analyzed by the selective reaction monitoring (SRM) transition of its molecular ion peak 324.09 (M+1) into 228.07, 200.07,183.11 and 122.18 m/z. An 8-point calibration curve ranging from 50 nM to 10 µM was used for quantification. Senicapoc plasma protein binding was determined with mouse plasma or mouse

brain extract in triplicate using rapid equilibrium devices with a molecular weight cut-off of 8 kD (RED, Fisher Scientific).

Neurological Scoring

Since filament MCAO induces infarction in both the striatum and the cortex we used the 14-point score tactile and proprioceptive limp-placing test to evaluate mice every 24 h. MCAO severely affects sensorimotor coordination in this test, in which a normal mouse scores 14, while mice subjected to MCAO typically exhibit scores of 0 or 1 when tested 12 h after surgery. The scoring was performed as previously described in detail (Chen et al., 2021; Chen et al., 2016). The investigator performing the scoring was blinded to the treatment groups.

Assessment of Infarct Area by MRI

Infarct volume was evaluated with T2-weighted MRI imaging in the Nuclear Magnetic Resonance (NMR) Facility at UC Davis. MRI was performed with a 7T (300 MHz) Bruker Biospec MR system running ParaVision version 5. The RF coil was Bruker's standard 35 mm ID mouse whole body resonator. Animals were anesthetized with isoflurane and placed under a heated circulating water blanket (37°C) to maintain body temperature. Fast spin echo (FSE) imaging, also known as RARE (Rapid Acquisition with Relaxation Enhancement), sequence was used to acquire tri-pilot geometry reference images. The multi-slice multi-echo (MSME) sequence (TE:56 ms; TR: 1681.2 ms) was used to acquire images of 7 coronal sections with 1 mm thickness from the junction of olfactory bulb and cortex. The infarct area was analyzed with Adobe Photoshop Elements by an investigator blinded to the treatments. On day-3 infarct area was corrected for edema and calculated with the equation: $(L - N)/L \times 100\%$; L: left (contralateral) hemisphere area;

N: non-infarcted tissue area in the ipsilateral hemisphere. By day-8 post tMCAO there typically is either only minimal or no associated cerebral edema (Chen et al., 2021; Chen et al., 2018), so no correction for edema (Swanson et al., 1990) is required and the percentage of infarcted area was calculated with the equation: (Infarct Area/Ipsilateral Hemisphere Area) × 100%.

Immunohistochemistry

After the MRI on day-8, animals were euthanized with an overdose of isoflurane, brains were quickly removed and sectioned into four 2-mm thick coronal slices starting from the frontal pole. Slices were fixed in 10% buffered formalin for 24 h and then stored in 70% ethanol before being embedded in paraffin and sectioned at 5 μm by the Histology Laboratory of the UC Davis School of Veterinary Medicine. Following rehydration and antigen retrieval (heating in 10 mM Na citrate for 15 min in a microwave) the 4-mm and the 6-mm sections were stained with antibodies for Iba-1 (Wako, 1:1000, polyclonal rabbit, Catalog # 019-19741) and for CD3 (Dako, 1:1000, polyclonal rabbit, Catalog # A045201-2) and NeuN (EMD Millipore, 1:800, polyclonal rabbit, Catalog # ABN78). The same secondary antibody was used for all stains (Alexa Fluor 647 Donkey anti-Rabbit IgG (H+L), 1:1000, Life Technologies, Catalog # A-31573). Cell nuclei were visualized with 4′,6-diamidino-2-phenylindole (DAPI).

The 4-mm and 6-mm sections of each animal were photographed on a Keyence BZ-X710 fluorescence microscope in the “stitching mode” with the 20x lens (545/25 nm excitation wavelength, 605/70 nm emission wavelength, 565 nm dichroic mirror wavelength). The images were then opened on the BZ-X Analyzer, the left (infarcted) hemisphere for each section extracted and analyzed with a macro within the “Hybrid Cell Count” feature of the BZ-X Analyzer program. Images were thresholded to exclusively the area of stained cells without considering artifacts, ventricles, or folds. Each macro-generated image was verified by careful visual inspection.

Results for Iba1 and CD3 are reported as percentage of section area (μm^2) that was positively stained, divided by total section area (μm^2) in the infarcted left hemisphere. NeuN is reported as the inverse of the percentage of section area (μm^2) that was positively stained, divided by total section area (μm^2) in the infarcted left hemisphere in order to quantify the Neu negative area.

RT-qPCR

After MRIs were completed, mice were euthanized with an overdose of isoflurane, brains harvested, split into ipsilateral and contralateral hemispheres, and immediately frozen with liquid N_2. Brain hemispheres were homogenized in mortar and pestles with liquid N_2. RNA was extracted from brain homogenates (Fig. 7b) or MMC cell pellets (Fig. 2) with Trizol (ThermoFisher, Catalog # 15596026) according to the manufacturer's protocol. RNA purity and concentration were assessed using a Nanodrop Spectrophotometer ND-1000 (Marshall Scientific). The 260 nm/280 nm absorption ratios for the samples ranged from 1.95 to 2.00. Subsequently, a cDNA library was made with a High-Capacity cDNA Reverse Transcription Kit (ThermoFisher Scientific, Catalog# 4374967), with 2 µg of total RNA per 20 µL reaction. Reactions were carried out in a PTC-200 Peltier Thermal Cycler; the conditions were as follows: 25°C for 10 min, 37°C for 120 min, 85°C for 5 min, with final storage at 4°C. RT-qPCR reactions were conducted in an Applied Biosystems Viia7 Real-Time PCR System using Maxima SYBR Green/ROX qPCR Master Mix (ThermoFisher Scientific, Catalog #K022) and with the recommended three-step cycling protocol. All CT values were normalized to the geometric mean of three housekeeping genes, β-actin, GAPDH, and 18S, as recommended by Vandesompele et al. (Vandesompele et al., 2002). Fold change was calculated by the ΔΔCt method. Primer sequences are provided in Supplementary Table 1. For brain samples relative mRNA levels were generated by normalizing to sham.

tPA Assay

The commercially available Tissue plasminogen activator (tPA) Activity Assay Kit (Abcam, ab108905) was used to assess whether senicapoc and TRAM-34 affect the ability of human tPA to cleave its substrate plasminogen similar to protocols published by Lapchak and Boitano (Lapchak & Boitano, 2014) and Lapchak et al. (Lapchak, Lara, & Boitano, 2017). Reactions were run in optically clear flat-bottom 96-well plates (Corning, Catalog #3904). Human plasminogen activator inhibitor-1 (PAI-1; Sigma-Aldrich CC4075) was used as a positive control. Human plasminogen, the chromogenic plasmin substrate, and human tPA were included in the tPA Activity Assay Kit. PBS with 10% human serum was used as assay medium; senicapoc or TRAM-34 were added at 500 nM and 5 μM with a final DMSO concentration of 0.1%. The reactions were pre-incubated at 37°C for 5 min prior to the addition of the chromogenic plasmin substrate and subsequently placed in a heated SpectraMax M5 spectrophotometer. Absorbances at 405 nm were measured every 30 seconds for 30 min.

Statistics

Using our previous work with the $K_{Ca}3.1$ blocker TRAM-34 in MCAO (Chen et al., 2016; Chen et al., 2011), where 11 animals per group allowed us to detect a ~50% reduction in infarct area, to provide conservative mean and standard deviation parameter estimates, sample size was powered to detect a reduction of 40% in mean percentage infarct area with 80% power.

Statistical analysis of infarct percentage comparing two groups was performed using unpaired t-test. Statistical analysis of three groups (e.g. vehicle vs senicapoc 10 mg/kg vs senicapoc 40 mg/kg) was performed with analysis of variance (ANOVA) with a post-hoc pair-wise comparison using Tukey's test (Origin software), as previously described (Chen et al., 2021; Chen

et al., 2016; Chen et al., 2018). All data are shown as box-and-whisker plots with an overlay of the individual animal data. The boxes show mean ± S.E.M, the whiskers show confidence intervals. The categorical neurological scoring data in Fig. 3b is shown as a scatter plot without means or S.E.M and was analyzed with the Mann-Whitney U test as per recommendations for optimal presentation and analysis of non-parametric data in pre-clinical stroke studies by Dirnagl (Dirnagl, 2016). For the IHC data in Figure 5 comparing two groups, unpaired t-tests were performed. The brain qPCR data in Figure 7 was analyzed in Prism using one-way ANOVA followed by Dunnett's test to correct for multiple comparisons. For all statistical testing, $p < 0.05$ was used as the level of significance. $* = p < 0.05$, $** = p < 0.01$, $*** = p < 0.001$.

Results

Senicapoc blocks microglial $K_{Ca}3.1$ currents and inhibits calcium signaling

Using a mouse microglial cell line as a model system, we confirmed that senicapoc inhibits microglial $K_{Ca}3.1$ currents as effectively as recombinantly expressed $K_{Ca}3.1$ currents (Stocker et al., 2003). Following dialysis of microglial cells with 1 µM of free Ca^{2+}, $K_{Ca}3.1$ currents were elicited by ramp pulses from -120 mV to +40 mV (Fig. 1a). Currents were blocked by senicapoc with an IC_{50} of 6.97 ± 3.17 nM (n = 4; mean ± 95% confidence interval) (Fig. 1b). In keeping with the channel's role in regulating calcium signaling, senicapoc also concentration-dependently reduced Ca^{2+} influx induced by perfusion of 100 µM of the purinergic receptor agonist ATP (Fig. 1c and 1d) suggesting that $K_{Ca}3.1$ counterbalances membrane depolarization induced by P2X4 receptor activation (Nguyen et al., 2020; Visentin, Renzi, Frank, Greco, & Levi, 1999) and thus sustains microglial calcium influx.

Senicapoc inhibits inflammatory cytokine and marker expression in microglia

MMC cells are an immortalized mouse microglial cell line which reacts to stimulation with amyloid-β, α-synuclein or the gram-negative cell wall component lipopolysaccharide (LPS) with a strong increase in the expression of inflammatory cytokines and other pro-inflammatory markers (Ramesha et al., 2021; Sarkar et al., 2020). Using RT-qPCR, we found that treatment with senicapoc concentration-dependently reduced expression of *IL-1β*, *TNF-α*, *IL-6* and *IL-10* induced by 24 hours of stimulation with 100 ng/mL LPS. Senicapoc also significantly reduced mRNA levels of the pro-inflammatory enzymes *iNOS* and *COX-2* and prevented induction of the inflammasome component *NLRP3*. Fig. 2 shows one representative experiment of three experiments performed. Interestingly, despite responding to ATP with a strong, immediate

calcium signal (Fig. 1c), MMCs did not respond with any significant increases in cytokine or inflammatory marker expression when exposed to 1 mM ATP for 24 hours (data not shown).

Senicapoc reduces infarction area and improves neurological deficits following transient MCAO in mice

Taken together, the results shown in Fig. 1 and Fig. 2 demonstrate that senicapoc reduces microglia activation *in vitro* similar to the more widely used $K_{Ca}3.1$ blocking tool compound TRAM-34. We next tested whether senicapoc would be as effective as TRAM-34 in reducing infarction in reperfusion MCAO (Chen et al., 2016; Chen et al., 2011) since demonstration of *in vivo* efficacy would be a prerequisite for repurposing senicapoc for stroke treatment. We previously found that senicapoc readily penetrates into the brain and achieves total brain concentrations in mice and rats that are 2- to 5-fold higher than plasma concentrations (Jin et al., 2019), while another group reported that following a dose of 10 mg/kg, senicapoc reached free concentrations in the brain and CSF of rats that were 3 or 12 times higher than the IC_{50} for $K_{Ca}3.1$ inhibition (Staal et al., 2017). However, in contrast to its long, 12-day half-life in humans, senicapoc metabolism in mice is much faster and the compound has a 1-hour half-life (Jin et al., 2019). We therefore chose to use senicapoc at the same doses at which we had previously tested TRAM-34 in mouse MCAO: a low dose of 10 mg/kg and a high dose of 40 mg/kg. Focal ischemic stroke was induced in 16-week-old, male C57BL/6J mice by 60-min occlusion of the left MCA and senicapoc administration was started following the first neurological deficit scoring at 12 h after reperfusion and then continued twice daily until evaluation of infarct area using T2-weighted MRI on day-8. This treatment paradigm was intended to simulate a long but clinically realistic delay to start of adjunctive therapy after EVT. Senicapoc treatment reduced the T2-weighted lesion area (Fig. 3a) from 20.5 ± 1.3% in vehicle treated mice (n = 10) to 11.6 ± 1.1% in the low dose group (n = 7, P

< 0.001) and 9.3 ± 1.3% in the high dose group (n = 7, P < 0.001). Mice treated with senicapoc also showed improvements in sensorimotor coordination (Fig. 3b) when assessed by the 14-point DeRyck tactile and proprioceptive limb placing test (De Ryck, Van Reempts, Borgers, Wauquier, & Janssen, 1989). All mice exhibited scores of close to 0 at 12 hours after the surgery (Fig. 3b). However, while vehicle treated mice only slowly improved and did not recover beyond an average score of 3 by day-8, senicapoc treated mice recovered more quickly and reached average scores of 7 in the 10 mg/kg and scores of 9 in the 40 mg/kg group by day-8. Supplementary Figure 1 shows the neurological deficits scoring as a stacked graph, which visualizes that vehicle treated animals only recover to a maximum score of 5 while senicapoc treated animals recover to maximum scores of 9 or 10 in the low or high dose group, respectively.

Senicapoc provides sufficient $K_{Ca}3.1$ target coverage in the brain

It is often hypothesized that blood brain barrier damage or breakdown in the wake of ischemic stroke could change drug uptake into the brain. In order to investigate if senicapoc's brain penetration is altered during stroke, we induced MCAO in a separate group of mice, administered senicapoc at 40 mg/kg 12 hours after reperfusion and then sacrificed animals 1, 4 and 12 hours later and collected ipsi- and contralateral forebrain samples following thorough cardiac perfusion with saline to remove all blood from the brain vasculature. Ultra-high-performance liquid chromatography (UPLC)/mass spectrometry (MS) analysis of plasma and brain samples showed that total senicapoc concentrations exceeded 10 μM for 12 hours and did not significantly vary between the infarcted and the non-infarcted hemisphere (Fig. 4 *left*). However, since only free drug is theoretically able to engage its target and exert a pharmacodynamic effect, we determined senicapoc's binding to plasma protein (96.8 ± 0.5%) and brain tissue extract (98.1 ± 0.5%) using equilibrium dialysis and converted total into free drug

concentrations (Fig. 4 *right*). Free senicapoc brain concentrations were above IC_{90} for $K_{Ca}3.1$ channel inhibition for at least 4 hours and remained above IC_{50} for 12 h after administration.

Senicapoc reduces microglia/macrophage activation and T-cell infiltration

In order to determine whether the reduction in infarction and improvements in neurological deficit we had observed with senicapoc treatment were accompanied by a reduction in immune cell activation and/or infiltration we quantified staining for microglia/macrophages and T cells in the infarcted hemisphere. When comparing Iba1 and CD3 staining intensity between vehicle and senicapoc treated animals in paraffin sections cut at 4 and 6 mm from the frontal pole using an unbiased, automated, pixel-based approach, we found that senicapoc at 40 mg/kg significantly reduced both microglia/macrophage activation and infiltration (Fig. 5a) and T cell infiltration (Fig. 5b). To confirm the MRI results at the microscopic level, we further stained the 4-mm and 6-mm sections from vehicle and senicapoc treated animals for NeuN, a protein found in the nuclei of mature neurons, and quantified the NeuN-negative area (Fig. 6) confirming that senicapoc treatment decreases neuronal death.

Earlier senicapoc administration is not more effective than delayed administration

Since many studies have described early pro-inflammatory changes following ischemic stroke, we next asked whether an earlier temporal administration paradigm for senicapoc, starting at 3 hours following tMCAO, would provide additional benefit. This is a clinically relevant time window as it matches the most common time frame for administration of IV tPA. To investigate whether senicapoc affects primary infarct growth or secondary infarct expansion and deterioration, we performed MRI on day-3 and day-8 in this experiment. Interestingly, compared

to vehicle (21.4 ± 2.3%, n = 8) senicapoc did not significantly reduce T2-weighetd lesion area (16.1 ± 3.1%, n = 8, P = 0.199) on day-3 (Fig. 7a), but reduced infarction on day-8 (vehicle 16.6 ± 1.0%; senicapoc 11.7 ± 1.8%, n = 8, P = 0.0318). Sensorimotor coordination in contrast was improved on both day-3 and day-8 by the earlier treatment paradigm (Fig. 7a). Taken together, these findings suggest that senicapoc does not prevent primary infarct growth but reduces secondary, immune mediated infarct expansion and reperfusion damage as indicated by the more pronounced effect on neurological deficit on day-3 than on infarction. Administration started at 3 hours was not more effective than administration started at 12 hours after tMCAO.

Following MRI on day-8, we removed brains from all animals in this experiment and analyzed 13 markers in the contralateral and ipsilateral hemisphere of senicapoc and vehicle treated animals by RT-qPCR. Normalization of relative mRNA levels to sham brains revealed that MCAO increased expression of many inflammatory markers such as *IL-1β, TNF-α*, *IL-6*, *IFN-γ iNOS* and *NLRP3* in both hemispheres on day-8, while expression of the phagocyte marker CD68 only increased in the infarcted hemisphere (Fig. 7b). Senicapoc treatment significantly reduced expression of *IL-1β, TNF-α*, *IL-6*, *CD68*, *NLRP3, IL-2*, *IFN-γ*, *IL-4*, and *IL-10* in the infarcted hemisphere compared to vehicle treated animals (Fig. 7b, for full statistics see Table S2). Since several of these cytokines are produced by T cells, reductions in their expression levels are in line with the inhibition of T cell infiltration observed following senicapoc treatment (Fig. 5b).

K_{Ca}3.1 blockers do not interfere with tPA in-vitro

With drug administration started at 12 hours post-MCAO, it is unlikely that senicapoc would affect the thrombolytic function of tPA because the two agents have disparate temporal administration paradigms that, combined with tPA's short half-life (Gravanis & Tsirka, 2008), should limit simultaneous exposure. However, in clinical use, senicapoc might not only be used

in combination with EVT but also together with, or shortly after thrombolysis with infused t-PA and we therefore carried out an *in-vitro* chromogenic assay to assess whether senicapoc affects the proteolytic function of tPA (Fig. 8). While the positive control, plasminogen activator inhibitor-1 (PAI-1) strongly inhibited tPA, senicapoc at concentrations of 0.5 μM and 5 μM had no effect on tPA activity *in-vitro* during the 30 min assay demonstrating that senicapoc has no effect on the proteolytic activity of tPA and therefore, would be unlikely to affect its fibrinolytic activity. Similar results were obtained with TRAM-34 (Supplementary Fig. 2) confirming that triarylmethane-type $K_{Ca}3.1$ blockers do not inhibit tPA in contrast to some cytoprotective chromones (Lapchak et al., 2017).

Discussion

Since its approval in 1995 (National Institute of Neurological & Stroke rt, 1995) until 2015, when endovascular thrombectomy (EVT) with stent-retriever devices in combination with advanced imaging was established as a new standard of care for selected patients with salvageable tissue (Goyal et al., 2016), intravenous t-PA employed as a thrombolytic has been the only FDA-approved pharmacological treatment for acute ischemic stroke. While EVT improves clinical outcomes (Goyal et al., 2016), many patients still experience substantial long-term neurological deficits (Zhou et al., 2023), and there is an urgent need to identify and develop adjunctive pharmacological approaches. Potential cerebroprotection could be achieved either by therapeutics that somehow “freeze” the penumbra (Baron, 2018) before EVT or that reduce the rate of infarct core expansion (Savitz et al., 2019; Savitz, Baron, Yenari, Sanossian, & Fisher, 2017). In the context of mechanical revascularization, reperfusion can help pharmacological agents penetrate into the ischemic core but also contributes to the inflammatory response in the wake of ischemic stroke by causing reperfusion injury (Savitz et al., 2017; Zhou et al., 2023). It therefore should be beneficial to administer immuno-modulators in combination with/or after EVT to enhance neurological recovery after ischemic stroke. In contrast to “classic” neuroprotectants like drugs targeting glutamate mediated excitotoxicity and which are only effective if administered rapidly, pharmacological interventions targeting neuroinflammation could potentially have a wider therapeutic time window (Iadecola & Anrather, 2011; Iadecola, Buckwalter, & Anrather, 2020). Attempts to target the immune response in ischemic stroke have included the IL-1 receptor antagonist anakinra, the leukocyte trafficking inhibitor fingolimod, antibodies against leukocyte adhesion molecules expressed on endothelial cells (enlimomab and natalizumab), or antioxidants such as Ebselen. So far none of these approaches have translated successfully from rodents to humans (Zera & Buckwalter, 2020). While there might be many reasons for this translational gap including the lack of reperfusion in the clinical trials evaluating these agents (Bosetti et al., 2017),

or inappropriate treatment timing (Zera & Buckwalter, 2020), many neuroimmune targets have not yet been fully explored. Given that approximately 70% of strokes are caused by occlusion of a major cerebral artery, typically the middle cerebral artery (Collaborators et al., 2018), suture induced tMCAO in rodents is a clinically relevant animal model because it simulates both the ischemia from a LVO and the rapid cerebral blood flow restoration occurring with mechanical thrombectomy (Sutherland et al., 2016). Thus, our study here, employing tMCAO in mice, is well suited to assess the efficacy of adjunctive immunomodulators like senicapoc within the context of the new clinical reality that patients with LVO and subsequent EVT face.

Microglia and macrophages are particularly attractive targets for immunomodulation. In rodent models of ischemic stroke, microglia initially increase their aborization and exploratory behavior, but then undergo deaborization and ameboid transformation within hours (Iadecola et al., 2020). Later, monocyte derived macrophages start infiltrating the brain and hypertrophic, CD68-positive microglia/macrophages become abundant in the infarcted area and the penumbra between 18 to 96 hours, peak between 7 to 14 days and are still present months after an insult (Buscemi, Price, Bezzi, & Hirt, 2019; Campanella, Sciorati, Tarozzo, & Beltramo, 2002; Hu et al., 2012). PET imaging and immunohistochemistry in postmortem brain has demonstrated a similar time course of microglia activation in humans (Beschorner, Schluesener, Gozalan, Meyermann, & Schwab, 2002; Price et al., 2006). Although microglia/macrophages can perform beneficial functions such as phagocytosing neuronal and myelin debris, they also produce pro-inflammatory cytokines/chemokines, reactive oxygen species, inflammatory lipid mediators and nitric oxide and presumably contribute to neuronal and axonal injury and expansion of the infarct border (Hu et al., 2012; Iadecola & Anrather, 2011). One approach to pharmacologically target detrimental microglia/macrophage functions is by inhibiting microglial calcium signaling processes which are regulated by several potassium channels including the calcium-activated potassium channel $K_{Ca}3.1$ (Nguyen, Grossinger, et al., 2017). By inducing membrane hyperpolarization, $K_{Ca}3.1$

enhances microglial calcium signaling, facilitates oxidative burst and microglia mediated neuronal killing (Chen et al., 2016; Kaushal, Koeberle, Wang, & Schlichter, 2007). The channel further plays an important role in microglia migration, proliferation and inflammatory cytokine production and secretion (D'Alessandro et al., 2013; Maezawa et al., 2016; Nguyen, Grossinger, et al., 2017). $K_{Ca}3.1$ inhibitors accordingly reduce neuroinflammation and ameliorate pathology in rodent models of Alzheimer's disease (Jin et al., 2019), traumatic brain injury (Mauler et al., 2004), and multiple sclerosis (Reich et al., 2005). In two previous studies our own group found that $K_{Ca}3.1$ inhibition with TRAM-34 reduces infarction and improves neurological deficit following tMCAO in both mice and rats (Chen et al., 2016; Chen et al., 2011). Based on these observations we postulated that senicapoc, which is structurally very similar to TRAM-34 and blocks $K_{Ca}3.1$ by binding to the same site in the inner pore of the channel (Nguyen, Singh, et al., 2017), could be repurposed for the treatment of ischemic stroke. In the current study, we show that senicapoc suppresses functions associated with *in-vitro* microglia activation such as calcium signaling and cytokine production as effectively as TRAM-34. Senicapoc also has similar effects *in vivo* and reduces infarction and improves sensorimotor deficits in mice subjected to tMCAO. Senicapoc provides this robust protection even when first administered 12 hours following MCAO. This extended time frame for protective efficacy is uncommon and would correspond to a more favorable time frame for successful clinical translation to human patients with acute stroke secondary to LVO that undergo EVT. We also demonstrate that, mechanistically, $K_{Ca}3.1$ inhibition targets both microglia/macrophages and infiltrating T cells. This is evidenced by the decreased $Iba1^+$ and $CD3^+$ staining seen in senicapoc-treated animals when compared to vehicle-treated animals and by the suppression of the expression of inflammatory markers produced by both microglia/macrophages and T cells. While it of course has long been known that $K_{Ca}3.1$ is expressed in T cells and that $K_{Ca}3.1$ blockers can inhibit T cell functions (Feske et al., 2015; Ghanshani et al., 2000), it had not previously been demonstrated that $K_{Ca}3.1$ inhibitors reduce T cell infiltration in the setting of ischemic stroke. These are interesting findings because they

suggest that $K_{Ca}3.1$ inhibitors could indeed be useful immunocytoprotectants for combination with EVT since they fulfill the postulated requirement of being “pleiotropic” in the sense of targeting multiple effector cells in the ischemic cascade (Savitz et al., 2019). An increasing T cell contribution to stroke pathophysiology has been proposed to be part of what is termed “inflammaging” (Carrasco et al., 2021) and might, in concert with other adaptive immune cells like B cells, be a significant driver of the post-stroke dementia and cognitive decline (Zera & Buckwalter, 2020).

In sum, we would like to propose that senicapoc could be repurposed as an adjunctive immunocytoprotectant for ischemic stroke. Senicapoc was well tolerated and safe in a large group of diverse patients, which can be seen in its previous failed sickle cell disease trials. Based on its safety and efficacy as a $K_{Ca}3.1$ blocker, senicapoc has also been proposed for the treatment of neuropathic pain (Staal et al., 2017), and is currently being trialed in a Phase-2 study for mild and prodromal Alzheimer’s disease with the goal of demonstrating biological activity and target engagement in humans with early AD (NCT04804241). Another explanatory, proof-of-concept study is evaluating Senicapoc in patients with familial dehydrated stomatocytosis caused by gain-of-function mutations in $K_{Ca}3.1$ (NCT04372498). This study has a number of strengths including incorporation of both infarct volume and neurobehavioral outcomes, inclusion of two senicapoc doses and two temporal administration paradigms, inclusion of true vehicle controls, confirmation of MCA occlusion and reperfusion by laser doppler, and confirmation of target engagement by brain drug concentration analysis by LC/MS. Limitations of this study include use of only young adult male mice and a single time point for the brain cytokine panel. Future studies should explore the efficacy of senicapoc in females, aged animals, and animals with comorbidities such as diabetes and hypertension.

Disclosures

Funding Information: This work was supported by the National Institute of Neurological Disease and Stroke (NS100294 to H.W. and R61NS123195 to J.W.).

Conflicts of interest/Competing interests: J.W. is listed as an inventor on US patent No. PCT/US18/16014, $K_{Ca}3.1$ inhibitor Senicapoc for use in Treatment of Stroke Patients. Filed 1/30/2018

Availability of data and material: Data are available from the corresponding author upon reasonable request. Senicapoc is available from several commercial vendors or from the corresponding author.

Authors contributions: Y-JC performed surgeries, and RL and Y-JC performed neurological scoring and MRI. HN performed electrophysioloy and calcium imaging. LS synthesized senicapoc and performed LC/MS. YC and BP performed IHC. RL performed qPCR and tPA assays. RL, CJD and Y-JC analyzed data and prepared figures. HW and JRW designed the study and obtained funding. All authors contributed to writing the manuscript.

Ethics approval: This study was approved by the University of California, Davis Institutional Animal Care and Use Committee and conduced in accordance with the IMPROVE guidelines for ischemic stroke in rodents.

References

Ataga, K. I., Orringer, E. P., Styles, L., Vichinsky, E. P., Swerdlow, P., Davis, G. A., Desimone, P. A., & Stocker, J. W. (2006). Dose-escalation study of ICA-17043 in patients with sickle cell disease. *Pharmacotherapy, 26*(11), 1557-1564. doi:10.1592/phco.26.11.1557

Ataga, K. I., Reid, M., Ballas, S. K., Yasin, Z., Bigelow, C., James, L. S., Smith, W. R., Galacteros, F., Kutlar, A., Hull, J. H., & Stocker, J. W. (2011). Improvements in haemolysis and indicators of erythrocyte survival do not correlate with acute vaso-occlusive crises in patients with sickle cell disease: a phase III randomized, placebo-controlled, double-blind study of the Gardos channel blocker senicapoc (ICA-17043). *Br J Haematol, 153*(1), 92-104. doi:10.1111/j.1365-2141.2010.08520.x

Ataga, K. I., Smith, W. R., De Castro, L. M., Swerdlow, P., Saunthararajah, Y., Castro, O., Vichinsky, E., Kutlar, A., Orringer, E. P., Rigdon, G. C., & Stocker, J. W. (2008). Efficacy and safety of the Gardos channel blocker, senicapoc (ICA-17043), in patients with sickle cell anemia. *Blood, 111*(8), 3991-3997. doi:blood-2007-08-110098 [pii] 10.1182/blood-2007-08-110098

Ataga, K. I., Staffa, S. J., Brugnara, C., & Stocker, J. W. (2021). Haemoglobin response to senicapoc in patients with sickle cell disease: a re-analysis of the Phase III trial. *Br J Haematol, 192*(5), e129-e132. doi:10.1111/bjh.17345

Ataga, K. I., & Stocker, J. (2009). Senicapoc (ICA-17043): a potential therapy for the prevention and treatment of hemolysis-associated complications in sickle cell anemia. *Expert Opin Investig Drugs, 18*(2), 231-239. doi:10.1517/13543780802708011

Baron, J. C. (2018). Protecting the ischaemic penumbra as an adjunct to thrombectomy for acute stroke. *Nat Rev Neurol, 14*(6), 325-337. doi:10.1038/s41582-018-0002-2

Beschorner, R., Schluesener, H. J., Gozalan, F., Meyermann, R., & Schwab, J. M. (2002). Infiltrating CD14+ monocytes and expression of CD14 by activated parenchymal microglia/macrophages contribute to the pool of CD14+ cells in ischemic brain lesions. *J Neuroimmunol, 126*(1-2), 107-115.

Blomster, L. V., Strobaek, D., Hougaard, C., Klein, J., Pinborg, L. H., Mikkelsen, J. D., & Christophersen, P. (2016). Quantification of the functional expression of the Ca(2+) -activated K(+) channel KCa 3.1 on microglia from adult human neocortical tissue. *Glia, 64*(12), 2065-2078. doi:10.1002/glia.23040

Bosetti, F., Koenig, J. I., Ayata, C., Back, S. A., Becker, K., Broderick, J. P., Carmichael, S. T., Cho, S., Cipolla, M. J., Corbett, D., Corriveau, R. A., Cramer, S. C., Ferguson, A. R., Finklestein, S. P., Ford, B. D., Furie, K. L., Hemmen, T. M., Iadecola, C., Jakeman, L. B., Janis, S., Jauch, E. C., Johnston, K. C., Kochanek, P. M., Kohn, H., Lo, E. H., Lyden, P. D., Mallard, C., McCullough, L. D., McGavern, L. M., Meschia, J. F., Moy, C. S., Perez-Pinzon, M. A., Ramadan, I., Savitz, S. I., Schwamm, L. H., Steinberg, G. K., Stenzel-Poore, M. P., Tymianski, M., Warach, S., Wechsler, L. R., Zhang, J. H., & Koroshetz, W. (2017). Translational Stroke Research: Vision and Opportunities. *Stroke, 48*(9), 2632-2637. doi:10.1161/STROKEAHA.117.017112

Brown, B. M., Shim, H., Christophersen, P., & Wulff, H. (2020). Pharmacology of Small- and Intermediate-Conductance Calcium-Activated Potassium Channels. *Annu Rev Pharmacol Toxicol, 60*, 219-240. doi:10.1146/annurev-pharmtox-010919-023420

Buscemi, L., Price, M., Bezzi, P., & Hirt, L. (2019). Spatio-temporal overview of neuroinflammation in an experimental mouse stroke model. *Sci Rep, 9*(1), 507. doi:10.1038/s41598-018-36598-4

Campanella, M., Sciorati, C., Tarozzo, G., & Beltramo, M. (2002). Flow cytometric analysis of inflammatory cells in ischemic rat brain. *Stroke, 33*(2), 586-592.

Carrasco, E., Gomez de Las Heras, M. M., Gabande-Rodriguez, E., Desdin-Mico, G., Aranda, J. F., & Mittelbrunn, M. (2021). The role of T cells in age-related diseases. *Nat Rev Immunol*. doi:10.1038/s41577-021-00557-4

Chen, Y. J., Cui, Y., Singh, L., & Wulff, H. (2021). The potassium channel Kv1.3 as a therapeutic target for immunocytoprotection after reperfusion. *Ann Clin Transl Neurol, 8*(10), 2070-2082. doi:10.1002/acn3.51456

Chen, Y. J., Nguyen, H. M., Maezawa, I., Grossinger, E. M., Garing, A. L., Kohler, R., Jin, L. W., & Wulff, H. (2016). The potassium channel KCa3.1 constitutes a pharmacological target for neuroinflammation associated with ischemia/reperfusion stroke. *J Cereb Blood Flow Metab, 36*(12), 2146-2161. doi:10.1177/0271678X15611434

Chen, Y. J., Nguyen, H. M., Maezawa, I., Jin, L. W., & Wulff, H. (2018). Inhibition of the potassium channel Kv1.3 reduces infarction and inflammation in ischemic stroke. *Ann Clin Transl Neurol, 5*(2), 147-161. doi:10.1002/acn3.513

Chen, Y. J., Raman, G., Bodendiek, S., O'Donnell, M. E., & Wulff, H. (2011). The KCa3.1 blocker TRAM-34 reduces infarction and neurological deficit in a rat model of ischemia/reperfusion stroke. *J Cereb Blood Flow Metab, 31*, 2363 - 2374. doi:jcbfm2011101 [pii] 10.1038/jcbfm.2011.101

Collaborators, G. B. D. L. R. o. S., Feigin, V. L., Nguyen, G., Cercy, K., Johnson, C. O., Alam, T., Parmar, P. G., Abajobir, A. A., Abate, K. H., Abd-Allah, F., Abejie, A. N., Abyu, G. Y., Ademi, Z., Agarwal, G., Ahmed, M. B., Akinyemi, R. O., Al-Raddadi, R., Aminde, L. N., Amlie-Lefond, C., Ansari, H., Asayesh, H., Asgedom, S. W., Atey, T. M., Ayele, H. T., Banach, M., Banerjee, A., Barac, A., Barker-Collo, S. L., Barnighausen, T., Barregard, L., Basu, S., Bedi, N., Behzadifar, M., Bejot, Y., Bennett, D. A., Bensenor, I. M., Berhe, D. F., Boneya, D. J., Brainin, M., Campos-Nonato, I. R., Caso, V., Castaneda-Orjuela, C. A., Rivas, J. C., Catala-Lopez, F., Christensen, H., Criqui, M. H., Damasceno, A., Dandona, L., Dandona, R., Davletov, K., de Courten, B., deVeber, G., Dokova, K., Edessa, D., Endres, M., Faraon, E. J. A., Farvid, M. S., Fischer, F., Foreman, K., Forouzanfar, M. H., Gall, S. L., Gebrehiwot, T. T., Geleijnse, J. M., Gillum, R. F., Giroud, M., Goulart, A. C., Gupta, R., Gupta, R., Hachinski, V., Hamadeh, R. R., Hankey, G. J., Hareri, H. A., Havmoeller, R., Hay, S. I., Hegazy, M. I., Hibstu, D. T., James, S. L., Jeemon, P., John, D., Jonas, J. B., Jozwiak, J., Kalani, R., Kandel, A., Kasaeian, A., Kengne, A. P., Khader, Y. S., Khan, A. R., Khang, Y. H., Khubchandani, J., Kim, D., Kim, Y. J., Kivimaki, M., Kokubo, Y., Kolte, D., Kopec, J. A., Kosen, S., Kravchenko, M., Krishnamurthi, R., Kumar, G. A., Lafranconi, A., Lavados, P. M., Legesse, Y., Li, Y., Liang, X., Lo, W. D., Lorkowski, S., Lotufo, P. A., Loy, C. T., Mackay, M. T., Abd El Razek, H. M., Mahdavi, M., Majeed,

A., Malekzadeh, R., Malta, D. C., Mamun, A. A., Mantovani, L. G., Martins, S. C. O., Mate, K. K., Mazidi, M., Mehata, S., Meier, T., Melaku, Y. A., Mendoza, W., Mensah, G. A., Meretoja, A., Mezgebe, H. B., Miazgowski, T., Miller, T. R., Ibrahim, N. M., Mohammed, S., Mokdad, A. H., Moosazadeh, M., Moran, A. E., Musa, K. I., Negoi, R. I., Nguyen, M., Nguyen, Q. L., Nguyen, T. H., Tran, T. T., Nguyen, T. T., Anggraini Ningrum, D. N., Norrving, B., Noubiap, J. J., O'Donnell, M. J., Olagunju, A. T., Onuma, O. K., Owolabi, M. O., Parsaeian, M., Patton, G. C., Piradov, M., Pletcher, M. A., Pourmalek, F., Prakash, V., Qorbani, M., Rahman, M., Rahman, M. A., Rai, R. K., Ranta, A., Rawaf, D., Rawaf, S., Renzaho, A. M., Robinson, S. R., Sahathevan, R., Sahebkar, A., Salomon, J. A., Santalucia, P., Santos, I. S., Sartorius, B., Schutte, A. E., Sepanlou, S. G., Shafieesabet, A., Shaikh, M. A., Shamsizadeh, M., Sheth, K. N., Sisay, M., Shin, M. J., Shiue, I., Silva, D. A. S., Sobngwi, E., Soljak, M., Sorensen, R. J. D., Sposato, L. A., Stranges, S., Suliankatchi, R. A., Tabares-Seisdedos, R., Tanne, D., Nguyen, C. T., Thakur, J. S., Thrift, A. G., Tirschwell, D. L., Topor-Madry, R., Tran, B. X., Nguyen, L. T., Truelsen, T., Tsilimparis, N., Tyrovolas, S., Ukwaja, K. N., Uthman, O. A., Varakin, Y., Vasankari, T., Venketasubramanian, N., Vlassov, V. V., Wang, W., Werdecker, A., Wolfe, C. D. A., Xu, G., Yano, Y., Yonemoto, N., Yu, C., Zaidi, Z., El Sayed Zaki, M., Zhou, M., Ziaeian, B., Zipkin, B., Vos, T., Naghavi, M., Murray, C. J. L., & Roth, G. A. (2018). Global, Regional, and Country-Specific Lifetime Risks of Stroke, 1990 and 2016. *N Engl J Med, 379*(25), 2429-2437. doi:10.1056/NEJMoa1804492

D'Alessandro, G., Catalano, M., Sciaccaluga, M., Chece, G., Cipriani, R., Rosito, M., Grimaldi, A., Lauro, C., Cantore, G., Santoro, A., Fioretti, B., Franciolini, F., Wulff, H., & Limatola, C. (2013). KCa3.1 channels are involved in the infiltrative behavior of glioblastoma in vivo. *Cell Death Dis, 4*, e773. doi:10.1038/cddis.2013.279

De Ryck, M., Van Reempts, J., Borgers, M., Wauquier, A., & Janssen, P. A. (1989). Photochemical stroke model: flunarizine prevents sensorimotor deficits after neocortical infarcts in rats. *Stroke, 20*(10), 1383-1390.

Dirnagl, U. (2016). Neuromethods 120; Springer Protocols. In U. Dirnagl (Ed.), *Rodent Models of Stroke* (pp. 301-316): Humana Press.

Feske, S., Wulff, H., & Skolnik, E. Y. (2015). Ion channels in innate and adaptive immunity. *Annu Rev Immunol, 33*, 291-353. doi:10.1146/annurev-immunol-032414-112212

Ghanshani, S., Wulff, H., Miller, M. J., Rohm, H., Neben, A., Gutman, G. A., Cahalan, M. D., & Chandy, K. G. (2000). Up-regulation of the IKCa1 potassium channel during T-cell activation: Molecular mechanism and functional consequences. *J Biol Chem, 275*, 37137-37149.

Goyal, M., Menon, B. K., van Zwam, W. H., Dippel, D. W., Mitchell, P. J., Demchuk, A. M., Davalos, A., Majoie, C. B., van der Lugt, A., de Miquel, M. A., Donnan, G. A., Roos, Y. B., Bonafe, A., Jahan, R., Diener, H. C., van den Berg, L. A., Levy, E. I., Berkhemer, O. A., Pereira, V. M., Rempel, J., Millan, M., Davis, S. M., Roy, D., Thornton, J., Roman, L. S., Ribo, M., Beumer, D., Stouch, B., Brown, S., Campbell, B. C., van Oostenbrugge, R. J., Saver, J. L., Hill, M. D., Jovin, T. G., & collaborators, H. (2016). Endovascular thrombectomy after large-vessel ischaemic stroke: a meta-analysis of individual patient data from five randomised trials. *Lancet, 387*(10029), 1723-1731. doi:10.1016/S0140-6736(16)00163-X

Gravanis, I., & Tsirka, S. E. (2008). Tissue-type plasminogen activator as a therapeutic target in stroke. *Expert Opin Ther Targets, 12*(2), 159-170. doi:10.1517/14728222.12.2.159

Hu, X., Li, P., Guo, Y., Wang, H., Leak, R. K., Chen, S., Gao, Y., & Chen, J. (2012). Microglia/macrophage polarization dynamics reveal novel mechanism of injury expansion after focal cerebral ischemia. *Stroke, 43*(11), 3063-3070. doi:10.1161/STROKEAHA.112.659656

Iadecola, C., & Anrather, J. (2011). The immunology of stroke: from mechanisms to translation. *Nat Med, 17*(7), 796-808. doi:10.1038/nm.2399

Iadecola, C., Buckwalter, M. S., & Anrather, J. (2020). Immune responses to stroke: mechanisms, modulation, and therapeutic potential. *J Clin Invest, 130*(6), 2777-2788. doi:10.1172/JCI135530

Jin, L. W., Di Lucente, J., Nguyen, H. M., Singh, V., Singh, L., Chavez, M., Bushong, T., Wulff, H., & Maezawa, I. (2019). Repurposing the KCa3.1 inhibitor senicapoc for Alzheimer's disease. *Ann Clin Transl Neurol*.

Kaushal, V., Koeberle, P. D., Wang, Y., & Schlichter, L. C. (2007). The Ca2+-activated K+ channel KCNN4/KCa3.1 contributes to microglia activation and nitric oxide-dependent neurodegeneration. *J Neurosci, 27*(1), 234-244.

Lapchak, P. A., & Boitano, P. D. (2014). Effect of the Pleiotropic Drug CNB-001 on Tissue Plasminogen Activator (tPA) Protease Activity in vitro: Support for Combination Therapy to Treat Acute Ischemic Stroke. *J Neurol Neurophysiol, 5*(4).

Lapchak, P. A., Lara, J. M., & Boitano, P. D. (2017). Cytoprotective Drug-Tissue Plasminogen Activator Protease Interaction Assays: Screening of Two Novel Cytoprotective Chromones. *Transl Stroke Res*. doi:10.1007/s12975-017-0533-7

Lin, J., Liang, Y., & Lin, J. (2020). Endovascular therapy versus intravenous thrombolysis in cervical artery dissection-related ischemic stroke: a meta-analysis. *J Neurol, 267*(6), 1585-1593. doi:10.1007/s00415-019-09474-y

Longa, E. Z., Weinstein, P. R., Carlson, S., & Cummins, R. (1989). Reversible middle cerebral artery occlusion without craniectomy in rats. *Stroke, 20*(1), 84-91.

Maezawa, I., Jenkins, D. P., Jin, B. E., & Wulff, H. (2012). Microglial KCa3.1 Channels as a Potential Therapeutic Target for Alzheimer's Disease. *Int J Alzheimers Dis, 2012*, 868972. doi:10.1155/2012/868972

Maezawa, I., Nguyen, H. M., DiLucente, J., Singh, V., Chavez, M., Wulff, H., & Jin, L. W. (2016). Microglial KCa3.1 channels as a potential therapeutic target for Alzheimer's disease. *2016 Neuroscience Meeting Planner. San Diego, CA: Society for Neuroscience, 2016. Online., 38.11/G30*.

Maezawa, I., Zimin, P., Wulff, H., & Jin, L. W. (2011). A-beta oligomer at low nanomolar concentrations activates microglia and induces microglial neurotoxicity. *J Biol Chem, 286*, 3693-3706. doi:M110.135244 [pii] 10.1074/jbc.M110.135244

Mauler, F., Hinz, V., Horvath, E., Schuhmacher, J., Hofmann, H. A., Wirtz, S., Hahn, M. G., & Urbahns, K. (2004). Selective intermediate-/small-conductance calcium-activated potassium channel (KCNN4) blockers are potent and effective therapeutics in experimental brain oedema and traumatic brain injury caused by acute subdural haematoma. *Eur J Neurosci, 20*(7), 1761-1768.

McNaughton-Smith, G. A., Burns, J. F., Stocker, J. W., Rigdon, G. C., Creech, C., Arrington, S., Shelton, T., & de Franceschi, L. (2008). Novel inhibitors of the Gardos channel for the treatment of sickle cell disease. *J Med Chem, 51*(4), 976-982. doi:10.1021/jm070663s

Mulder, M., Jansen, I. G. H., Goldhoorn, R. B., Venema, E., Chalos, V., Compagne, K. C. J., Roozenbeek, B., Lingsma, H. F., Schonewille, W. J., van den Wijngaard, I. R., Boiten, J., Albert Vos, J., Roos, Y., van Oostenbrugge, R. J., van Zwam, W. H., Majoie, C., van der Lugt, A., Dippel, D. W. J., & Investigators, M. C. R. (2018). Time to Endovascular Treatment and Outcome in Acute Ischemic Stroke: MR CLEAN Registry Results. *Circulation, 138*(3), 232-240. doi:10.1161/CIRCULATIONAHA.117.032600

National Institute of Neurological, D., & Stroke rt, P. A. S. S. G. (1995). Tissue plasminogen activator for acute ischemic stroke. *N Engl J Med, 333*(24), 1581-1587. doi:10.1056/NEJM199512143332401

Nguyen, H. M., Blomster, L. V., Christophersen, P., & Wulff, H. (2017). Potassium channel expression and function in microglia: Plasticity and possible species variations. *Channels (Austin), 11*(4), 305-315. doi:10.1080/19336950.2017.1300738

Nguyen, H. M., di Lucente, J., Chen, Y. J., Cui, Y., Ibrahim, R. H., Pennington, M. W., Jin, L. W., Maezawa, I., & Wulff, H. (2020). Biophysical basis for Kv1.3 regulation of membrane potential changes induced by P2X4-mediated calcium entry in microglia. *Glia, 68*, 2377-2394. doi:10.1002/glia.23847

Nguyen, H. M., Grossinger, E. M., Horiuchi, M., Davis, K. W., Jin, L. W., Maezawa, I., & Wulff, H. (2017). Differential Kv1.3, KCa3.1, and Kir2.1 expression in "classically" and "alternatively" activated microglia. *Glia, 65*(1), 106-121. doi:10.1002/glia.23078

Nguyen, H. M., Singh, V., Pressly, B., Jenkins, D. P., Wulff, H., & Yarov-Yarovoy, V. (2017). Structural Insights into the Atomistic Mechanisms of Action of Small Molecule Inhibitors Targeting the KCa3.1 Channel Pore. *Mol Pharmacol, 91*(4), 392-402. doi:10.1124/mol.116.108068

Palaniswami, M., & Yan, B. (2015). Mechanical Thrombectomy Is Now the Gold Standard for Acute Ischemic Stroke: Implications for Routine Clinical Practice. *Interv Neurol, 4*(1-2), 18-29. doi:10.1159/000438774

Percie du Sert, N., Alfieri, A., Allan, S. M., Carswell, H. V., Deuchar, G. A., Farr, T. D., Flecknell, P., Gallagher, L., Gibson, C. L., Haley, M. J., Macleod, M. R., McColl, B. W., McCabe, C., Morancho, A., Moon, L. D., O'Neill, M. J., Perez de Puig, I., Planas, A., Ragan, C. I., Rosell, A., Roy, L. A., Ryder, K. O., Simats, A., Sena, E. S., Sutherland, B. A., Tricklebank, M. D., Trueman, R. C., Whitfield, L., Wong, R., & Macrae, I. M. (2017). The IMPROVE Guidelines (Ischaemia Models: Procedural Refinements Of in Vivo Experiments). *J Cereb Blood Flow Metab, 37*(11), 3488-3517. doi:10.1177/0271678X17709185

Prabhakaran, S., Ruff, I., & Bernstein, R. A. (2015). Acute stroke intervention: a systematic review. *JAMA, 313*(14), 1451-1462. doi:10.1001/jama.2015.3058

Price, C. J., Wang, D., Menon, D. K., Guadagno, J. V., Cleij, M., Fryer, T., Aigbirhio, F., Baron, J. C., & Warburton, E. A. (2006). Intrinsic activated microglia map to the peri-infarct zone in the subacute phase of ischemic stroke. *Stroke, 37*(7), 1749-1753. doi:01.STR.0000226980.95389.0b [pii] 10.1161/01.STR.0000226980.95389.0b

Ramesha, S., Rayaprolu, S., Bowen, C. A., Giver, C. R., Bitarafan, S., Nguyen, H. M., Gao, T., Chen, M. J., Nwabueze, N., Dammer, E. B., Engstrom, A. K., Xiao, H., Pennati, A., Seyfried, N. T., Katz, D. J., Galipeau, J., Wulff, H., Waller, E. K., Wood, L. B., Levey, A. I., & Rangaraju, S. (2021). Unique molecular characteristics and microglial origin of Kv1.3 channel-positive brain myeloid cells in Alzheimer's disease. *Proc Natl Acad Sci U S A, 118*(11). doi:10.1073/pnas.2013545118

Reich, E. P., Cui, L., Yang, L., Pugliese-Sivo, C., Golovko, A., Petro, M., Vassileva, G., Chu, I., Nomeir, A. A., Zhang, L. K., Liang, X., Kozlowski, J. A., Narula, S. K., Zavodny, P. J., & Chou, C. C. (2005). Blocking ion channel KCNN4 alleviates the symptoms of experimental autoimmune encephalomyelitis in mice. *Eur J Immunol, 35*(4), 1027-1036.

Sarkar, S., Nguyen, H. M., Malovic, E., Luo, J., Langley, M., Palanisamy, B. N., Singh, N., Manne, S., Neal, M., Gabrielle, M., Abdalla, A., Anantharam, P., Rokad, D., Panicker, N., Singh, V., Ay, M., Charli, A., Harischandra, D., Jin, L. W., Jin, H., Rangaraju, S., Anantharam, V., Wulff, H., & Kanthasamy, A. G. (2020). Kv1.3 modulates neuroinflammation and neurodegeneration in Parkinson's disease. *J Clin Invest, 130*(8), 4195-4212. doi:10.1172/JCI136174

Savitz, S. I., Baron, J. C., Fisher, M., & Consortium, S. X. (2019). Stroke Treatment Academic Industry Roundtable X: Brain Cytoprotection Therapies in the Reperfusion Era. *Stroke, 50*(4), 1026-1031. doi:10.1161/STROKEAHA.118.023927

Savitz, S. I., Baron, J. C., Yenari, M. A., Sanossian, N., & Fisher, M. (2017). Reconsidering Neuroprotection in the Reperfusion Era. *Stroke, 48*(12), 3413-3419. doi:10.1161/STROKEAHA.117.017283

Schindelin, J., Arganda-Carreras, I., Frise, E., Kaynig, V., Longair, M., Pietzsch, T., Preibisch, S., Rueden, C., Saalfeld, S., Schmid, B., Tinevez, J. Y., White, D. J., Hartenstein, V., Eliceiri, K., Tomancak, P., & Cardona, A. (2012). Fiji: an open-source platform for biological-image analysis. *Nat Methods, 9*(7), 676-682. doi:10.1038/nmeth.2019

Staal, R. G., Khayrullina, T., Zhang, H., Davis, S., Fallon, S. M., Cajina, M., Nattini, M. E., Hu, A., Zhou, H., Poda, S. B., Zorn, S., Chandrasena, G., Dale, E., Cambpell, B., Biilmann Ronn, L. C., Munro, G., & Mller, T. (2017). Inhibition of the potassium channel KCa3.1 by senicapoc reverses tactile allodynia in rats with peripheral nerve injury. *Eur J Pharmacol, 795*, 1-7. doi:10.1016/j.ejphar.2016.11.031

Stocker, J. W., De Franceschi, L., McNaughton-Smith, G. A., Corrocher, R., Beuzard, Y., & Brugnara, C. (2003). ICA-17043, a novel Gardos channel blocker, prevents sickled red blood cell dehydration in vitro and in vivo in SAD mice. *Blood, 101*(6), 2412-2418. doi:10.1182/blood-2002-05-14332002-05-1433 [pii]

Sutherland, B. A., Neuhaus, A. A., Couch, Y., Balami, J. S., DeLuca, G. C., Hadley, G., Harris, S. L., Grey, A. N., & Buchan, A. M. (2016). The transient intraluminal filament middle cerebral artery occlusion model as a model of endovascular thrombectomy in stroke. *J Cereb Blood Flow Metab, 36*(2), 363-369. doi:10.1177/0271678X15606722

Swanson, R. A., Morton, M. T., Tsao-Wu, G., Savalos, R. A., Davidson, C., & Sharp, F. R. (1990). A semiautomated method for measuring brain infarct volume. *J Cereb Blood Flow Metab, 10*(2), 290-293. doi:10.1038/jcbfm.1990.47

Thomas, L., & Gehrig, J. (2020). ImageJ/Fiji ROI 1-click tools for rapid manual image annotations and measurements. *MicroPubl Biol, 2020*. doi:10.17912/micropub.biology.000215

Vandesompele, J., De Preter, K., Pattyn, F., Poppe, B., Van Roy, N., De Paepe, A., & Speleman, F. (2002). Accurate normalization of real-time quantitative RT-PCR data by geometric averaging of multiple internal control genes. *Genome Biol, 3*(7), RESEARCH0034. doi:10.1186/gb-2002-3-7-research0034

Virani, S. S., Alonso, A., Benjamin, E. J., Bittencourt, M. S., Callaway, C. W., Carson, A. P., Chamberlain, A. M., Chang, A. R., Cheng, S., Delling, F. N., Djousse, L., Elkind, M. S. V., Ferguson, J. F., Fornage, M., Khan, S. S., Kissela, B. M., Knutson, K. L., Kwan, T. W., Lackland, D. T., Lewis, T. T., Lichtman, J. H., Longenecker, C. T., Loop, M. S., Lutsey, P. L., Martin, S. S., Matsushita, K., Moran, A. E., Mussolino, M. E., Perak, A. M., Rosamond, W. D., Roth, G. A., Sampson, U. K. A., Satou, G. M., Schroeder, E. B., Shah, S. H., Shay, C. M., Spartano, N. L., Stokes, A., Tirschwell, D. L., VanWagner, L. B., Tsao, C. W., American Heart Association Council on, E., Prevention Statistics, C., & Stroke Statistics, S. (2020). Heart Disease and Stroke Statistics-2020 Update: A Report From the American Heart Association. *Circulation, 141*(9), e139-e596. doi:10.1161/CIR.0000000000000757

Visentin, S., Renzi, M., Frank, C., Greco, A., & Levi, G. (1999). Two different ionotropic receptors are activated by ATP in rat microglia. *J Physiol, 519 Pt 3*, 723-736. doi:10.1111/j.1469-7793.1999.0723n.x

Wulff, H., Miller, M. J., Haensel, W., Grissmer, S., Cahalan, M. D., & Chandy, K. G. (2000). Design of a potent and selective inhibitor of the intermediate-conductance Ca2+-activated K+ channel, IKCa1: A potential immunosuppressant. *Proc Natl Acad Sci USA, 97*, 8151-8156.

Zera, K. A., & Buckwalter, M. S. (2020). The Local and Peripheral Immune Responses to Stroke: Implications for Therapeutic Development. *Neurotherapeutics, 17*(2), 414-435. doi:10.1007/s13311-020-00844-3

Zhou, Y., He, Y., Yan, S., Chen, L., Zhang, R., Xu, J., Hu, H., Liebeskind, D. S., & Lou, M. (2023). Reperfusion Injury Is Associated With Poor Outcome in Patients With Recanalization After Thrombectomy. *Stroke, 54*(1), 96-104. doi:10.1161/STROKEAHA.122.039337

Figures

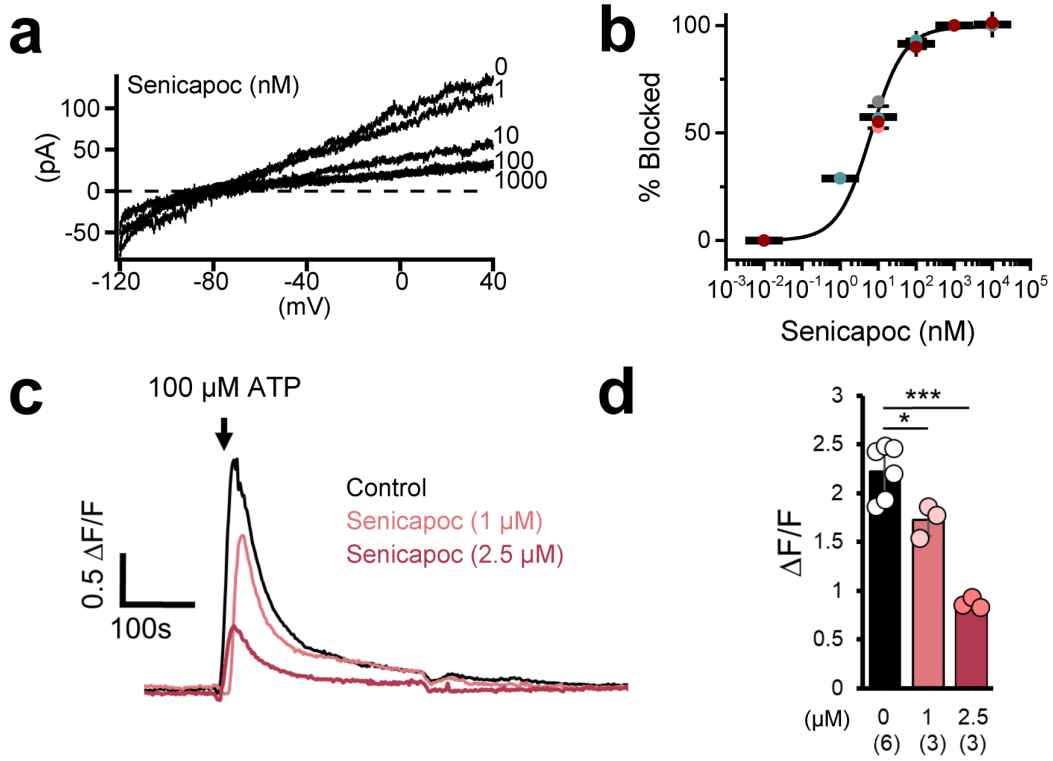

Figure 1. Senicapoc inhibits microglia $K_{Ca}3.1$ currents and ATP-induced calcium signaling. (**a**) Calcium-activated $K_{Ca}3.1$ currents elicited by a voltage ramp from -120 mV to 40 mV are shown before and after addition of increasing concentrations of senicapoc. (**b**) Inhibition of $K_{Ca}3.1$ currents was measured as shown in (a) and plotted as a function of senicapoc concentration for individual cells (filled circles) and mean (thick bars) ± standard deviation. Fitting the Hill equation (coefficient = 1) to the data yielded a mean IC_{50} value of 6.97 ± 3.17 nM (n = 4; mean ± 95% confidence interval). (**c**) Senicapoc reduces calcium indicator fluorescence signaling elicited by 100 µM ATP in MMC. Changes in $[Ca^{2+}]_i$ are represented as ΔF/F and quantified in (**d**). All calcium data are presented as mean ± SEM for measurements made from three to six independent experiments (different cultures) with 150–245 cells per experiment. Statistical significance determined by paired *t* test. *p < 0.05, ***p < 0.001.

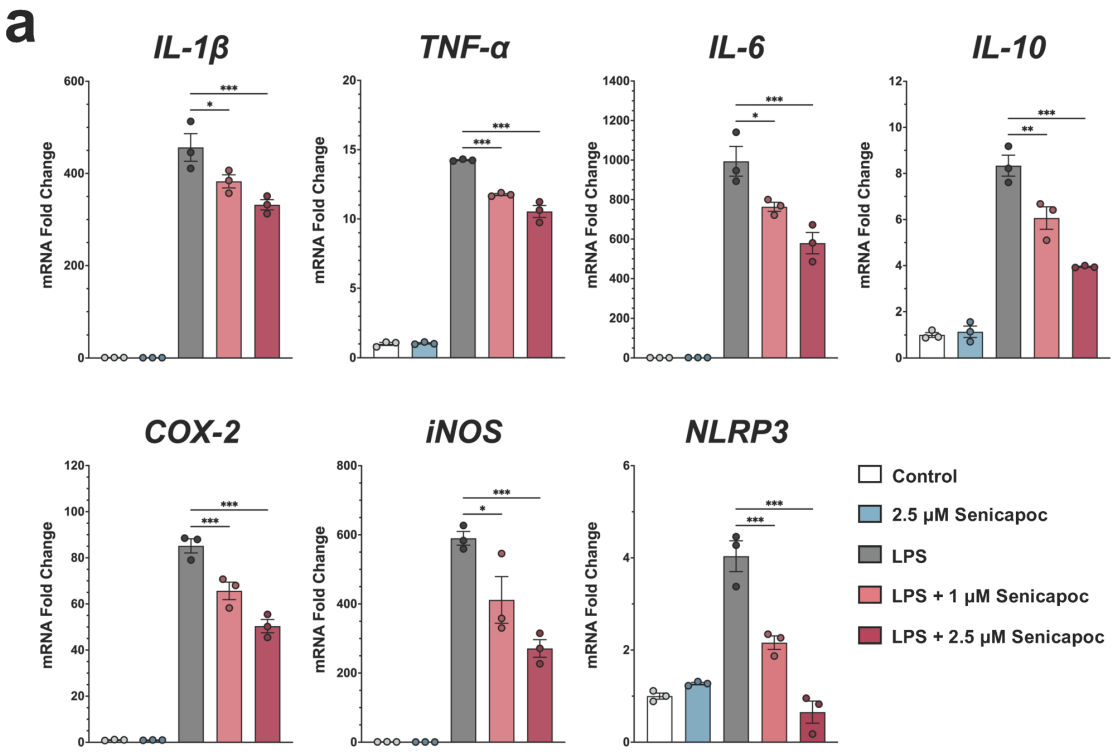

Figure 2. Senicapoc reduces inflammatory cytokines and inflammatory marker expression in MMC cells. Shown are fold increases in mRNA expression of the cytokines *il1β*, *tnfα*, *il6*, and *il10* and the markers *cox2*, *inos*, and *nlrp3* from one representative experiment following 24 h of stimulation with 100 ng/mL LPS**.** Data are shown as mean ± SEM (n = 3). *P<0.05, **P<0.01, ***P<0.001.

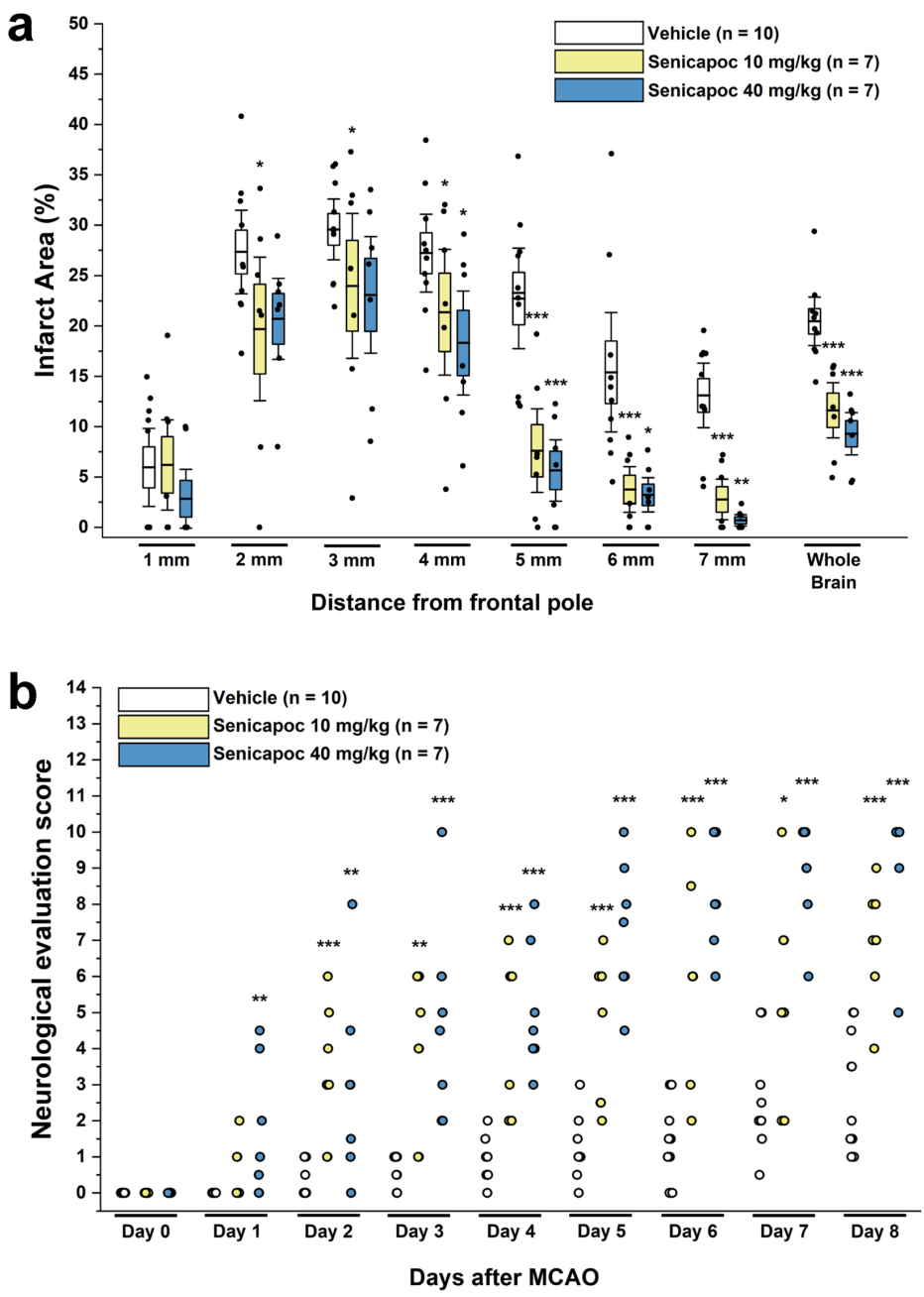

Figure 3. Senicapoc reduces infarction and improves neurological deficit in mice. Infarct area (**a**) and deficit score (**b**) in vehicle treated mice (n = 10) compared to mice treated with 10 mg/kg (n = 7) or 40 mg/kg (n = 7) senicapoc started at 12 h after reperfusion. Infarct areas are shown as whisker plots with data overlay. The boxes show mean ± S.E.M, the whiskers show confidence intervals. DeRyck scoring is shown as a scatter plot and was analyzed with the Mann-Whitney U test.

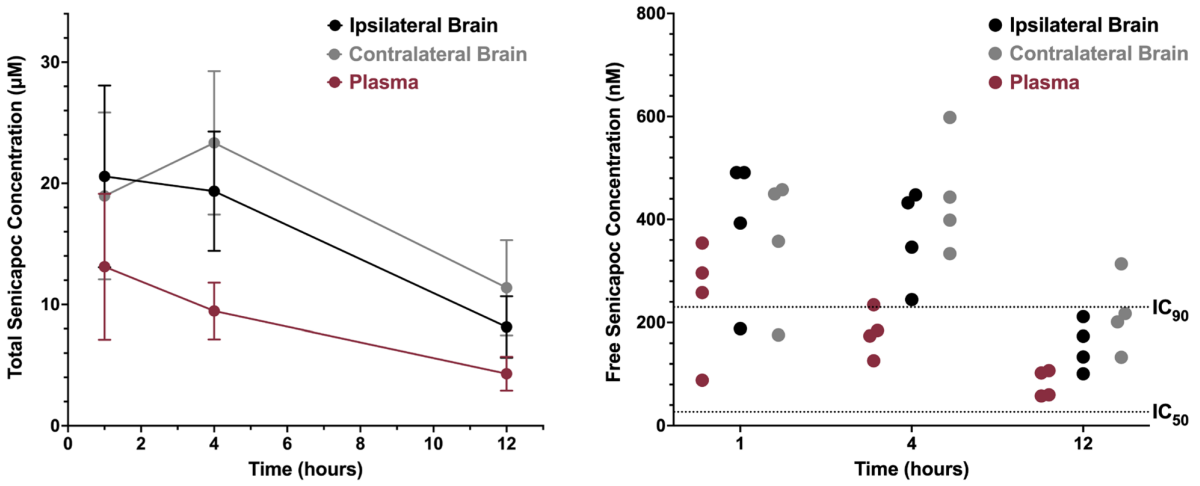

Figure 4. Senicapoc achieves $K_{Ca}3.1$ blocking concentrations. (**a**) Time course of total senicapoc concentrations in plasma and ipsi- and contralateral brain hemisphere following i.p. administration of 40 mg/kg. Data are mean ± S.D., n = 4 mice per time point. (**b**) Free senicapoc concentrations in plasma and brain hemispheres shown as scatter plots with the senicapoc $K_{Ca}3.1$ IC_{50} and IC_{90} shown as broken lines. n = 4 mice per time point.

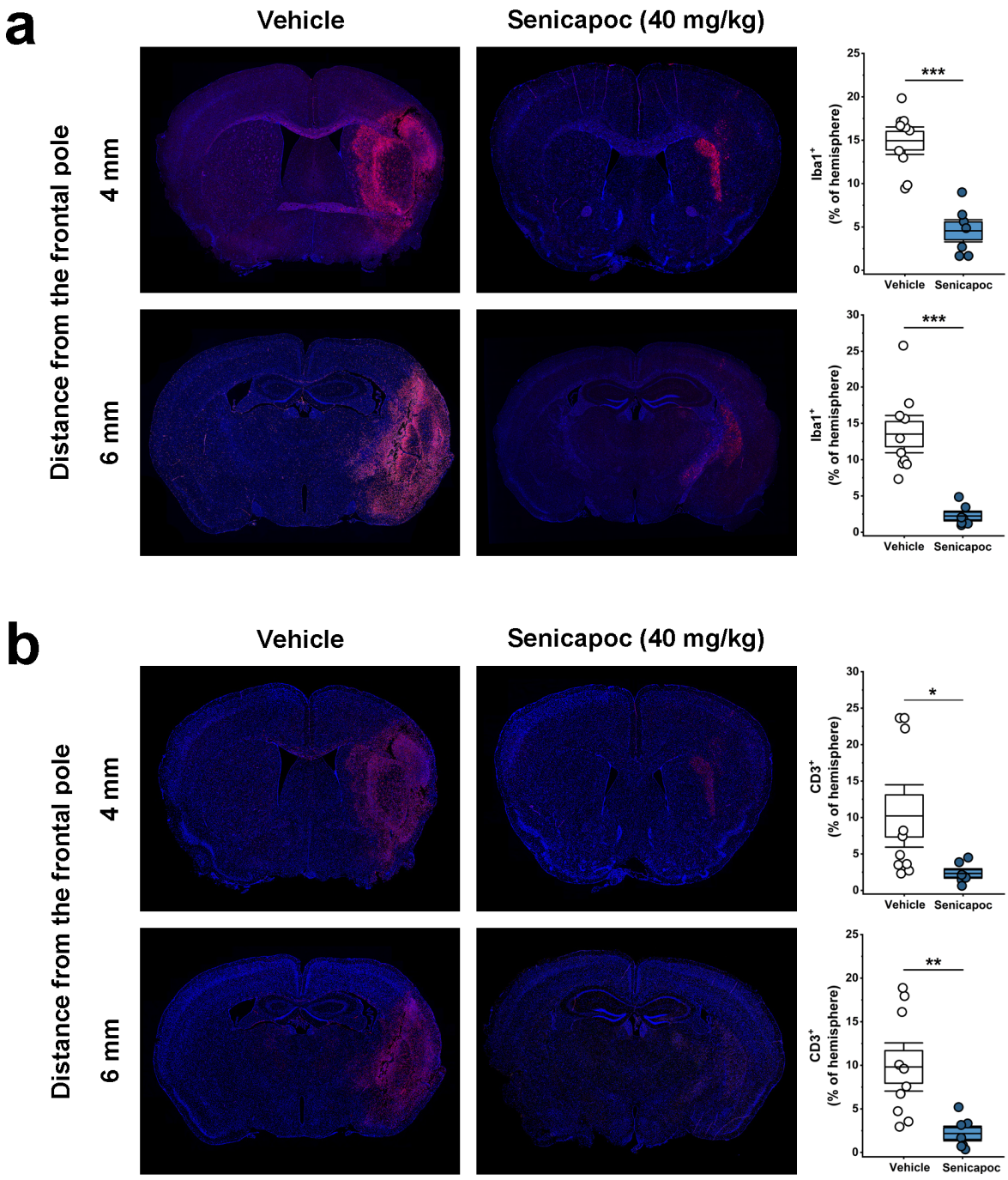

Figure 5. Senicapoc reduces Iba-1 (a) and CD3 (b) staining intensity in the infarcted hemisphere on day-8 after MCAO. Serial paraffin sections (5 μm thick) cut at 4- and the 6-mm from the frontal pole were stained for Iba-1 and CD3. Data are shown as whisker plots with individual data overlay. The boxes show mean ± S.E.M, the whiskers show confidence intervals.

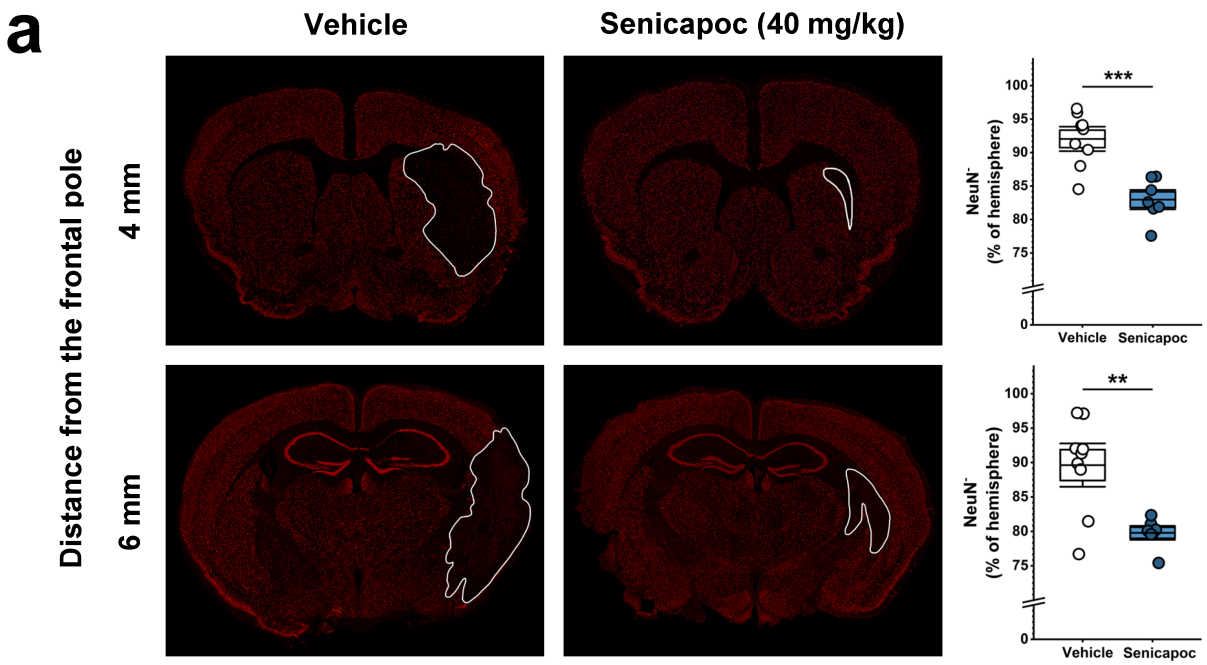

Figure 6. Senicapoc decreases neuronal death on day-8 after MCAO. Staining of neurons with the nuclear stain NeuN in 4- and 6-mm sections of vehicle and senicapoc treated mice. The NeuN-negative area is shown as whisker plots with individual data overlay. The boxes show mean ± S.E.M, the whiskers show confidence intervals. The infarct area is outlined in white.

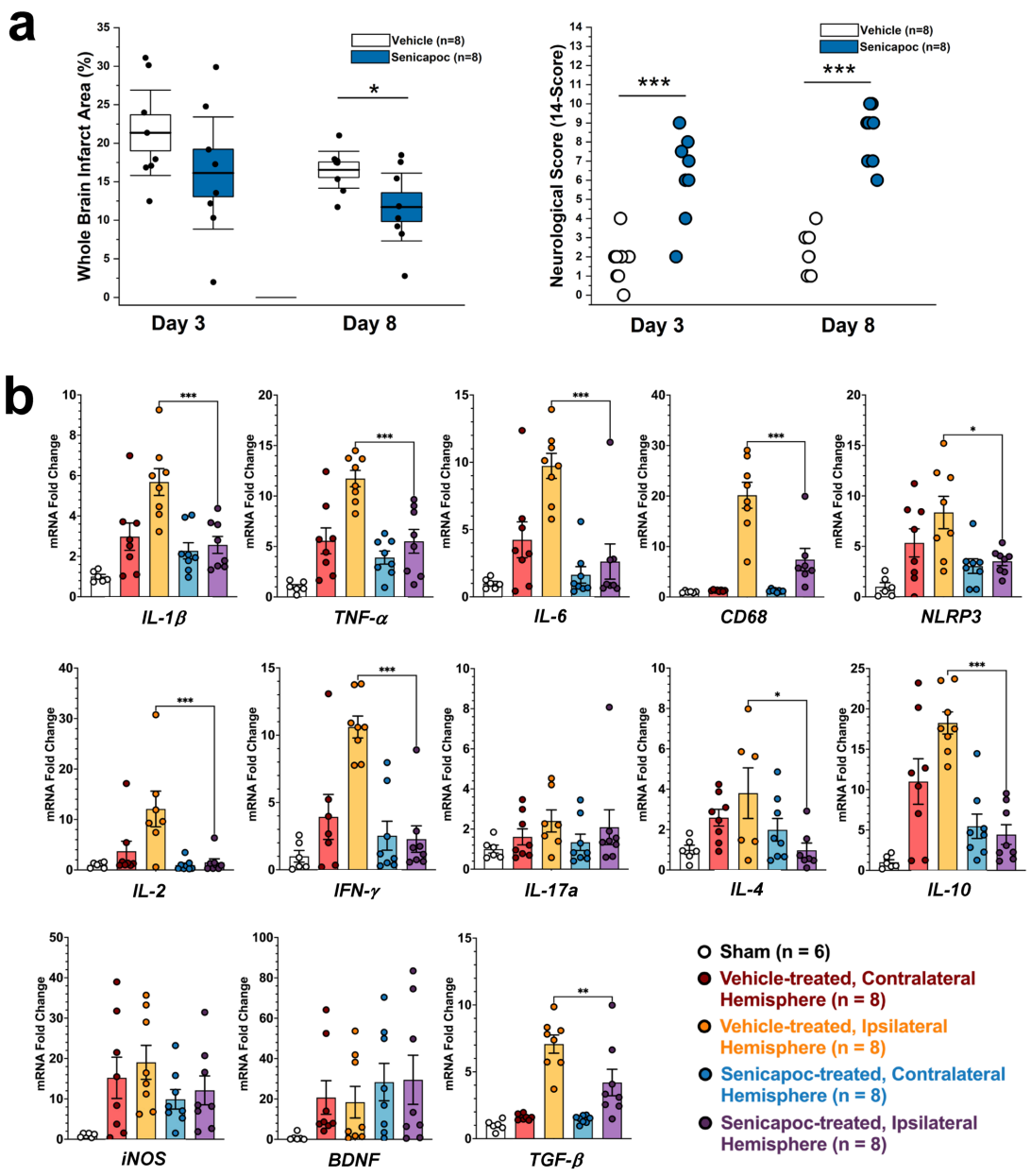

Figure 7. Senicapoc treatment started at 3 hours after tMCAO. (**a**) Effect of senicapoc (40 mg/kg compared to vehicle on infarct area and neurological deficit score on day-3 and day-8 (n = 8). Shown are whisker plots with data overlay. The boxes show mean ± S.E.M, the whiskers show confidence intervals. (**b**) Effect of senicapoc on inflammatory brain markers measured by RT-qPCR. mRNA expression levels are reported as a fold-change relative to sham. Values were normalized to sham mouse brain and to the geometric mean of three housekeeping genes, *β-actin*, *GAPDH*, and *18S*. Data were analyzed with one-way ANOVA followed by Dunnett's test and are shown as mean ± S.E.M; the whiskers show confidence intervals. For full statistics see Supplementary Table 2.

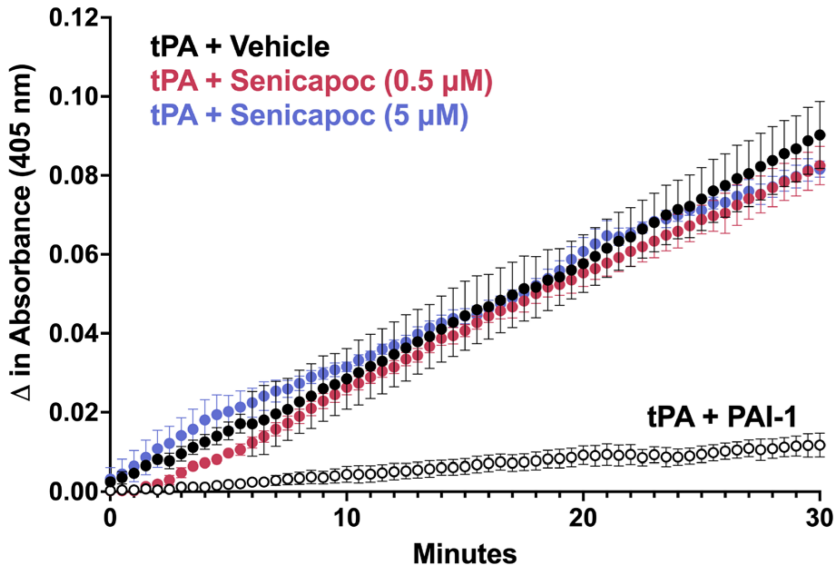

Figure 8. Senicapoc at 0.5 µM and 5 µM does not inhibit tPA activity as measured by increases in absorbance at 405 nm of a chromogenic tPA substrate. Each data point shown is the average of three independent experimental runs ± S.E.M. Each reaction was performed in triplicate wells.

Supplementary Tables and Figures

Marker (*Gene*)	Forward Primer Sequence	Reverse Primer Sequence
β-actin (*actb*)	GGCTGTATTCCCCTCCATCG	CCAGTTGGTAACAATGCCATGT
GAPDH (*gapdh*)	AGGTCGGTGTGAACGGATTTG	TGTAGACCATGTAGTTGAGGTCA
18S (*rps18*)	CCTGGATACCGCAGCTAGGA	GCGGCGCAATACGAATGCCCC
IL-1β (*il1b*)	GAGTGTGGATCCCAAGCAAT	TACCAGTTGGGGAACTCTGC
TNF-α (*tnfa*)	CAGCCGATGGGTTGTACCTT	GGCAGCCTTGTCCCTTGA
IFN-γ (*ifng*)	TGCTGATGGGAGGAGATGTCT	TGCTGTCTGGCCTGCTGTTA
IL-2 (*il2*)	CCTGAGCAGGATGGAGAATTACA	TCCAGAACATGCCGCAGAG
IL-4 (*il4*)	AGATGGATGTGCCAAACGTCCTCA	AATATGCGAAGCACCTTGGAAGCC
IL-6 (*il6*)	CCACGGCCTTCCCTACTTC	TGGGAGTGGTATCCTCTGTGAA
IL-10 (*il10*)	GATGCCCCAGGCAGAGAA	CACCCAGGGAATTCAAATGC
IL-17 (*il17*)	ATCCCTCAAAGCTCAGCGTGTC	GGGTCTTCATTGCGGTGGAGAG
COX-2 (*cox2*)	GATGACTGCCCAACTCCC	AACCCAGGTCCTCGCTTA
iNOS (*inos*)	CAGCTGGGCTGTACAAACCTT	CATTGGAAGTGAAGCGTTTCG
NLRP3 (*nlrp3*)	GGTCCTCTTTACCATGTGCTTC	AAGTCATGTGGCTGAAGCTGTA
BDNF (*bdnf*)	TGCAGGGGCATAGACAAAAGG	CTTATGAATCGCCAGCCAATTCTC
TGF-β (*tgfb1*)	TGATACGCCTGAGTGGCTGTCT	CACAAGAGCAGTGAGCGCTGAA
CD68 (*cd68*)	ACTTCGGGCCATGTTTCTCT	GCTGGTAGGTTGATTGTCGT

Supplementary Table 1. Primer sequences for the RT-qPCR experiments.

Il1b

Dunnett's multiple comparisons test	Mean Diff.	95.00% CI of diff.	Adjusted P Value
Vehicle-treated, Ipsi vs. Sham	4.683	2.668 to 6.698	<0.001
Sham vs. Vehicle-treated, Contra	-1.977	-3.971 to 0.01746	0.05
Vehicle treated, Ipsi vs Vehicle treated Contra	2.707	0.8412 to 4.572	0.003
Vehicle-treated, Ipsi vs. Senicapoc-treated, Ipsi	3.115	1.250 to 4.981	<0.001

tnfa

Dunnett's multiple comparisons test	Mean Diff.	95.00% CI of diff.	Adjusted P Value
Vehicle-treated, Ipsi vs. Sham	10.73	7.060 to 14.40	<0.001
Sham vs. Vehicle-treated, Contra	-4.562	-8.194 to -0.9301	0.01
Vehicle treated, Ipsi vs Vehicle treated Contra	6.168	2.770 to 9.566	<0.001
Vehicle-treated, Ipsi vs. Senicapoc-treated, Ipsi	6.221	2.823 to 9.619	<0.001

il6

Dunnett's multiple comparisons test	Mean Diff.	95.00% CI of diff.	Adjusted P Value
Vehicle-treated, Ipsi vs. Sham	8.728	4.790 to 12.67	<0.001
Sham vs. Vehicle-treated, Contra	-3.237	-7.134 to 0.6597	0.12
Vehicle treated, Ipsi vs Vehicle treated Contra	5.491	1.845 to 9.136	0.002
Vehicle-treated, Ipsi vs. Senicapoc-treated, Ipsi	7.107	3.462 to 10.75	<0.001

cd68

Dunnett's multiple comparisons test	Mean Diff.	95.00% CI of diff.	Adjusted P Value
Vehicle-treated, Ipsi vs. Sham	19.15	13.24 to 25.06	<0.001
Sham vs. Vehicle-treated, Contra	-0.2782	-6.126 to 5.570	>0.99
Vehicle treated, Ipsi vs Vehicle treated Contra	18.87	13.40 to 24.34	<0.001
Vehicle-treated, Ipsi vs. Senicapoc-treated, Ipsi	12.76	7.100 to 18.42	<0.001

nlrp3

Dunnett's multiple comparisons test	Mean Diff.	95.00% CI of diff.	Adjusted P Value
Vehicle-treated, Ipsi vs. Sham	7.358	3.194 to 11.52	<0.001
Sham vs. Vehicle-treated, Contra	-4.349	-8.469 to -0.2281	0.04
Vehicle treated, Ipsi vs Vehicle treated Contra	3.01	-0.8457 to 6.865	0.16
Vehicle-treated, Ipsi vs. Senicapoc-treated, Ipsi	4.839	0.9842 to 8.695	0.01

il2

Dunnett's multiple comparisons test	Mean Diff.	95.00% CI of diff.	Adjusted P Value
Vehicle-treated, Ipsi vs. Sham	11.09	4.015 to 18.16	0.001
Sham vs. Vehicle-treated, Contra	-2.703	-9.527 to 4.122	0.69
Vehicle treated, Ipsi vs Vehicle treated Contra	8.384	1.806 to 14.96	0.009
Vehicle-treated, Ipsi vs. Senicapoc-treated, Ipsi	10.6	4.020 to 17.18	<0.001

ifng

Dunnett's multiple comparisons test	Mean Diff.	95.00% CI of diff.	Adjusted P Value
Vehicle-treated, Ipsi vs. Sham	9.606	5.496 to 13.72	<0.001
Sham vs. Vehicle-treated, Contra	-2.926	-7.117 to 1.265	0.23
Vehicle treated, Ipsi vs Vehicle treated Contra	6.68	2.741 to 10.62	<0.001
Vehicle-treated, Ipsi vs. Senicapoc-treated, Ipsi	8.327	4.522 to 12.13	<0.001

il17a

Dunnett's multiple comparisons test	Mean Diff.	95.00% CI of diff.	Adjusted P Value
Vehicle-treated, Ipsi vs. Sham	1.404	-0.7716 to 3.580	0.3
Sham vs. Vehicle-treated, Contra	-0.6106	-2.710 to 1.489	0.86
Vehicle treated, Ipsi vs Vehicle treated Contra	0.7936	-1.230 to 2.818	0.7
Vehicle-treated, Ipsi vs. Senicapoc-treated, Ipsi	0.3131	-1.711 to 2.337	0.98

Il4

Dunnett's multiple comparisons test	Mean Diff.	95.00% CI of diff.	Adjusted P Value
Vehicle-treated, Ipsi vs. Sham	2.805	0.3649 to 5.246	0.02
Sham vs. Vehicle-treated, Contra	-1.589	-3.872 to 0.6935	0.24
Vehicle treated, Ipsi vs Vehicle treated Contra	1.216	-1.067 to 3.499	0.45
Vehicle-treated, Ipsi vs. Senicapoc-treated, Ipsi	2.833	0.4816 to 5.185	0.01

Il10

Dunnett's multiple comparisons test	Mean Diff.	95.00% CI of diff.	Adjusted P Value
Vehicle-treated, Ipsi vs. Sham	17.25	10.58 to 23.93	<0.001
Sham vs. Vehicle-treated, Contra	-10	-16.61 to -3.399	0.002
Vehicle treated, Ipsi vs Vehicle treated Contra	7.247	1.067 to 13.43	0.02
Vehicle-treated, Ipsi vs. Senicapoc-treated, Ipsi	13.82	7.638 to 20.00	<0.001

inos

Dunnett's multiple comparisons test	Mean Diff.	95.00% CI of diff.	Adjusted P Value
Vehicle-treated, Ipsi vs. Sham	18.05	3.760 to 32.34	0.01
Sham vs. Vehicle-treated, Contra	-14.23	-28.37 to -0.08833	0.05

Vehicle treated, Ipsi vs Vehicle treated Contra	3.821	-9.411 to 17.05	0.87
Vehicle-treated, Ipsi vs. Senicapoc-treated, Ipsi	6.938	-6.294 to 20.17	0.48

bdnf

Dunnett's multiple comparisons test	**Mean Diff.**	**95.00% CI of diff.**	**Adjusted P Value**
Vehicle-treated, Ipsi vs. Sham	17.41	-17.14 to 51.97	0.52
Sham vs. Vehicle-treated, Contra	-19.74	-53.94 to 14.46	0.38
Vehicle treated, Ipsi vs Vehicle treated Contra	-2.328	-34.32 to 29.67	>0.99
Vehicle-treated, Ipsi vs. Senicapoc-treated, Ipsi	-11.09	-43.08 to 20.91	0.79

tgfb

Dunnett's multiple comparisons test	**Mean Diff.**	**95.00% CI of diff.**	**Adjusted P Value**
Vehicle-treated, Ipsi vs. Sham	6.076	3.883 to 8.268	<0.001
Sham vs. Vehicle-treated, Contra	-0.629	-2.799 to 1.541	0.86
Vehicle treated, Ipsi vs Vehicle treated Contra	5.447	3.417 to 7.477	<0.001
Vehicle-treated, Ipsi vs. Senicapoc-treated, Ipsi	2.876	0.8461 to 4.906	0.003

Supplementary Table 2. Statistics for the RT-qPCR experiment in Figure 7b.

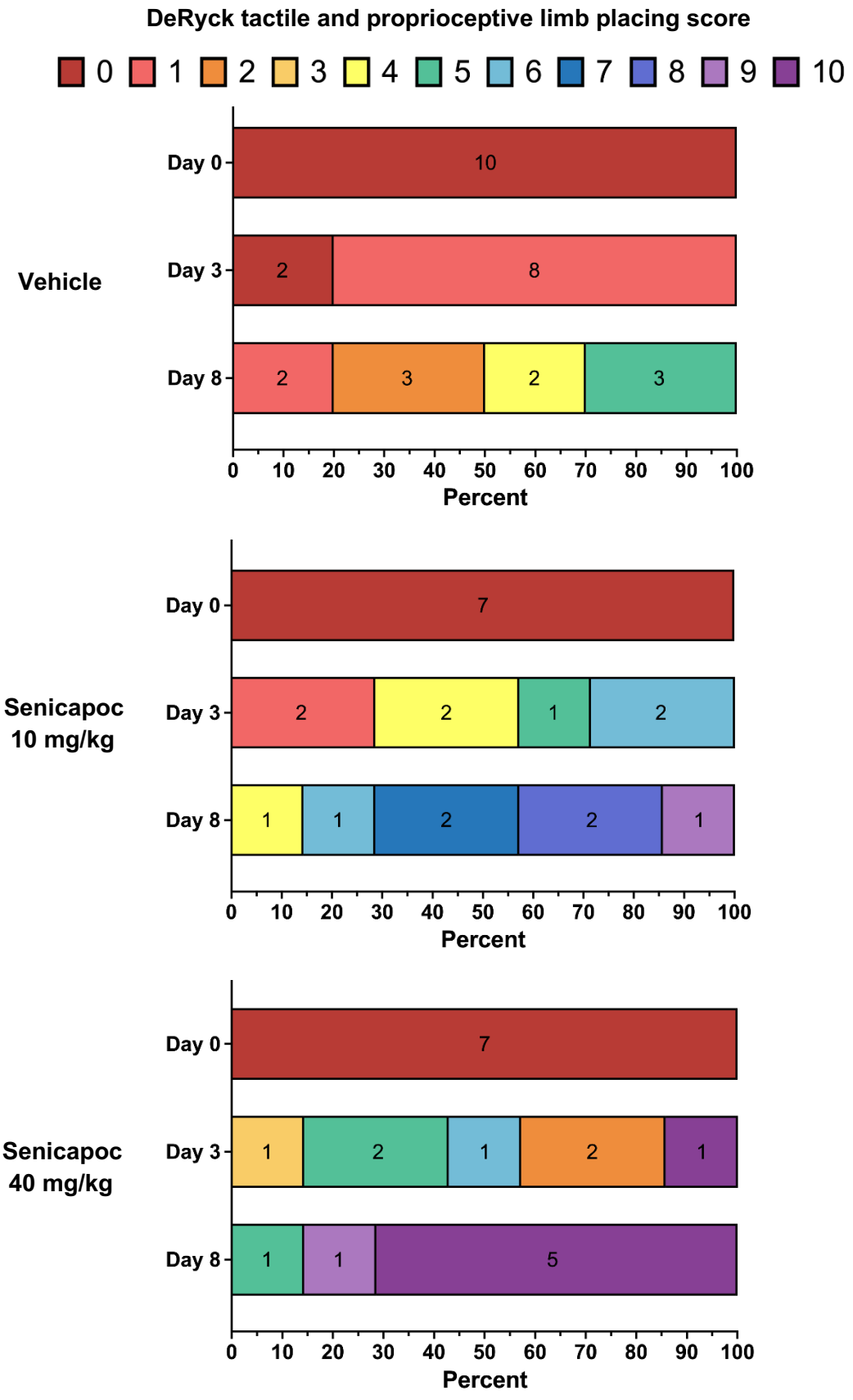
DeRyck tactile and proprioceptive limb placing score
0
1
2
3
4
5
6
7
8
9
10
Vehicle
Day 0
10
Day 3
2
8
Day 8
2
3
2
3
0
10
20
30
40
50
60
70
80
90
100
Percent
Senicapoc
10 mg/kg
Day 0
7
Day 3
2
2
1
2
Day 8
1
1
2
2
1
0
10
20
30
40
50
60
70
80
90
100
Percent
Senicapoc
40 mg/kg
Day 0
7
Day 3
1
2
1
2
1
Day 8
1
1
5
0
10
20
30
40
50
60
70
80
90
100
Percent

Supplementary Figure 1. Neurological deficit scoring on day-0, day-3 and day-8 shown as stacked bar graphs. Rainbow colors are used to represent the different scores according to the color scheme on top. Numbers represent the number of animals in each score category.

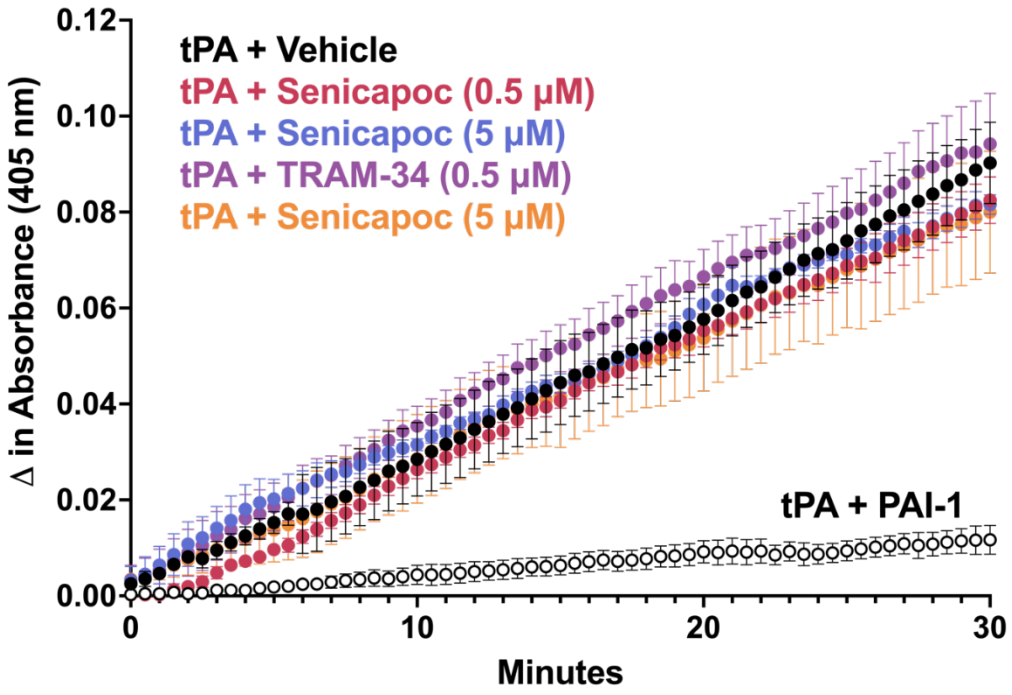

Supplementary Figure 2. Both $K_{Ca}3.1$ blockers, senicapoc and TRAM-34, do not interfere with tPA activity. tPA activity (measured by change in absorbance at 405 nm) was compared between conditions containing: tPA and vehicle (buffer) vs. tPA and 0.5 μM Senicapoc vs. tPA and 5 μM Senicapoc vs tPA and 0.5 μM TRAM-34 vs. tPA and 5 μM TRAM-34 vs tPA and PAI-1, a tPA inhibitor. Each data point shown is the average of three independent experimental runs ± S.E. M. Each reaction was performed in triplicate wells.

CHAPTER 3

Immunocytoprotection after Reperfusion with $K_V1.3$ Inhibitors has an Extended Treatment Window for Ischemic Stroke

Ruth D. Lee, MS[1]*, Yi-Je Chen, DVM, PhD[1,2]*, Latika Singh, PhD[1], Hai M. Nguyen, PhD[1], Heike Wulff, PhD[1]

* These authors contributed equally.

[1]Department of Pharmacology, School of Medicine, University of California, Davis, CA 95616, USA; [2]Animal Models Core, Department of Pharmacology, School of Medicine, University of California, Davis, CA 95616, USA

Address Correspondence to Heike Wulff, PhD, Department of Pharmacology, School of Medicine, University of California, Davis; 451 Health Sciences Drive, GBSF 3502, Davis, CA 95616. Email: hwulff@ucdavis.edu

Abstract

Objective: Mechanical thrombectomy has improved treatment options and outcomes for acute ischemic stroke with large artery occlusion. However, as the time window of endovascular thrombectomy is extended there is an increasing need to develop immunocytoprotective therapies that can reduce inflammation in the penumbra and prevent reperfusion injury. We previously demonstrated, that by reducing neuroinflammation, $K_V1.3$ inhibitors can improve outcomes not only in young male rodents but also in female and aged animals. To further explore the therapeutic potential of $K_V1.3$ inhibitors for stroke therapy, we here directly compared a peptidic and a small molecule $K_V1.3$ blocker and asked whether $K_V1.3$ inhibition would still be beneficial when started at 72 hours after reperfusion.

Methods: Transient middle cerebral artery occlusion (tMCAO, 90-min) was induced in male Wistar rats and neurological deficit assessed daily. On day-8 infarction was determined by T2-weighted MRI and inflammatory marker expression in the brain by quantitative PCR. Potential interactions with tissue plasminogen activator (tPA) were evaluated *in-vitro* with a chromogenic assay.

Results: In a direct comparison with administration started at 2 hours after reperfusion, the small molecule PAP-1 significantly improved outcomes on day-8, while the peptide ShK-223 failed to reduce infarction and neurological deficits despite reducing inflammatory marker expression. PAP-1 still provided benefits when started 72 hours after reperfusion. PAP-1 does not reduce the proteolytic activity of tPA.

Interpretation: Our studies suggest that $K_V1.3$ inhibition for immunocytoprotection after ischemic stroke has a wide therapeutic window and requires brain-penetrant small molecules.

Introduction

The goal of acute ischemic stroke therapy is to minimize damage by restoring blood flow to ischemic brain areas as soon as possible while minimizing reperfusion injury. Since the first endovascular device was approved by the FDA in 2004, door-to-reperfusion times have been slowly improving, with an increasing number of patients receiving and benefiting from Endovascular Therapy (EVT) (Goyal et al., 2016; Smith & Furlan, 2016). For acute ischemic stroke patients with a proximal cerebral arterial occlusion and salvageable brain tissue seen on Computerized Tomography (CT) imaging, EVT has been shown to be safe and efficacious within 6 hours after symptom onset (Campbell et al., 2015; Goyal et al., 2015). And, for a subset of patients who have severe symptom deficits despite a relatively small infarct volume, several studies have extended this treatment window to 24 hours and beyond (Nogueira et al., 2018).

Even though patient outcomes are significantly improved when EVT is initiated as soon as possible (Saver et al., 2016), door-to-reperfusion times can vary widely, depending on factors like patient education about stroke, and distance from and access to EVT-capable hospitals (Saver et al., 2016). Today's acute stroke algorithm entails transporting patients to the nearest hospital, capable of providing diagnostic imaging and intravenous tissue-type plasminogen activator (IV-tPA), but not necessarily EVT; only about 20% of stroke patients in the USA are within fifteen minutes of transportation time to an EVT-capable hospital (Saver et al., 2016). Thus, most patients must be subsequently transferred to an EVT-capable facility, with an average symptom onset-to-procedure time of 260 minutes (Saver et al., 2016). This broad range of door-to-reperfusion times can result in an enlarging ischemic core (Gauberti, De Lizarrondo, & Vivien, 2016; Savitz, Baron, Yenari, Sanossian, & Fisher, 2017). which in turn, may explain why some patients have such poor outcomes after thrombectomy. Most of the injury in the ischemic core results from the lack of blood flow itself, which is why it is salvageable by reperfusion via thrombectomy, but with time, this core can enlarge into the ischemic or "inflammatory" penumbra

(Gauberti et al., 2016). which are areas at risk of damage by immune cells like microglia and infiltrating neutrophiles, macrophages and T-cells (Chamorro et al., 2012; Iadecola & Anrather, 2011; Weinstein, Koerner, & Moller, 2010). Because there is a strong neuroinflammatory component to the penumbra, lesion growth, and the poor neurological outcomes associated with it despite successful thrombectomy (Zhou et al., 2023), may be preventable by immunomodulatory drugs providing what has been termed “immunocytoprotection” (Gauberti et al., 2016; Savitz et al., 2017). A recent study reported radiological observed reperfusion injury (RORI) in 47% of stroke patients after mechanical thrombectomy (Zhou et al., 2023).

Here, we focus on one possible target of immunomodulation for ischemic stroke. We previously showed that blocking the voltage-gated potassium channel $K_V1.3$, which is expressed on microglia and T cells, with our small molecule drug, PAP-1, results in reduced neuroinflammation without compromising the beneficial functions of the immune system such as phagocytosis of neuronal debris by microglia in two rodent models of ischemic stroke (Chen, Cui, Singh, & Wulff, 2021; Chen, Nguyen, Maezawa, Jin, & Wulff, 2018). Using middle cerebral artery occlusion (MCAO) with reperfusion in both mice (60 min occlusion) and rats (90 min occlusion), we demonstrated that $K_V1.3$ inhibition with PAP-1 reduces infarct size and improves neurological deficits on day-8 in young adult male mice and rats when compound administration was started 12 hour after reperfusion (Chen et al., 2018). We subsequently further validated $K_V1.3$ as a target for immunocytoprotection in ischemic stroke by demonstrating that pharmacological $K_V1.3$ blockade and genetic $K_V1.3$ deletion benefits young (16-week-old) and aged (80-week-old) mice of both sexes (Chen et al., 2021). Here, we explore the therapeutic window of PAP-1 and assess the degree of immunocytoprotection PAP-1 confers when given earlier and later than our previous 12-hour timepoint, at 2 hours and 3 days after MCAO in rats. We also evaluated a peptidic $K_V1.3$ blocker in order to compare peripherally restricted $K_V1.3$ inhibition with the brain-penetrant $K_V1.3$ blocker PAP-1.

Materials and Methods

Middle Cerebral Artery Occlusion Surgeries

This study was approved by the University of California, Davis, Animal Use and Care Committee and conducted in accordance with the guidelines of Animal Use and Care of the National Institutes of Health, the University of California, Davis for survival surgery, and the IMPROVE guidelines for ischemic stroke in rodents (Percie du Sert et al., 2017). Adult male Wistar IGS rats (Strain 003 WISTAR) weighing 160 to 180 g were purchased from Charles River (Wilmington, MA, USA), acclimatized to the vivarium for 7 to 10 days and used for surgery when they weighed 250 to 300 g. Rats were anesthetized using box induction with 5% isoflurane and then maintained on 0.5 to 1.5% isoflurane in medical grade oxygen via a facemask. To assure consistent reduction of cerebral blood flow (CBF) throughout the procedure, a small area of skull was shaved, and the Laser Doppler probe (Moor Instruments, Wilmington, DE, USA) affixed to the surface of the skull with a hand-made adapter 5 mm lateral to the central fusion line and 2.5 mm posterior to bregma after the skull bone had been thinned with a drill (5 mm diameter). Instant adhesive and dental cement were applied to the base and around the edges of the small plastic adapter to hold the Doppler probe. The adapter with the attached probe remained in place throughout the MCAO surgery to confirm continuous occlusion and later the establishment of reperfusion. Focal cerebral ischemia was then induced by occlusion of the left middle cerebral artery (MCA) according to Zea Longa (Longa, Weinstein, Carlson, & Cummins, 1989). Briefly, the left common carotid artery was surgically exposed, the external carotid artery was ligated distally from the common carotid artery, and a silicone rubber-coated nylon monofilament with a tip diameter of 0.43 ± 0.02 mm (Doccol Corp., Redlands, CA, USA) was inserted into the external carotid artery and advanced into the internal carotid artery to block the origin of the MCA (when maximum CBF reduction observed). The filament was kept in place for 90 min and then withdrawn to restore blood supply. Animals received subcutaneous Buprenex at 0.02 mg/kg every 12 h to

limit postsurgical pain for 24 h after surgery. For sham surgeries, the filament was placed into the external carotid artery but not advanced into the internal carotid artery.

The survival rate for MCAO surgeries was 92%. Animals where CBF was not reduced by at least 70% and which did not display any obvious neurological deficit 2 hours after reperfusion were excluded. The average CBF reduction in this study was 76.3 ± 5.8%. Animals that met these inclusion criteria were assigned to treatment or vehicle groups based on a computer-generated randomization scheme. Out of the animals surviving to day-8 (52 out of 56), 4 animals were excluded due to insufficient occlusion and insufficient neurological deficit.

Drug Treatments

Starting at 2 hours or 3 days post-MCAO, rats received either miglyol-812 neutral oil (Caprylic/Capric Triglyceride, Spectrum Chemicals), saline, ShK-223 at 100 μg/kg once daily, or PAP-1 at 40 mg/kg intraperitoneally twice daily until sacrifice on day-8 (Fig. 1). Miglyol 812 is a low viscosity oily vehicle, which is widely used as a pharmaceutical excipient and well tolerated for i.p. or oral administration. It can be autoclaved and allows for the dissolution of lipophilic compounds like PAP-1 at high concentrations (20 mg/mL for this study). PAP-1 was synthesized in our laboratory and chemical identity and purity (>98%) confirmed by ^{1}H and ^{13}C-NMR and HPLC (Schmitz et al., 2005). ShK-223, a highly Kv1.3-selective derivative of the sea anemone *Stichodactyla helianthus* toxin peptide ShK (Pennington et al., 2015) was synthesized at AmbioPharm Inc. (North Augusta, SC).

Neurological Scoring

Neurological deficits were scored according to a 14-score test tactile and proprioceptive limb-placing test (De Ryck, Van Reempts, Borgers, Wauquier, & Janssen, 1989) as follows: proprioception, forward extension, lateral abduction, and adduction were tested with vision or tactile stimuli (lower score for more severe neurological deficits). For visual limb placing, rats were held and slowly moved forward or lateral toward the top of a table. Normal rats placed both forepaws on the tabletop. Tactile forward and lateral limb placing were tested by lightly contacting the table edge with the dorsal or lateral surface of a rat's paw while avoiding whisker contact and covering the eyes to avoid vision. For proprioceptive hindlimb placing, each rat was pushed along the edge of an elevated platform to test proprioceptive hindlimb adduction. The paw was pulled down and away from the platform edge, and the ability to retrieve and place the paw on the table surface upon sudden release was assessed. For each test, limb-placing scores were 0=no placing; 1=incomplete and delayed (>2 seconds) placing; or 2=immediate and complete placing. For each body side, the maximum summed tactile and proprioceptive limb-placing score, including the platform test, was 14.

The investigator performing the drug administration, neurological scoring, and analyses was blinded to the treatments.

Assessment of Infarct Area with MRI

Infarct volume on day-8 was evaluated with T2-weighted MRI imaging in the Nuclear Magnetic Resonance (NMR) Facility at UC Davis. MRI was performed with a 7T (300 MHz) Bruker Biospec MR system running ParaVision version 5. The RF coil was Bruker’s standard 42 mm ID rat resonator. Animals were anesthetized with isoflurane and placed under a heated circulating

water blanket (37°C) to maintain body temperature. Fast spin echo (FSE) imaging, also known as RARE (Rapid Acquisition with Relaxation Enhancement), sequence was used to acquire tri-pilot geometry reference images. The multi-slice multi-echo (MSME) sequence (TE:56 ms; TR: 1681.2 ms) was used to acquire images of 12 coronal sections with 1 mm thickness from the junction of olfactory bulb and cortex. The infarct area was analyzed with Adobe Photoshop Elements by an investigator blinded to the treatments. The percentage of infarcted area was calculated with the equation: (Infarct Area ÷ Ipsilateral Hemisphere Area) × 100% MRI.

Statistics

Based on our previous work with PAP-1 in MCAO (Chen et al., 2018), sample size was powered to detect a reduction of 40% in mean percentage infarct area with 80% power. Statistical analysis comparing two groups was done using unpaired t-test. Comparison of three groups was done using one-way ANOVA in Prism, with post-hoc pairwise comparison of the treatment groups with Tukey's method (Schlattmann & Dirnagl, 2010). $P<0.05$ was used as the level of significance; *$P<0.05$, **$P<0.01$, and ***$P<0.001$. All data are given as mean ± S.E.M.

RT-qPCR

After the MRI was completed, rats were euthanized with an overdose of isoflurane, and brains were harvested. The brains were split into ipsilateral and contralateral hemispheres and were immediately frozen with liquid N_2. Brain hemispheres were homogenized in mortar and pestles with liquid N_2. RNA was subsequently extracted with Trizol (ThermoFisher, Catalog # 15596026) according to the manufacturer's protocol. RNA purity and concentration were assessed using a Nanodrop Spectrophotometer ND-1000 (Marshall Scientific). The 260 nm/280

nm absorption ratios for the samples ranged from 1.90 to 2.00. Subsequently, a cDNA library was made with a High-Capacity cDNA Reverse Transcription Kit (ThermoFisher Scientific, Catalog# 4374967), with 2 µg of total RNA per 20 uL reaction. Reactions were carried out in a PTC-200 Peltier Thermal Cycler; the conditions were as follows: 25°C for 10 min, 37°C for 120 min, 85°C for 5 min, with final storage at 4°C. RT-qPCR reactions were conducted in triplicate in an Applied Biosystems Viia7 Real-Time PCR System using Maxima SYBR Green/ROX qPCR Master Mix (ThermoFisher Scientific, Catalog #K022) and with the recommended three-step cycling protocol. RT-qPCR primer sequences are provided in Supplementary Table 1; The primers for rat *IL-2*, *IL-4*, *IL-10*, and *IL-17a* did not work as determined with concanavalin A stimulated rat splenocytes.

All CT values were normalized to the geometric mean of three housekeeping genes, β-*actin*, *hmbs*, and *ywhaz*, as recommended by Vandesompele *et al* (Vandesompele et al., 2002). Fold changes were calculated by the ΔΔCt method; relative mRNA levels were generated by normalizing to sham. The three housekeeping genes were selected from a panel of the 17 most commonly used housekeeping genes in the stroke field because they were the most stably expressed genes (with the lowest M values) in two age-matched male Wistar rats and two representative ipsilateral MCAO Wistar rats; this ranking was generated by a stepwise exclusion of the least stable genes, using the GeNorm analysis software (Kang, Wu, Cai, & Lu, 2018; Vandesompele et al., 2002). We chose both normal brain and ipsilateral MCAO hemispheres for the housekeeping gene panel because we wanted genes that remained stable during stroke. Primers were purchased from BioRad as part of their PrimePCR plate and sequences are provided in Supplementary Table 2. Outliers were defined as datapoints that deviated more than 5 standard deviations from the mean and were removed (modified Grubb's test). The remaining 612 data points were analyzed and are shown. Statistical analysis comparing the ipsilateral hemisphere of the various treatment groups to the ipsilateral hemisphere of the vehicle treated

animals was performed in Prism using one-way ANOVA followed by Dunnett's test to correct for multiple comparisons. All data are given as mean ± S.E.M.

tPA Assay

The commercially available Tissue tPA Activity Assay Kit (Abcam, ab108905) was used to assess whether PAP-1 affects the ability of human tPA to cleave its substrate plasminogen (Lapchak & Boitano, 2014; Lapchak, Lara, & Boitano, 2017). All reactions were run in optically clear flat-bottom 96-well plates (Corning, Catalog #3904). Human plasminogen activator inhibitor-1 (PAI-1, Sigma-Aldrich CC4075) was used as a positive control. Human plasminogen, the chromogenic plasmin substrate, and human tPA were included in the Tissue tPA Activity Assay Kit (Abcam, ab108905). PBS with 10% human serum was used as the assay medium; PAP-1 was added at 500 nM and 5 μM with a final DMSO concentration of 0.1%. The reactions were pre-incubated at 37°C for 5 min prior to addition of the chromogenic substrate and placed into a SpectraMax M5 spectrophotometer heated to 37°C. Absorbances at 405 nm were measured every 30 seconds for 30 min.

Results

K_V1.3 inhibition with the small molecule PAP-1 but not the peptide ShK-223 reduces infarction and improves neurological deficit after tMCAO in rats

K_V1.3 can be targeted with small molecules or with biologics such as venom-derived peptides, antibodies and nanobodies. We here chose two K_V1.3 blockers, our small molecule PAP-1 (Schmitz et al., 2005) and ShK-223 (Pennington et al., 2015), a more selective and stable analog of ShK-186 (Dalazatide) (Tarcha et al., 2012), as representatives of the two modalities for testing in MCAO in adult male Wistar rats. The doses of ShK-223 (IC_{50} 25 pM) and PAP-1 (IC_{50} for 2 nM) were chosen considering their Kv1.3 blocking potency and are based on previously reported efficacy in rat models of experimental autoimmune encephalomyelitis (EAE) or of ischemic stroke (Chen et al., 2018; Tarcha et al., 2012).

Following 90 min of occlusion of the MCA (76.3 ± 5.8% flow reduction) and subsequent reperfusion, rats were randomized and treated either with 100 μg/kg ShK-223, 40 mg/kg PAP-1 or the respective compound vehicles (PBS or miglyol) starting 2 hours after reperfusion (Fig. 1). The treatments were administered twice daily and continued until day-8, when infarct areas were measured by T2-weighted MRI and brains subsequently removed for qPCR analysis. Neurological deficit scoring using the De Ryck 14-score tactile and proprioceptive limb-placing test (De Ryck et al., 1989) was performed daily, starting 12 hours after reperfusion. While ShK-223 did not reduce infarction (Fig. 2A) or improve neurological deficit scores (Fig. 2B) compared to vehicle-treated rats, PAP-1 treatment significantly reduced infarct area on day-8 (Fig. 2C) and ameliorated neurological deficit starting from day-4 after MCAO (Fig. 2D) when compared to its vehicle miglyol, which is a low viscosity triglyceride. Since we had used two different vehicles, we next compared the two vehicles to each other and found no differences in stroke outcomes (Fig. S1 A and B). We, therefore, combined the two vehicles into one large vehicle group (n = 16) and

compared it to ShK-223 and PAP-1 treated animals. This comparison using Turkey's method for *post hoc* comparison, again demonstrated that the small molecule PAP-1 improved stroke outcomes, while the peptidic K_V1.3 blocker ShK-223, did not significantly reduce infarction (Fig. S1C) or improved neurological deficit (Fig. S1D).

K_V1.3 inhibition with PAP-1 still improves MCAO outcomes when administration is started 3 days after reperfusion

Following MCAO in rats and mice, hypertrophic, CD68-positive mononuclear phagocytes, arising from both activated microglia and infiltrating monocytes become abundant in the infarcted area and the penumbra between 18 to 96 hours after an ischemic stroke and have been described to peak between 7-14 days (Campanella, Sciorati, Tarozzo, & Beltramo, 2002; Hu et al., 2012). Using immunohistochemistry and electrophysiology on acutely isolated CD11b+ cells we previously characterized the time course of K_V1.3 expression on microglia/macrophages following ischemic stroke in mice. While K_V1.3 currents were barely detectable on microglia isolated from normal brain or from the contralateral side, K_V1.3 current amplitudes from CD11b+ cells from the infarcted hemisphere started to significantly increase at two and five days after MCAO and peaked around day-8 (Chen et al., 2018). Similar to mice, we here observed large, PAP-1-sensitive K_V1.3 currents on Iba-1 and $CD68^+$ microglia/macrophages acutely isolated from the infarcted area with CD11b-selective magnetic beads (Fig. S2). A significant percentage of the CD11b+ cells were clearly activated and stained positive for K_V1.3, confirming our previous observations made in mice, here in rats.

Based on these time courses for microglia/macrophage activation and K_V1.3 expression, we hypothesized that K_V1.3 inhibition might still be beneficial when started as late as 3 days after ischemic stroke and therefore also treated a group of rats with 40 mg/kg of PAP-1 starting at 72

h after reperfusion. A comparison of these animals to vehicle-treated rats and rats that had started receiving PAP-1 at 2 hours after reperfusion, revealed that delayed PAP-1 treatment was as effective as early PAP-1 treatment in reducing infarction as determined by T2-weighted MRI by day-8 after MCAO (Fig. 3A). As expected, neurological deficit scoring was initially not altered in comparison to vehicle but started to be significantly improved by day-6 and was similar to early PAP-1 by day-8 (Fig. 3B).

Early and late administration of K_V1.3 inhibitors reduces inflammatory marker expression in the infarcted hemisphere

Following the MRI on day-8, brains from all animals were removed for RT-qPCR analysis. As recommended by Vandesompele *et al*., CT values were normalized to three housekeeping genes (Vandesompele et al., 2002), *β-actin*, *hmbs*, and *ywhaz,* which were selected from a panel of the 17 most commonly used housekeeping genes in the stroke field based on their stable expression when comparing age matched male Wistar rats and ipsilateral MCAO tissue (see Methods). Relative mRNA levels of all analyzed markers were normalizing to sham. MCAO significantly increased expression of inflammatory cytokines (*IL-1β*, *IL-6*, *TNF-α* and *IFN-γ*), the phagocyte marker CD68, and the enzymes *COX-2* and *iNOS* in the infarcted hemisphere compared to the contralateral hemisphere (Fig. 4, for full statistics see Table S3). Interestingly, *TGF-β* expression was increased in the contralateral hemisphere by day-8 compared to sham, but drastically decreased in the infarcted side (Fig. 4). K_V1.3 inhibition with early and late PAP-1 or with the peptide ShK-223, reduced mRNA expression of *IL-1β*, *IL-6*, *TNF-α, COX-2* and *iNOS* (Fig. 4) and increased expression of *TGF-β* in the infarcted hemisphere. Expression of *IFN-γ* was only significantly reduced by early PAP-1 treatment, while CD68 expression was not significantly affected by K_V1.3 blocker treatment.

In contrast to previously published qPCR data from isolated microglia, whole brain tissue expression analysis of the microglial ion channels (*P2X4*, *P2X7*, $K_V1.3$ and $K_{Ca}3.1$) was not very informative on day-8 (Fig. 4). While there were trends towards increased mRNA expression with MCAO and decreased mRNA with treatment, only early PAP-1 treatment significantly decreased $K_V1.3$ mRNA expression compared to vehicle treatment (Fig. 4).

PAP-1 does not interfere with tPA in-vitro

In clinical use, $K_V1.3$ inhibitors might not only be employed in combination with mechanical thrombectomy but also together with, or shortly after tPA infusion. We, therefore, tested whether PAP-1 affects the proteolytic function of tPA (Fig. 5). While the positive control, plasminogen activator inhibitor-1 (PAI-1) strongly inhibited the enzymatic activity of tPA in a chromogenic assay, PAP-1, at 0.5 µM and 5 µM, had no effect on tPA activity during the 30 min assay suggesting that it is unlikely to affect its fibrinolytic activity.

Discussion

Since $K_V1.3$ was first discovered in T-cells in 1984 (DeCoursey, Chandy, Gupta, & Cahalan, 1984), the channel has been studied as a potential target for immunosuppression and immunomodulation in multiple sclerosis, autoimmune diabetes, rheumatoid arthritis, psoriasis and ulcerative colitis (Beeton et al., 2006; Kundu-Raychaudhuri, Chen, Wulff, & Raychaudhuri, 2014; Unterweger et al., 2021). $K_V1.3$ blockers, like ShK-peptides or the small molecules PAP-1 and DES1, work well in treating these T-cell mediated pathologies because $K_V1.3$ is overexpressed on $CCR7^-$ effector memory T cells (Beeton et al., 2006), which are a subset of T-cells that home to sites of inflammation, secrete pro-inflammatory cytokines, and display immediate effector functions (Sallusto, Lenig, Forster, Lipp, & Lanzavecchia, 1999). More recently, $K_V1.3$ has been investigated as a target for inflammation in the central nervous system where $K_V1.3$ expression has been described on activated, “M1-like” or disease-associated microglia in human brain or in rodent models of Alzheimer’s disease (Maezawa et al., 2018; Ramesha et al., 2021), multiple sclerosis (Rus et al., 2005), Parkinson’s disease (Sarkar et al., 2020), and ischemic stroke (Chen et al., 2018). Network analysis of transcriptomic datasets revealed that $K_V1.3$ is part of a pro-inflammatory microglial gene signature in neurodegenerative disease models (Ramesha et al., 2021; Rangaraju et al., 2017). The physiological function of $K_V1.3$ in T cells and microglia is similar; this voltage-gated potassium channel regulates membrane potential and controls store-operated calcium influx through CRAC (calcium release activated calcium) channels and downstream signaling events such as activation and nuclear translocation of NF-kB and NFAT (Feske, Wulff, & Skolnik, 2015; Fomina, Nguyen, & Wulff, 2021). In microglia, $K_V1.3$ also plays a crucial role in enabling these cells to resist depolarizations produced by P2X4 receptor activation by the danger signal ATP (Nguyen et al., 2020). In assays with cultured microglia or organotypic hippocampal slices, $K_V1.3$ blockers reduce expression of iNOS and COX-2 and production of inflammatory cytokines and NO following stimulation with LPS, amyloid-β, α-synuclein or

ischemia/hypoxia (Chen et al., 2018; Maezawa et al., 2018; Sarkar et al., 2020). K_V1.3 blockers, which are generally well tolerated, and do not affect the ability of rodents to clear infections or of rhesus macaques to develop protective vaccine responses (Beeton et al., 2006; Pereira et al., 2007), therefore constitute attractive therapeutic candidates for immunocytoprotection in ischemic stroke.

In our efforts to translate K_V1.3 into a therapeutic target for ischemic stroke, we initially performed proof-of-concept experiments in young male mice, where we characterized the time course of K_V1.3 expression on microglia after MCAO and demonstrated that PAP-1 treatment started at 12 hours after reperfusion decreased infarct size and improved neurological deficits after one week (Chen et al., 2018). We subsequently evaluated whether K_V1.3 inhibition would also be beneficial in females and aged animals. At the target level, there are no sex differences; microglia from both male and female mice express similar levels of K_V1.3 in culture or after acute isolation out of the infarcted area following MCAO (Chen et al., 2021; Nguyen et al., 2020). In treatment experiments, PAP-1 started at 12 hours after reperfusion benefited young and aged mice of both sexes, but was particularly effective in 20-month-old animals (Chen et al., 2021), presumably because of the increasing T-cell contribution to stroke pathology due to a process that has been termed “inflammaging” (Carrasco et al., 2021), and which is characterized by a shrinking of the naïve T cell compartment and an expansion of the tissue homing effector memory T-cell pool. In keeping with this hypothesis, we observed that both treatment with PAP-1 or genetic K_V1.3 deletion, not only reduced microglia/macrophage activation as measured by Iba-1 pixel density but also very effectively reduced T cell infiltration into the infarcted hemisphere in aged animals (Chen et al., 2021).

In this present study, we focus on exploring the treatment window for K_V1.3 inhibition and the treatment modalities. Specifically, we wanted to determine whether K_V1.3 blockers for the treatment of ischemic stroke need to be brain-penetrant small molecules or whether biologics

would also be effective. While our small molecule PAP-1 penetrates well into the brain and reaches equal concentrations in brain tissue and - plasma (C_{brain}/C_{plasma} = 1.1) (Beeton et al., 2006), positively charged ShK peptides are only minimally brain penetrant based on studies with radiolabeled peptides that showed 0.05% of the total injected radioactivity in the brain (Tarcha et al., 2012). To answer this question about the treatment modality, we decided to directly compare PAP-1 and the peptide ShK-223 in MCAO in male rats with treatment started 2 hours after reperfusion, a time point that would simulate administration relatively early after mechanical thrombectomy. In this setting, where both PAP-1 and ShK-223 were given at doses at which they had previously been effective in stroke or EAE in rats (Chen et al., 2018; Tarcha et al., 2012), the peptide ShK-223 failed to significantly reduce T2-weighted infarct area or improve neurological deficit scoring on day-8, while the small molecule PAP-1 improved both parameters. When delaying the start of PAP-1 administration, we found that even if treatment is started at 3 days after reperfusion, PAP-1 is still effective at reducing infarct area and improving neurological deficit on day-8.

One very interesting observation from our study is that both the peptide ShK-223 and early or late administration of the small molecule PAP-1 were similarly effective at reducing expression of *IL-1β*, *IL-6*, *TNF-α, COX-2* and *iNOS* in the infarcted hemisphere on day-8. Yet only PAP-1 treatment resulted in a significant reduction in infarction and an improvement in neurological deficits. Why is there such a mismatch between inflammatory marker expression and functional outcomes? Our interpretation of these findings is that a large proportion of the mRNA in the infarcted tissue on day-8 originates from infiltrating peripheral immune cells that have migrated to and proliferated in the infarcted tissue. These cells would have been exposed to ShK-223 in the periphery and susceptible to the effects of this membrane-impermeable peptide. A limitation of our study in this respect is that we used all animals for qPCR and did not directly compare the extent of immune cell infiltration/activation by immunohistochemistry or flow cytometry between

ShK-223, early PAP-1 and late PAP-1 treatment. Another explanation for the lack of effect of the peptide on functional outcomes is, that it was not able to access the infarcted tissue sufficiently. Opening of the blood brain barrier (BBB) in tMCAO has been reported to be biphasic, once at 6 hours and once at 72 hours, with no Evans blue or fluorescein extravasation occurring at 24 or 48 hours (Hone et al., 2018). However, even under conditions where the brain is inflamed, and the BBB confirmed to be compromised, only very small amounts of ShK-sized peptides (4 kDa) penetrate into the brain as a recently published PET imaging study using HsTX1 labeled with a long-lived ^{64}Cu-isotope demonstrated (Reddiar et al., 2022). Similar to ShK-223, HsTX1[R14A] is a 34-residue, C-terminally amidated peptide cross-linked by four disulfide bridges, that inhibits K_V1.3 with picomolar affinity. When LPS treatment was used to open-up the blood brain barrier, brain uptake of the ^{64}Cu-labeled HsTX1[R14A] only increased from less than 0.1 SUV (standard uptake value) to 0.25 SUV compared to SUVs of 40-95 in the kidney, demonstrating very limited bioavailability in the brain even with a compromised BBB (Reddiar et al., 2022). Similar results had been obtained with an LS-MS/MS assay (Reddiar et al., 2021). While no HsTX1[R14A] was detectable in the brains of normal mice, brain concentrations reached 2% of plasma concentrations following treatment with a high dose of systemic LPS. The small molecule PAP-1, in contrast, is highly brain penetrant and provides solid brain exposure with total concentrations in the micromolar range and free brain concentrations providing IC_{50}-IC_{90} coverage of K_V1.3 for at least 8 hours after administration in mice or rats (Beeton et al., 2006; Chen et al., 2018; Maezawa et al., 2018). One major conclusion from our study is, therefore, that K_V1.3 inhibitors used for immunocytoprotection after ischemic stroke need to be brain penetrant to prevent inflammatory lesion expansion. These findings are similar to observations made with targeting P2X7 for stroke and other conditions associated with neuroinflammation. P2X7 targeted nanobodies can only occupy microglial P2X7 receptor channels following intracerebroventricular delivery (Pinto-Espinoza et al., 2022).

Our other major finding in this study is that K_V1.3 inhibition with PAP-1 still improves MCAO outcomes when administration is started as late as 3 days after reperfusion. This is an exciting observation that is in keeping with the time course of microglia/macrophages activation (Campanella et al., 2002; Hu et al., 2012) and K_V1.3 expression after ischemic stroke, which starts to significantly increase between 2-5 days and peaks around day-8 after MCAO (Chen et al., 2018). From a therapeutic perspective, these findings suggest that K_V1.3 inhibition has a wide treatment window and could be a useful, adjunctive pharmacological treatment that could be administered either together with EVT or fibrinolytic drugs or up to days later to reduce inflammation in the penumbra and prevent reperfusion injury.

Disclosures

Funding Information: This work was supported by the National Institute of Neurological Disease and Stroke (NS100294 to H.W.).

Conflict of Interest: H.W. is an inventor on a University of California patent claiming PAP-1 for immunosuppression. This patent has been abandoned because of its short remaining patent life.

Author Contributions: RDL, YJC and HW developed the concept and designed the study. YJC performed all surgeries. LS synthesized PAP-1. RDL and YC acquired and analyzed the data. HMN performed the electrophysiology, RDL, YJC, and HW prepared the figures. RDL, YJC and HW wrote the manuscript with input from all co-authors.

References

Beeton, C., Wulff, H., Standifer, N. E., Azam, P., Mullen, K. M., Pennington, M. W., Kolski-Andreaco, A., Wei, E., Grino, A., Counts, D. R., Wang, P. H., Leehealey, C. J., B, S. A., Sankaranarayanan, A., Homerick, D., Roeck, W. W., Tehranzadeh, J., Stanhope, K. L., Zimin, P., Havel, P. J., Griffey, S., Knaus, H. G., Nepom, G. T., Gutman, G. A., Calabresi, P. A., & Chandy, K. G. (2006). Kv1.3 channels are a therapeutic target for T cell-mediated autoimmune diseases. *Proc Natl Acad Sci U S A, 103*(46), 17414-17419.

Campanella, M., Sciorati, C., Tarozzo, G., & Beltramo, M. (2002). Flow cytometric analysis of inflammatory cells in ischemic rat brain. *Stroke, 33*(2), 586-592.

Campbell, B. C., Mitchell, P. J., Kleinig, T. J., Dewey, H. M., Churilov, L., Yassi, N., Yan, B., Dowling, R. J., Parsons, M. W., Oxley, T. J., Wu, T. Y., Brooks, M., Simpson, M. A., Miteff, F., Levi, C. R., Krause, M., Harrington, T. J., Faulder, K. C., Steinfort, B. S., Priglinger, M., Ang, T., Scroop, R., Barber, P. A., McGuinness, B., Wijeratne, T., Phan, T. G., Chong, W., Chandra, R. V., Bladin, C. F., Badve, M., Rice, H., de Villiers, L., Ma, H., Desmond, P. M., Donnan, G. A., Davis, S. M., & Investigators, E.-I. (2015). Endovascular therapy for ischemic stroke with perfusion-imaging selection. *N Engl J Med, 372*(11), 1009-1018. doi:10.1056/NEJMoa1414792

Carrasco, E., Gomez de Las Heras, M. M., Gabande-Rodriguez, E., Desdin-Mico, G., Aranda, J. F., & Mittelbrunn, M. (2021). The role of T cells in age-related diseases. *Nat Rev Immunol*. doi:10.1038/s41577-021-00557-4

Chamorro, A., Meisel, A., Planas, A. M., Urra, X., van de Beek, D., & Veltkamp, R. (2012). The immunology of acute stroke. *Nat Rev Neurol, 8*(7), 401-410. doi:10.1038/nrneurol.2012.98

Chen, Y. J., Cui, Y., Singh, L., & Wulff, H. (2021). The potassium channel Kv1.3 as a therapeutic target for immunocytoprotection after reperfusion. *Ann Clin Transl Neurol, 8*(10), 2070-2082. doi:10.1002/acn3.51456

Chen, Y. J., Nguyen, H. M., Maezawa, I., Jin, L. W., & Wulff, H. (2018). Inhibition of the potassium channel Kv1.3 reduces infarction and inflammation in ischemic stroke. *Ann Clin Transl Neurol, 5*(2), 147-161. doi:10.1002/acn3.513

De Ryck, M., Van Reempts, J., Borgers, M., Wauquier, A., & Janssen, P. A. (1989). Photochemical stroke model: flunarizine prevents sensorimotor deficits after neocortical infarcts in rats. *Stroke, 20*(10), 1383-1390.

DeCoursey, T. E., Chandy, K. G., Gupta, S., & Cahalan, M. D. (1984). Voltage-gated K+ channels in human T lymphocytes: a role in mitogenesis? *Nature, 307*(5950), 465-468.

Feske, S., Wulff, H., & Skolnik, E. Y. (2015). Ion channels in innate and adaptive immunity. *Annu Rev Immunol, 33*, 291-353. doi:10.1146/annurev-immunol-032414-112212

Fomina, A. F., Nguyen, H. M., & Wulff, H. (2021). Kv1.3 inhibition attenuates neuroinflammation through disruption of microglial calcium signaling. *Channels (Austin), 15*(1), 67-78. doi:10.1080/19336950.2020.1853943

Gauberti, M., De Lizarrondo, S. M., & Vivien, D. (2016). The "inflammatory penumbra" in ischemic stroke: From clinical data to experimental evidence. *Eur Stroke J, 1*(1), 20-27. doi:10.1177/2396987316630249

Goyal, M., Demchuk, A. M., Menon, B. K., Eesa, M., Rempel, J. L., Thornton, J., Roy, D., Jovin, T. G., Willinsky, R. A., Sapkota, B. L., Dowlatshahi, D., Frei, D. F., Kamal, N. R., Montanera, W. J., Poppe, A. Y., Ryckborst, K. J., Silver, F. L., Shuaib, A., Tampieri, D., Williams, D., Bang, O. Y., Baxter, B. W., Burns, P. A., Choe, H., Heo, J. H., Holmstedt, C. A., Jankowitz, B., Kelly, M., Linares, G., Mandzia, J. L., Shankar, J., Sohn, S. I., Swartz, R. H., Barber, P. A., Coutts, S. B., Smith, E. E., Morrish, W. F., Weill, A., Subramaniam, S., Mitha, A. P., Wong, J. H., Lowerison, M. W., Sajobi, T. T., Hill, M. D., & Investigators, E. T. (2015). Randomized assessment of rapid endovascular treatment of ischemic stroke. *N Engl J Med, 372*(11), 1019-1030. doi:10.1056/NEJMoa1414905

Goyal, M., Menon, B. K., van Zwam, W. H., Dippel, D. W., Mitchell, P. J., Demchuk, A. M., Davalos, A., Majoie, C. B., van der Lugt, A., de Miquel, M. A., Donnan, G. A., Roos, Y. B., Bonafe, A., Jahan, R., Diener, H. C., van den Berg, L. A., Levy, E. I., Berkhemer, O. A., Pereira, V. M., Rempel, J., Millan, M., Davis, S. M., Roy, D., Thornton, J., Roman, L. S., Ribo, M., Beumer, D., Stouch, B., Brown, S., Campbell, B. C., van Oostenbrugge, R. J., Saver, J. L., Hill, M. D., Jovin, T. G., & collaborators, H. (2016). Endovascular thrombectomy after large-vessel ischaemic stroke: a meta-analysis of individual patient data from five randomised trials. *Lancet, 387*(10029), 1723-1731. doi:10.1016/S0140-6736(16)00163-X

Hone, E. A., Hu, H., Sprowls, S. A., Farooqi, I., Grasmick, K., Lockman, P. R., simpkins, J. W., & Ren, X. (2018). Biphasic blood-brain barrier openings after stroke. *Neurologcial Disorders and Stroke International, 1*(2), Article 1011.

Hu, X., Li, P., Guo, Y., Wang, H., Leak, R. K., Chen, S., Gao, Y., & Chen, J. (2012). Microglia/macrophage polarization dynamics reveal novel mechanism of injury expansion after focal cerebral ischemia. *Stroke, 43*(11), 3063-3070. doi:10.1161/STROKEAHA.112.659656

Iadecola, C., & Anrather, J. (2011). The immunology of stroke: from mechanisms to translation. *Nat Med, 17*(7), 796-808. doi:10.1038/nm.2399

Kang, Y., Wu, Z., Cai, D., & Lu, B. (2018). Evaluation of reference genes for gene expression studies in mouse and N2a cell ischemic stroke models using quantitative real-time PCR. *BMC Neurosci, 19*(1), 3. doi:10.1186/s12868-018-0403-6

Kundu-Raychaudhuri, S., Chen, Y. J., Wulff, H., & Raychaudhuri, S. P. (2014). Kv1.3 in psoriatic disease: PAP-1, a small molecule inhibitor of Kv1.3 is effective in the SCID mouse psoriasis--xenograft model. *J Autoimmun, 55*, 63-72. doi:10.1016/j.jaut.2014.07.003

Lapchak, P. A., & Boitano, P. D. (2014). Effect of the Pleiotropic Drug CNB-001 on Tissue Plasminogen Activator (tPA) Protease Activity in vitro: Support for Combination Therapy to Treat Acute Ischemic Stroke. *J Neurol Neurophysiol, 5*(4).

Lapchak, P. A., Lara, J. M., & Boitano, P. D. (2017). Cytoprotective Drug-Tissue Plasminogen Activator Protease Interaction Assays: Screening of Two Novel Cytoprotective Chromones. *Transl Stroke Res*. doi:10.1007/s12975-017-0533-7

Longa, E. Z., Weinstein, P. R., Carlson, S., & Cummins, R. (1989). Reversible middle cerebral artery occlusion without craniectomy in rats. *Stroke, 20*(1), 84-91.

Maezawa, I., Nguyen, H. M., Di Lucente, J., Jenkins, D. P., Singh, V., Hilt, S., Kim, K., Rangaraju, S., Levey, A. I., Wulff, H., & Jin, L. W. (2018). Kv1.3 inhibition as a potential microglia-targeted therapy for Alzheimer's disease: preclinical proof of concept. *Brain, 141*(2), 596-612. doi:10.1093/brain/awx346

Nguyen, H. M., di Lucente, J., Chen, Y. J., Cui, Y., Ibrahim, R. H., Pennington, M. W., Jin, L. W., Maezawa, I., & Wulff, H. (2020). Biophysical basis for Kv1.3 regulation of membrane potential changes induced by P2X4-mediated calcium entry in microglia. *Glia, 68*, 2377-2394. doi:10.1002/glia.23847

Nogueira, R. G., Jadhav, A. P., Haussen, D. C., Bonafe, A., Budzik, R. F., Bhuva, P., Yavagal, D. R., Ribo, M., Cognard, C., Hanel, R. A., Sila, C. A., Hassan, A. E., Millan, M., Levy, E. I., Mitchell, P., Chen, M., English, J. D., Shah, Q. A., Silver, F. L., Pereira, V. M., Mehta, B. P., Baxter, B. W., Abraham, M. G., Cardona, P., Veznedaroglu, E., Hellinger, F. R., Feng, L., Kirmani, J. F., Lopes, D. K., Jankowitz, B. T., Frankel, M. R., Costalat, V., Vora, N. A., Yoo, A. J., Malik, A. M., Furlan, A. J., Rubiera, M., Aghaebrahim, A., Olivot, J. M., Tekle, W. G., Shields, R., Graves, T., Lewis, R. J., Smith, W. S., Liebeskind, D. S., Saver, J. L., Jovin, T. G., & Investigators, D. T. (2018). Thrombectomy 6 to 24 Hours after Stroke with a Mismatch between Deficit and Infarct. *N Engl J Med, 378*(1), 11-21. doi:10.1056/NEJMoa1706442

Pennington, M. W., Chang, S. C., Chauhan, S., Huq, R., Tajhya, R. B., Chhabra, S., Norton, R. S., & Beeton, C. (2015). Development of highly selective Kv1.3-blocking peptides based on the sea anemone peptide ShK. *Mar Drugs, 13*(1), 529-542. doi:10.3390/md13010529

Percie du Sert, N., Alfieri, A., Allan, S. M., Carswell, H. V., Deuchar, G. A., Farr, T. D., Flecknell, P., Gallagher, L., Gibson, C. L., Haley, M. J., Macleod, M. R., McColl, B. W., McCabe, C., Morancho, A., Moon, L. D., O'Neill, M. J., Perez de Puig, I., Planas, A., Ragan, C. I., Rosell, A., Roy, L. A., Ryder, K. O., Simats, A., Sena, E. S., Sutherland, B. A., Tricklebank, M. D., Trueman, R. C., Whitfield, L., Wong, R., & Macrae, I. M. (2017). The IMPROVE Guidelines (Ischaemia Models: Procedural Refinements Of in Vivo Experiments). *J Cereb Blood Flow Metab, 37*(11), 3488-3517. doi:10.1177/0271678X17709185

Pereira, L. E., Villinger, F., Wulff, H., Sankaranarayanan, A., Raman, G., & Ansari, A. A. (2007). Pharmacokinetics, toxicity, and functional studies of the selective Kv1.3 channel blocker 5-(4-phenoxybutoxy)psoralen in rhesus macaques. *Exp Biol Med (Maywood), 232*(10), 1338-1354.

Pinto-Espinoza, C., Guillou, C., Rissiek, B., Wilmes, M., Javidi, E., Schwarz, N., Junge, M., Haag, F., Liaukouskaya, N., Wanner, N., Nicke, A., Stortelers, C., Tan, Y. V., Adriouch, S., Magnus, T., & Koch-Nolte, F. (2022). Effective targeting of microglial P2X7 following intracerebroventricular delivery of nanobodies and nanobody-encoding AAVs. *Front Pharmacol, 13*, 1029236. doi:10.3389/fphar.2022.1029236

Ramesha, S., Rayaprolu, S., Bowen, C. A., Giver, C. R., Bitarafan, S., Nguyen, H. M., Gao, T., Chen, M. J., Nwabueze, N., Dammer, E. B., Engstrom, A. K., Xiao, H., Pennati, A., Seyfried, N. T., Katz, D. J., Galipeau, J., Wulff, H., Waller, E. K., Wood, L. B., Levey, A. I., & Rangaraju, S. (2021). Unique molecular characteristics and microglial origin of Kv1.3

channel-positive brain myeloid cells in Alzheimer's disease. *Proc Natl Acad Sci U S A, 118*(11). doi:10.1073/pnas.2013545118

Rangaraju, S., Raza, S. A., Pennati, A., Deng, Q., Dammer, E. B., Duong, D., Pennington, M. W., Tansey, M. G., Lah, J. J., Betarbet, R., Seyfried, N. T., & Levey, A. I. (2017). A systems pharmacology-based approach to identify novel Kv1.3 channel-dependent mechanisms in microglial activation. *J Neuroinflammation, 14*(1), 128. doi:10.1186/s12974-017-0906-6

Reddiar, S. B., de Veer, M., Paterson, B. M., Sepehrizadeh, T., Wai, D. C. C., Csoti, A., Panyi, G., Nicolazzo, J. A., & Norton, R. S. (2022). A Biodistribution Study of the Radiolabeled Kv1.3-Blocking Peptide DOTA-HsTX1[R14A] Demonstrates Brain Uptake in a Mouse Model of Neuroinflammation. *Mol Pharm*. doi:10.1021/acs.molpharmaceut.2c00614

Reddiar, S. B., Jin, L., Wai, D. C. C., Csoti, A., Panyi, G., Norton, R. S., & Nicolazzo, J. A. (2021). Lipopolysaccharide influences the plasma and brain pharmacokinetics of subcutaneously-administered HsTX1[R14A], a K(V)1.3-blocking peptide. *Toxicon, 195*, 29-36. doi:10.1016/j.toxicon.2021.03.002

Rus, H., Pardo, C. A., Hu, L., Darrah, E., Cudrici, C., Niculescu, T., Niculescu, F., Mullen, K. M., Allie, R., Guo, L., Wulff, H., Beeton, C., Judge, S. I., Kerr, D. A., Knaus, H. G., Chandy, K. G., & Calabresi, P. A. (2005). The voltage-gated potassium channel Kv1.3 is highly expressed on inflammatory infiltrates in multiple sclerosis brain. *Proc Natl Acad Sci U S A, 102*, 11094-11099.

Sallusto, F., Lenig, D., Forster, R., Lipp, M., & Lanzavecchia, A. (1999). Two subsets of memory T lymphocytes with distinct homing potentials and effector functions. *Nature, 401*(6754), 708-712.

Sarkar, S., Nguyen, H. M., Malovic, E., Luo, J., Langley, M., Palanisamy, B. N., Singh, N., Manne, S., Neal, M., Gabrielle, M., Abdalla, A., Anantharam, P., Rokad, D., Panicker, N., Singh, V., Ay, M., Charli, A., Harischandra, D., Jin, L. W., Jin, H., Rangaraju, S., Anantharam, V., Wulff, H., & Kanthasamy, A. G. (2020). Kv1.3 modulates neuroinflammation and neurodegeneration in Parkinson's disease. *J Clin Invest, 130*(8), 4195-4212. doi:10.1172/JCI136174

Saver, J. L., Goyal, M., van der Lugt, A., Menon, B. K., Majoie, C. B., Dippel, D. W., Campbell, B. C., Nogueira, R. G., Demchuk, A. M., Tomasello, A., Cardona, P., Devlin, T. G., Frei, D. F., du Mesnil de Rochemont, R., Berkhemer, O. A., Jovin, T. G., Siddiqui, A. H., van Zwam, W. H., Davis, S. M., Castano, C., Sapkota, B. L., Fransen, P. S., Molina, C., van Oostenbrugge, R. J., Chamorro, A., Lingsma, H., Silver, F. L., Donnan, G. A., Shuaib, A., Brown, S., Stouch, B., Mitchell, P. J., Davalos, A., Roos, Y. B., Hill, M. D., & Collaborators, H. (2016). Time to Treatment With Endovascular Thrombectomy and Outcomes From Ischemic Stroke: A Meta-analysis. *JAMA, 316*(12), 1279-1288. doi:10.1001/jama.2016.13647

Savitz, S. I., Baron, J. C., Yenari, M. A., Sanossian, N., & Fisher, M. (2017). Reconsidering Neuroprotection in the Reperfusion Era. *Stroke, 48*(12), 3413-3419. doi:10.1161/STROKEAHA.117.017283

Schlattmann, P., & Dirnagl, U. (2010). Statistics in experimental cerebrovascular research: comparison of more than two groups with a continuous outcome variable. *J Cereb Blood Flow Metab, 30*(9), 1558-1563. doi:jcbfm201095 [pii] 10.1038/jcbfm.2010.95

Schmitz, A., Sankaranarayanan, A., Azam, P., Schmidt-Lassen, K., Homerick, D., Hansel, W., & Wulff, H. (2005). Design of PAP-1, a selective small molecule Kv1.3 blocker, for the suppression of effector memory T cells in autoimmune diseases. *Mol Pharmacol, 68*, 1254-1270.

Smith, W. S., & Furlan, A. J. (2016). Brief History of Endovascular Acute Ischemic Stroke Treatment. *Stroke, 47*(2), e23-26. doi:10.1161/STROKEAHA.115.010863

Tarcha, E. J., Chi, V., Munoz-Elias, E. J., Bailey, D., Londono, L. M., Upadhyay, S. K., Norton, K., Banks, A., Tjong, I., Nguyen, H., Hu, X., Ruppert, G. W., Boley, S. E., Slauter, R., Sams, J., Knapp, B., Kentala, D., Hansen, Z., Pennington, M. W., Beeton, C., Chandy, K. G., & Iadonato, S. P. (2012). Durable pharmacological responses from the peptide drug ShK-186, a specific Kv1.3 channel inhibitor that suppresses T cell mediators of autoimmune disease. *J Pharmacol Exp Ther*. doi:10.1124/jpet.112.191890

Unterweger, A. L., Jensen, M. O., Giordanetto, F., Jogini, V., Ruschher, A., Seuss, M., Winkelmann, P., Koletzko, L., Shaw, D. E., Siebeck, M., Gropp, R., Beigel, F., & Aszodi, A. (2021). Suppressing Kv1.3 Ion Channel Activity with a Novel Small Molecule Inhibitor Ameliorates Inflammation in a Humanised Mouse Model of Ulcerative Colitis. *J Crohns Colitis, 15*(11), 1943-1958. doi:10.1093/ecco-jcc/jjab078

Vandesompele, J., De Preter, K., Pattyn, F., Poppe, B., Van Roy, N., De Paepe, A., & Speleman, F. (2002). Accurate normalization of real-time quantitative RT-PCR data by geometric averaging of multiple internal control genes. *Genome Biol, 3*(7), RESEARCH0034. doi:10.1186/gb-2002-3-7-research0034

Weinstein, J. R., Koerner, I. P., & Moller, T. (2010). Microglia in ischemic brain injury. *Future Neurol, 5*(2), 227-246. doi:10.2217/fnl.10.1

Zhou, Y., He, Y., Yan, S., Chen, L., Zhang, R., Xu, J., Hu, H., Liebeskind, D. S., & Lou, M. (2023). Reperfusion Injury Is Associated With Poor Outcome in Patients With Recanalization After Thrombectomy. *Stroke, 54*(1), 96-104. doi:10.1161/STROKEAHA.122.039337

Figures

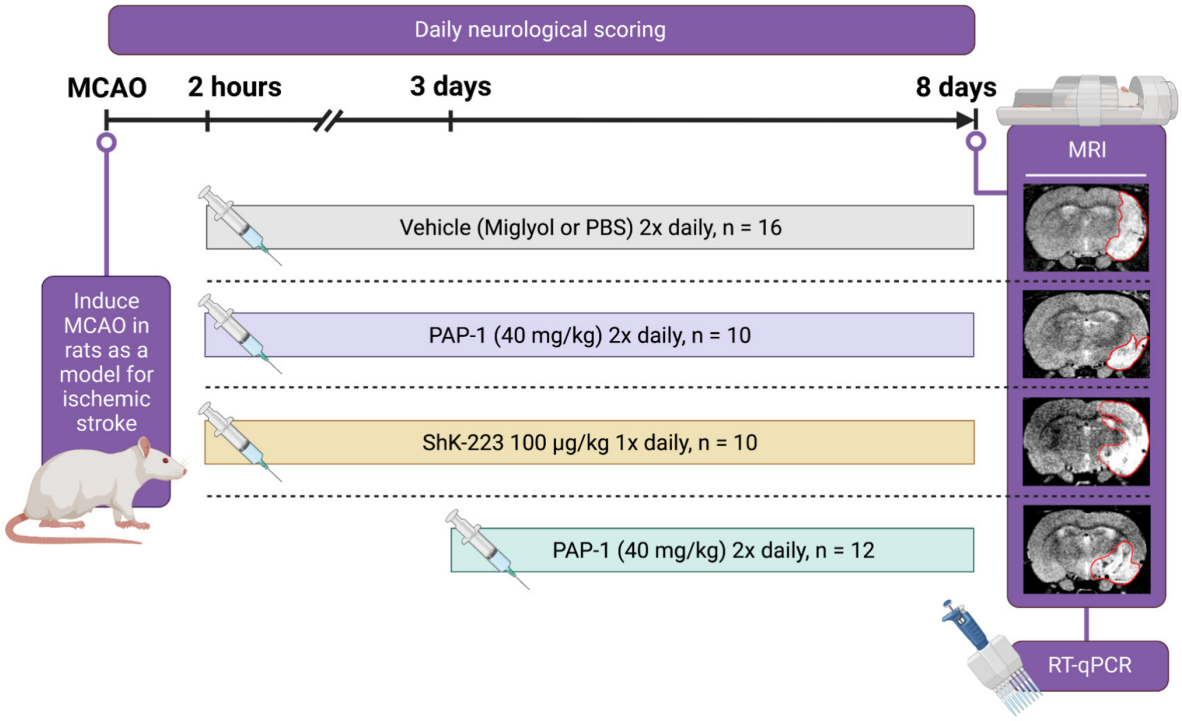

Figure 1. Experimental Paradigm. Cartoon showing the experimental design, the timeline and the treatment groups.

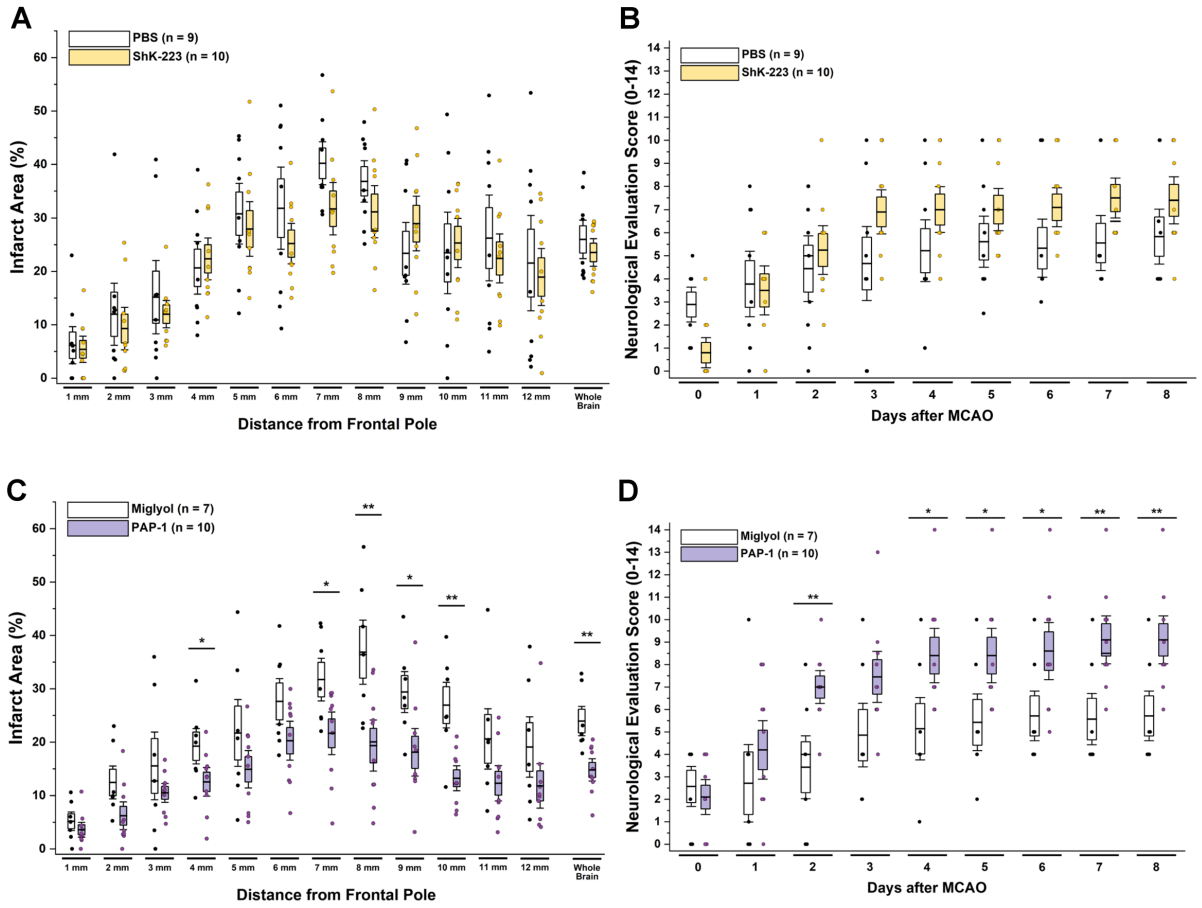

Figure 2. The $K_V1.3$ blocker PAP-1 but not the peptide ShK-223 reduces infarction and improves neurological deficit in adult male rats. (A) Infarct area and **(B)** neurological deficit score in PBS (n = 9) compared to ShK-223 (100 μg/kg; n = 10) treated male Wistar rat. **(C)** Infarct area and **(D)** neurological deficit score in miglyol vehicle (n = 7) compared to PAP-1 (40 mg/kg; n = 10) treated male rats (*P* = 0.002 for infarct, *P* =0.009 for NES on day-8). Data are shown as whisker plots with data from individual animals overlayed as scatter. The boxes show mean ± S.E.M; the whiskers show confidence intervals.

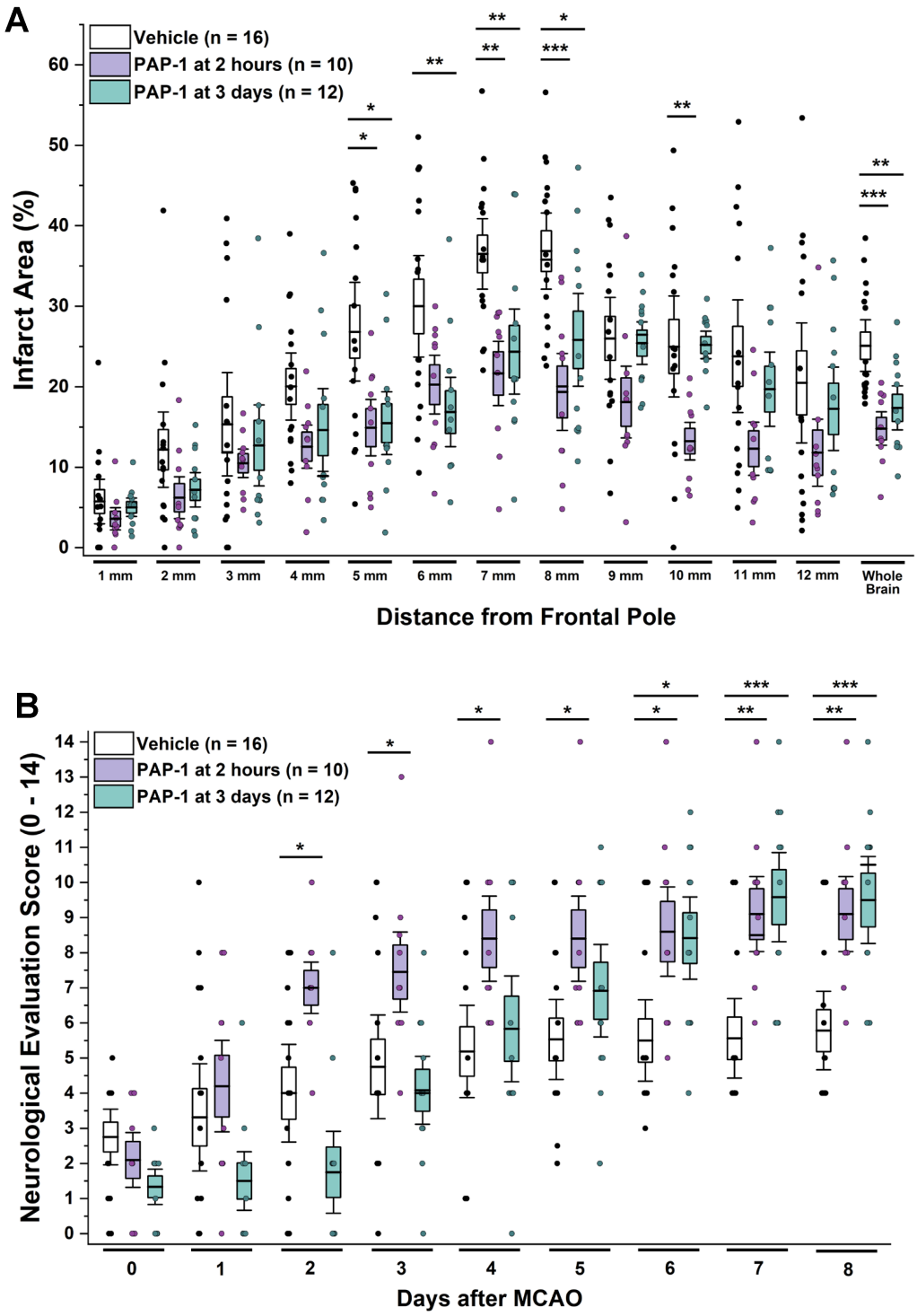

Figure 3. $K_V1.3$ inhibition with PAP-1 still improves MCAO outcomes when administration is started 3 days after reperfusion. (A) Infarct area and **(B)** neurological deficit score in vehicle treated male Wistar rats (n = 16) compared to animals treated with 40 mg/kg PAP-1 started at 2

hours (n = 10, *P* = 0.0004 for infarct, *P* =0.005 for NES on day-8) or started at 3 days (n = 12, *P* = 0.005 for infarct, *P* =0.0009 for NES on day-8) after reperfusion. Data are shown as whisker plots with data from individual animals overlayed as scatter. The boxes show mean ± S.E.M; the whiskers show confidence intervals. PAP-1 started at 2 hours was not significantly different from PAP-1 started at 3 days.

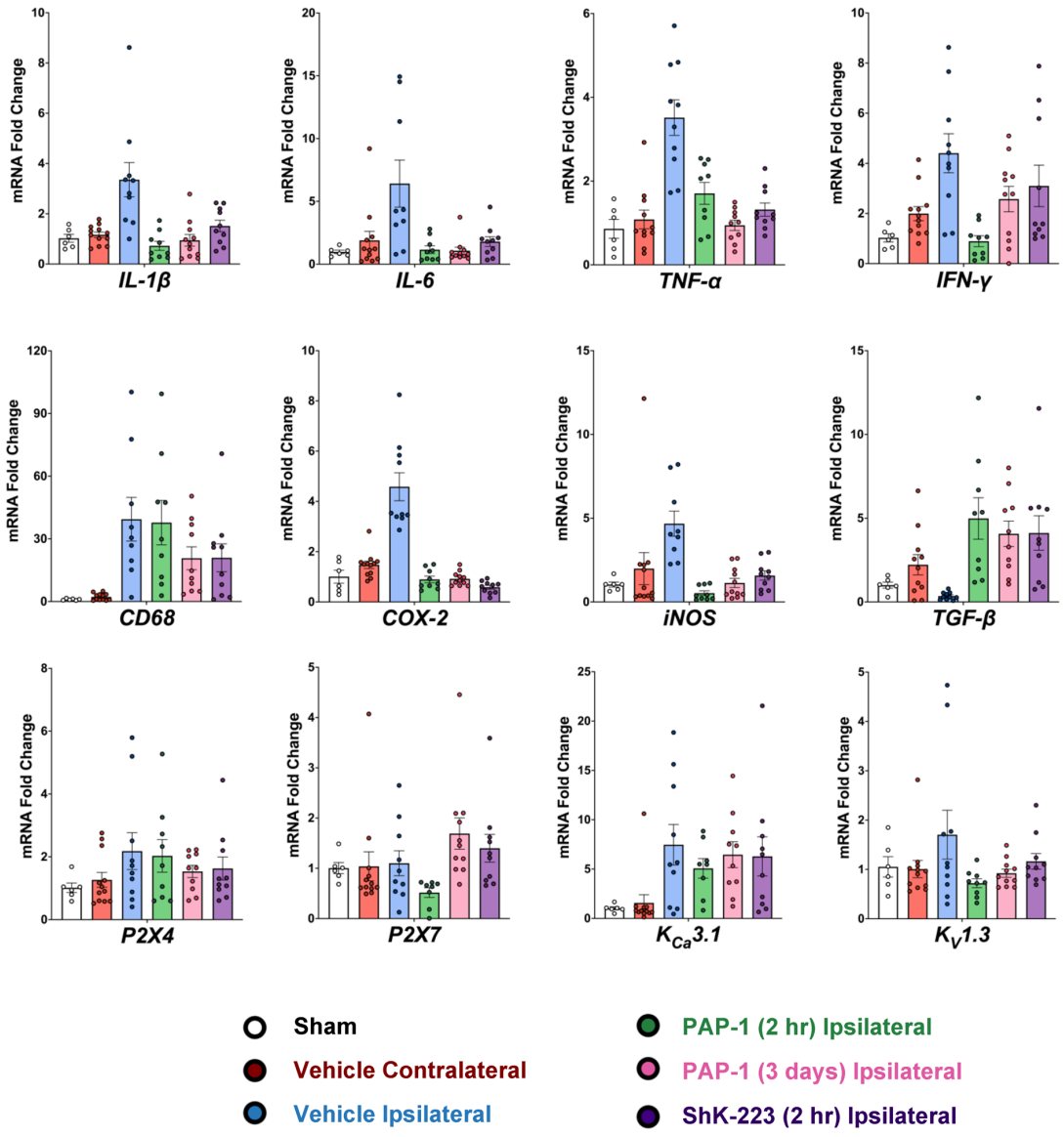

Figure 4. Blocking $K_V1.3$ with a brain-penetrant small molecule, PAP-1, and brain-impermeable peptide, ShK-223, both reduce pro-inflammatory cytokines in-vivo at 2 hours and 3 days, as measured by RT-qPCR. mRNA expression levels are reported as a fold-change respective to the ipsilateral hemisphere of vehicle-treated MCAO mice. Values were normalized to sham rat brain and to the geometric mean of three housekeeping genes, *β-actin*, *ywhaz*, and *hmbs*. Data was analyzed with one-way ANOVA followed by Dunnett's test and are shown as mean ± S.E.M; the whiskers show confidence intervals. For full statistics see Supplementary Table 3.

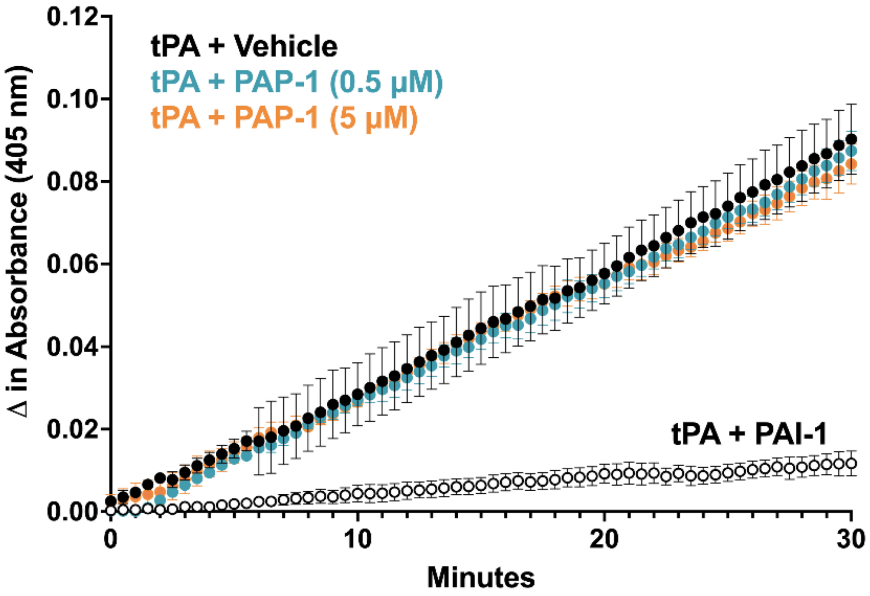

Figure 5. PAP-1 does not interfere with tPA activity in vitro. PAP-1 at 0.5 μM and 5 μM does not inhibit tPA activity as measured by increases in absorbance at 405 nm of a chromogenic tPA substrate. Each data point shown is the average of three independent experimental runs ± S.E.M. Each reaction was performed in triplicate wells.

Supplementary Tables and Figures

Gene	F Primer	R Primer
il1b	CACCTCTCAAGCAGAGCACAG	GGGTTCCATGGTGAAGTCAAC
il6	TCCTACCCCAACTTCCAATGCTC	TTGGATGGTCTTGGTCCTTAGCC
cd68	CTCATCATTGGCCTGGTCCT	GTTGATTGTCGTCTGCGGG
cox2	TGTATGCTACCATCTGGCTTCGG	GTTTGGAACAGTCGCTCGTCATC
ifng	ATGAGTGCTACACGCCGCGTCTTGG	GAGTTCATTGACAGCTTTGTGCTGG
inos	GACCAGAAACTGTCTCACCTG	CGAACATCGAACGTCTCACA
tnfa	AAATGGGCTCCCTCTCATCAGTTC	TCTGCTTGGTGGTTTGCTACGAC
tgfb	CAAAGACATCACACACAGTA	GGTGTTGAGCCCTTTCCAGG
*il2**	CATGTACAGCATGCAGCTCGCATCC	CCACCACAGTTGCTGGCTCATCATC
*il4**	TGCACCGAGATGTTTGTACC	GGATGCTTTTTAGGCTTTCC
*il10**	GCAGGACTTTAAGGGTTACTTGG	GGGGAGAAATCGATGACAGC
*il17a**	CTACCTCAACCGTTCCACT	TTCTCAGGCTCCCTCTTC

Gene	Biorad Unique Assay ID
actb	qRnoCID0056984
hmbs	qRnoCED0057013
ywhaz	qRnoCID0056990
kcnn4	qRnoCID0003361
kcna3	qRnoCED0018850
p2rx4	qRnoCID0003238
p2rx7	qRnoCID0007779

*These primers did not work in our hands.

Supplementary Table 1. Primer sequences for the RT-qPCR experiments.

Gene	PrimePCR Unique Assay ID
actb	qRnoCID0056984
b2m	qRnoCED0056999
camlg	qRnoCED0009273
cd163	qRnoCID0008321
gapdh	qRnoCID0057018
hmbs	qRnoCED0057013
hprt1	qRnoCED0057020
pgk1	qRnoCED0002588
polr2a	qRnoCED0007537
ppib	qRnoCED0006997
ppox	qRnoCED0012992
rpl13a	qRnoCED0056993
rps13	qRnoCED0002931
rps18	qRnoCED0003920
sdha	qRnoCID0057011
tubb5	qRnoCED0053789
ywhaz	qRnoCID0056990

Supplementary Table 2. Housekeeping Gene plate from BioRad

Treatment group	Samples
Sham	6
Vehicle Contralateral	12
Vehicle Ipsilateral	10
PAP-1 (2 hr) Ipsilateral	9
PAP-1 (3 days) Ipsilateral	11
ShK-223 (2 hr) Ipsilateral	12

il-1b

Dunnett's multiple comparisons test	Mean Diff.	95.00% CI of diff.	P-Value	Summary
Ipsilateral + Vehicle vs. Sham	2.331	0.9230 to 3.739	<0.001	***
Ipsilateral + Vehicle vs. Contralateral + Vehicle	2.19	1.004 to 3.377	<0.001	***
Ipsilateral + Vehicle vs. PAP-1 (2 hour)	2.63	1.357 to 3.904	<0.001	***
Ipsilateral + Vehicle vs. PAP-1 (3 day)	2.412	1.201 to 3.623	<0.001	***
Ipsilateral + Vehicle vs. ShK	1.84	0.6010 to 3.080	0.001	**

il-6

Dunnett's multiple comparisons test	Mean Diff.	95.00% CI of diff.	P-Value	Summary
Ipsilateral + Vehicle vs. Sham	5.436	1.851 to 9.022	0.001	**
Ipsilateral + Vehicle vs. Contralateral + Vehicle	4.524	1.466 to 7.583	0.001	**
Ipsilateral + Vehicle vs. PAP-1 (2 hour)	5.261	1.992 to 8.531	<0.001	***
Ipsilateral + Vehicle vs. PAP-1 (3 day)	5.346	2.229 to 8.463	<0.001	***
Ipsilateral + Vehicle vs. ShK	4.621	1.434 to 7.808	0.002	**

tnfa

Dunnett's multiple comparisons test	Mean Diff.	95.00% CI of diff.	P-Value	Summary
Ipsilateral + Vehicle vs. Sham	2.655	1.582 to 3.727	<0.001	***
Ipsilateral + Vehicle vs. Contralateral + Vehicle	2.431	1.500 to 3.363	<0.001	***
Ipsilateral + Vehicle vs. PAP-1 (2 hour)	1.809	0.8295 to 2.789	<0.001	***
Ipsilateral + Vehicle vs. PAP-1 (3 day)	2.571	1.617 to 3.524	<0.001	***
Ipsilateral + Vehicle vs. ShK	2.195	1.241 to 3.148	<0.001	***

ifng

Dunnett's multiple comparisons test	Mean Diff.	95.00% CI of diff.	P-Value	Summary
Ipsilateral + Vehicle vs. Sham	3.376	1.032 to 5.720	0.002	**
Ipsilateral + Vehicle vs. Contralateral + Vehicle	2.412	0.4320 to 4.392	0.01	*
Ipsilateral + Vehicle vs. PAP-1 (2 hour)	3.512	1.388 to 5.637	<0.001	***
Ipsilateral + Vehicle vs. PAP-1 (3 day)	1.832	-0.1888 to 3.852	0.09	ns
Ipsilateral + Vehicle vs. ShK	1.306	-0.7622 to 3.374	0.38	ns

Cd68

Dunnett's multiple comparisons test	Mean Diff.	95.00% CI of diff.	P-Value	Summary
Ipsilateral + Vehicle vs. Sham	38.4	9.213 to 67.59	0.006	**
Ipsilateral + Vehicle vs. Contralateral + Vehicle	37.15	10.90 to 63.40	0.002	**
Ipsilateral + Vehicle vs. PAP-1 (2 hour)	1.615	-26.44 to 29.68	>0.99	ns
Ipsilateral + Vehicle vs. PAP-1 (3 day)	18.67	-8.676 to 46.02	0.3	ns
Ipsilateral + Vehicle vs. ShK	18.45	-8.901 to 45.80	0.31	ns

cox2

Dunnett's multiple comparisons test	Mean Diff.	95.00% CI of diff.	P-Value	Summary
Ipsilateral + Vehicle vs. Sham	3.581	2.477 to 4.684	<0.001	***
Ipsilateral + Vehicle vs. Contralateral + Vehicle	3.107	2.199 to 4.015	<0.001	***
Ipsilateral + Vehicle vs. PAP-1 (2 hour)	3.688	2.713 to 4.662	<0.001	***
Ipsilateral + Vehicle vs. PAP-1 (3 day)	3.662	2.736 to 4.589	<0.001	***
Ipsilateral + Vehicle vs. ShK	3.997	3.048 to 4.945	<0.001	***

inos

Dunnett's multiple comparisons test	Mean Diff.	95.00% CI of diff.	P-Value	Summary
Ipsilateral + Vehicle vs. Sham	3.634	1.080 to 6.188	0.003	**
Ipsilateral + Vehicle vs. Contralateral + Vehicle	2.684	0.5077 to 4.860	0.01	**
Ipsilateral + Vehicle vs. PAP-1 (2 hour)	4.148	1.821 to 6.475	<0.001	***
Ipsilateral + Vehicle vs. PAP-1 (3 day)	3.541	1.322 to 5.759	<0.001	***
Ipsilateral + Vehicle vs. ShK	3.097	0.8289 to 5.364	0.003	**

tgfb

Dunnett's multiple comparisons test	Mean Diff.	95.00% CI of diff.	P-Value	Summary
Ipsilateral + Vehicle vs. Sham	-0.6499	-3.937 to 2.638	0.98	ns
Ipsilateral + Vehicle vs. Contralateral + Vehicle	-1.869	-4.955 to 1.217	0.42	ns
Ipsilateral + Vehicle vs. PAP-1 (2 hour)	-4.63	-7.876 to -1.385	0.002	**
Ipsilateral + Vehicle vs. PAP-1 (3 day)	-3.716	-6.875 to -0.5573	0.01	*
Ipsilateral + Vehicle vs. ShK	-3.764	-6.922 to -0.6049	0.01	*

p2x4

Dunnett's multiple comparisons test	Mean Diff.	95.00% CI of diff.	P-Value	Summary
Ipsilateral + Vehicle vs. Sham	1.166	-0.4555 to 2.787	0.24	ns
Ipsilateral + Vehicle vs. Contralateral + Vehicle	0.9141	-0.4772 to 2.305	0.34	ns
Ipsilateral + Vehicle vs. PAP-1 (2 hour)	0.1509	-1.342 to 1.644	>0.99	ns
Ipsilateral + Vehicle vs. PAP-1 (3 day)	0.6475	-0.8057 to 2.101	0.72	ns
Ipsilateral + Vehicle vs. ShK	0.5527	-0.9005 to 2.006	0.83	ns

p2x7

Dunnett's multiple comparisons test	Mean Diff.	95.00% CI of diff.	P-Value	Summary
Ipsilateral + Vehicle vs. Sham	0.09769	-1.014 to 1.210	>0.99	ns
Ipsilateral + Vehicle vs. Contralateral + Vehicle	0.06285	-0.9863 to 1.112	>0.99	ns
Ipsilateral + Vehicle vs. PAP-1 (2 hour)	0.584	-0.5783 to 1.746	0.61	ns
Ipsilateral + Vehicle vs. PAP-1 (3 day)	-0.5905	-1.661 to 0.4801	0.52	ns
Ipsilateral + Vehicle vs. ShK	-0.2983	-1.394 to 0.7975	0.96	ns

kcnn4

Dunnett's multiple comparisons test	Mean Diff.	95.00% CI of diff.	P-Value	Summary
Ipsilateral + Vehicle vs. Sham	6.439	0.3250 to 12.55	0.04	*
Ipsilateral + Vehicle vs. Contralateral + Vehicle	5.896	0.6723 to 11.12	0.02	*
Ipsilateral + Vehicle vs. PAP-1 (2 hour)	2.393	-3.394 to 8.180	0.78	ns
Ipsilateral + Vehicle vs. PAP-1 (3 day)	1.007	-4.449 to 6.463	>0.99	ns
Ipsilateral + Vehicle vs. ShK	1.175	-4.281 to 6.631	0.99	ns

kcna3

Dunnett's multiple comparisons test	Mean Diff.	95.00% CI of diff.	P-Value	Summary
Ipsilateral + Vehicle vs. Sham	0.6518	-0.3841 to 1.688	0.35	ns
Ipsilateral + Vehicle vs. Contralateral + Vehicle	0.6974	-0.1631 to 1.558	0.16	ns
Ipsilateral + Vehicle vs. PAP-1 (2 hour)	0.9841	0.06075 to 1.907	0.03	*
Ipsilateral + Vehicle vs. PAP-1 (3 day)	0.7824	-0.09568 to 1.660	0.1	ns
Ipsilateral + Vehicle vs. ShK	0.5407	-0.3581 to 1.439	0.43	ns

Supplementary Table 3. Statistics for the RT-qPCR experiments.

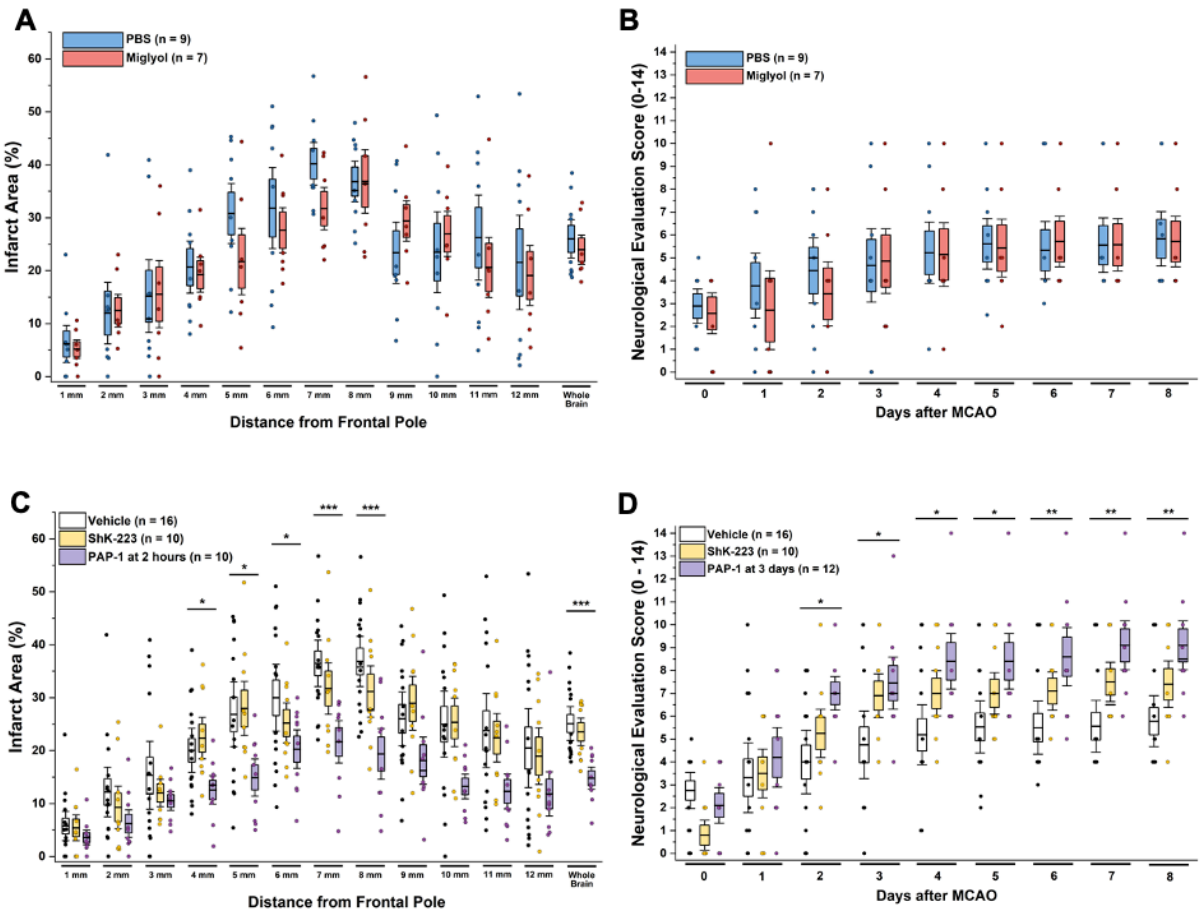

Supplementary Figure 1. The $K_V1.3$ blocker PAP-1 but not the peptide ShK-223 reduces infarction and improves neurological deficit in adult male rats. (A) Infarct area and **(B)** neurological deficit score in PBS (n = 9) compared to miglyol (n = 7) treated male Wistar rats demonstrating that there is no difference between the two vehicles. **(C)** Infarct and **(D)** neurological deficit score in vehicle treated male Wistar rats (n = 16) compared to PAP-1 (40 mg/kg; n = 10, *P* = 0.0004 for infarct, *P* = 0.003 for NES on day-8) treated rats and to ShK-223 (100 μg/kg; n = 10, *P* = 0.79103 for infarct, *P* = 0.2040 for NES on day-8) treated male Wistar rats. Data are shown as whisker plots with data from individual animals overlayed as scatter. The boxes show mean ± S.E.M, the whiskers show confidence intervals.

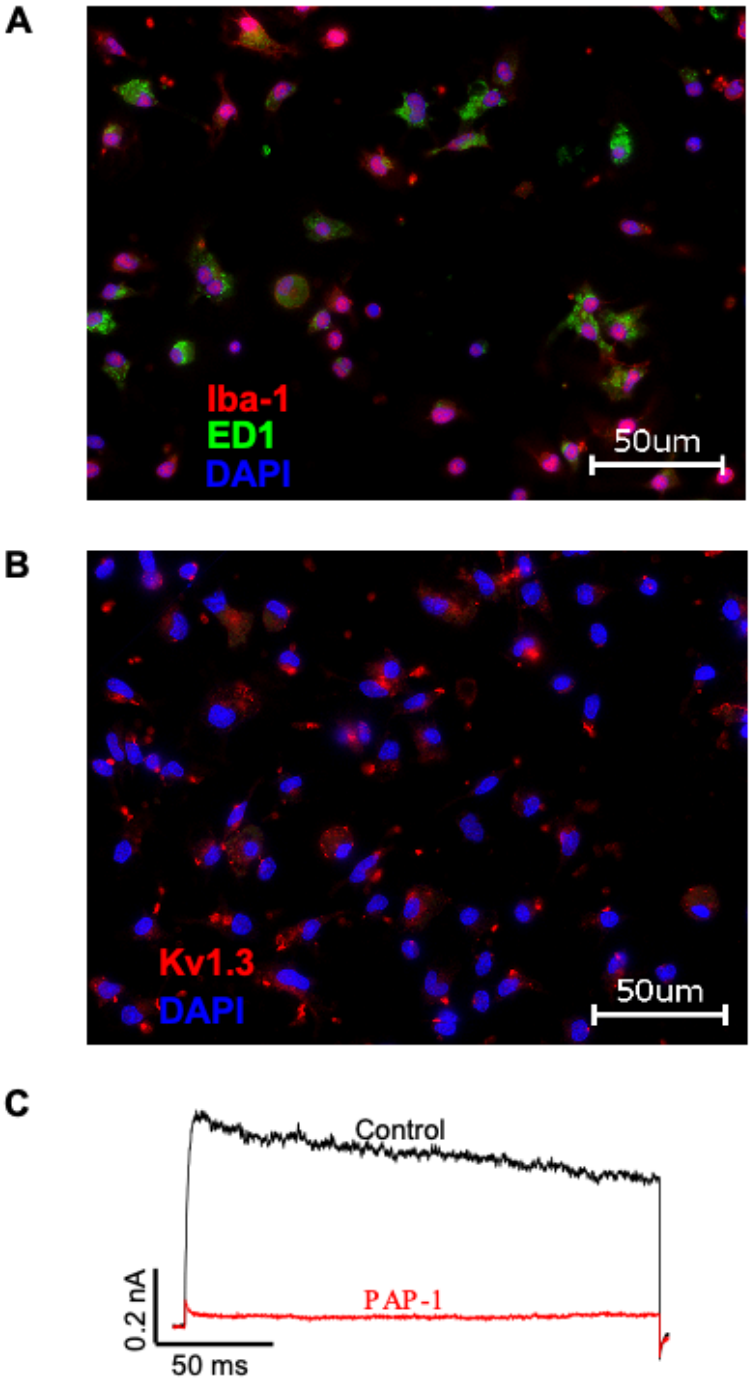

Supplementary Figure 2. Acutely isolated CD11b+ cells from the infarcted hemisphere on day-8 after MCAO in rats express $K_V1.3$ as determined by immunofluorescence and electrophysiology. Brain tissue was dissociated enzymatically with a Neural Tissue Dissociation Kit (Miltenyi Biotec), microglia isolated using anti-CD11b magnetic beads (Miltenyi Biotec) as

described previously [13] and plated on poly-L-lysine coated coverslips, permeabilized with 4% buffered formalin and then stained. **(A)** All isolated cells are positive for Iba-1 (rabbit anti-Iba1, Cat#019-19741,Wako 1:3000; secondary antibody is Alexa Fluo®546 goat anti-rabbit IgG(H+L), Cat# A11010, Life Technologies,1:1000) and many activated cells are positive for ED1 (= CD68; mouse anti-rat-CD68; Cat# MCA341R, Bio-Rad. 1:1000; secondary antibody is Alexa Fluo®488 donkey anti-mouse IgG(H+L), Cat# A21202, Life Technologies,1:1000). **(B)** Many activated cells stain for $K_V1.3$ (rabbit anti-$K_v1.3$, Cat# APC101, Alomone Labs 1:1000; secondary antibody is Alexa Fluo®546 goat Anti-rabbit IgG(H+L), Cat# A11010, Life Technologies,1:1000). **(C)** K_V currents were elicited by a 200-ms step pulse from -80 mV to + 40 mV as described [13]. The current is blocked completely by 1 μM of PAP-1.

CHAPTER 4

OUTLOOK

Conclusions and Future Directions

Most people in the general population understand that ischemic stroke is a major concern in the United States due to its impact on morbidity and mortality, and this dissertation is focused on discussing how we can use the science behind its pathophysiology to create tools (animal models) for studying its mechanisms and researching potential therapeutics to translate into human patients. Beyond the science, however—in an attempt to provide a multi-faceted argument as to why more research, discussions, and funding are needed to advance stroke research—it is also important to briefly discuss the economic burden of ischemic stroke for answering why improving stroke outcomes "pays off."

The economic burden of ischemic stroke includes both direct medical costs, such as hospitalization, medications, and rehabilitation, as well as indirect costs, such as lost productivity and disability-adjusted life years (DALYs). Using aggregate data from ischemic stroke patients of all age groups from the USA from 2003 to 2014, Girotra et al. (2019) showed that the estimated total direct and indirect costs of stroke in the United States was $103.5 billion per year. This includes $35 billion annually in direct medical costs, $38.1 billion annually in lost productivity due to disability, and $30.4 billion annually in lost productivity due to premature death (Girotra,

Lekoubou, Bishu, & Ovbiagele, 2019). According to the American Heart Association, the estimated per-patient lifetime cost of stroke in the United States is approximately $140,000 (Go et al., 2014).

The economic burden of ischemic stroke is not evenly distributed across all populations, with some groups experiencing a disproportionate burden (Brown et al., 2006). For example, minority populations, particularly African Americans and Hispanic Americans, have higher rates of stroke and are more likely to experience poor outcomes and greater disability compared to white Americans. Ikema et al. found that African Americans and Hispanic Americans had longer wait times at the emergency department, lower rates of treatment either with tPA or EVT even after controlling for stroke severity, and were less likely to be referred to endovascular-capable centers or another acute stroke care facility compared to White patients (Ikeme, Kottenmeier, Uzochukwu, & Brinjikji, 2022). Additionally, stroke patients and their families may face significant financial strain due to the costs of ongoing medical care, rehabilitation, and disability, which disproportionately affects individuals of lower socioeconomic statuses, and in turn, specific minority groups (Bravata et al., 2005).

Despite the high financial burden of ischemic stroke, studies have shown that stroke research is severely underfunded when compared to diseases like cancer and congestive heart failure (Pendlebury et al., 2004). The 2017 U.S. Census Bureau National Populations Projections states that in 2034, all baby boomers will be 65 years old or older and will outnumber children under 18 years old ("U.S. Census Bureau Population Projections," 2017). With this projected rapid increase in the elderly population, the total incidence of stroke is also expected to increase accordingly. There is no better time like the present for thinking about how to prepare for the future. We must be actively thinking about strategies for adapting to a new reality that also includes more stroke therapeutic options and improved clinical outcomes at later time points.

Overview of each chapter

In Chapter 1, we start by discussing the different types of ischemic strokes and how and why we use rodents to model MCA infarcts in humans (which represents the most common type of ischemic stroke). We also examine the pathophysiology of how an ischemic insult evolves from the ischemic core to the penumbra and discuss how the temporal evolution of this process compares in rodents versus in human patients. We subsequently explore the time courses of cerebral edema and inflammation and compare stroke functional outcome assessments in both humans and rodents. This chapter aimed to show the benefits and challenges of rodent models as a tool for enabling stroke research and drug development and how the time course of stroke in human patients, generally, progresses much more slowly compared to rodents. We also intended to prime the reader in thinking about what barriers currently exist for translating a stroke drug from the preclinical to clinical stages, and for repurposed drugs, what is actually necessary in order to make this transition. For scenarios regarding a repurposed drug or a drug with extensive safety and animal testing, we asked the question of whether translation can happen faster? Lastly, we introduced $K_V1.3$ and $K_{Ca}3.1$ as potential drug targets for immunocytoprotection in ischemic stroke, given their roles in the peripheral immune system (T cells) and central nervous system (microglia).

In Chapter 2, we evaluate the potential of repurposing senicapoc, a $K_{Ca}3.1$ blocker, for ischemic stroke. In 2011, senicapoc failed in Phase III clinical trials for sickle cell anemia (Ataga et al., 2011), but demonstrated that it is a safe drug in human patients. Here, we show that it is an attractive stroke drug candidate because it reduces infarct volume and improves neurological deficit at 8 days after stroke, when administered at two time points, after 3 hours and 12 hours post-transient (60 minutes) MCAO in adult male mice. We also found that senicapoc targets

microglia and infiltrating T cells from the periphery (via decreased Iba1$^+$ and CD3 staining$^+$), both of which have large roles in neuroinflammation in stroke (Y.-J. Chen et al., 2016; Y.-J. Chen, Raman, Bodendiek, O'Donnell, & Wulff, 2011). Mechanistically, we show that senicapoc inhibited $K_{Ca}3.1$ currents in a microglia cell line by regulating calcium signaling. And in two other in-vitro experiments, we demonstrate that: senicapoc inhibits inflammatory cytokines when a microglia cell line was stimulated with a lipopolysaccharide (a bacterial cell-wall derivative that promotes inflammation), and senicapoc does not interfere with tPA. Taken together, we show that senicapoc is a good candidate for repurposing as an immunocytoprotective drug when used in conjunction with EVT for ischemic stroke. Nonetheless, more work still needs to be done before translation into human patients. Future studies should expand on testing senicapoc's efficacy in female and senescent rodents, rodents with comorbidities, and on exploring senicapoc's window of therapeutic effect past 12 hours after reperfusion (Lee et al., 2023).

We transition to discussing another K^+ channel inhibitor in Chapter 3, where we explore the treatment window of PAP-1, a brain-penetrant $K_V1.3$ blocker, for ischemic stroke. In previous work, we showed that PAP-1, when given 12 hours after reperfusion, reduces infarct size and improves neurological deficits 8 days after MCAO in adult male mice and rats (Y. Chen, Nguyen, Maezawa, Jin, & Wulff, 2018). A few years later, we expanded on this work and further validated $K_V1.3$ as good drug target for ischemic stroke with MCAO experiments in young and senescent mice of both sexes, in addition to a $K_V1.3$ knockout mouse (Y. J. Chen, Cui, Singh, & Wulff, 2021). We demonstrate in this study that PAP-1 continues to be beneficial when given at earlier and later time points (2 hours and 3 days after reperfusion). We show these effects both with in-vitro assessments of inflammatory marker expression and in-vivo assessments of infarct size and neurological testing. We specifically chose 3 days because we previously demonstrated that microglia/macrophages (isolated with CD11b$^+$ beads from ischemic stroke brains) start increasing in number at 2 days after MCAO and reach a peak around 8 days post-stroke (Y. Chen et al.,

2018); 3 days after reperfusion is an early time point in this uphill rise in microglia. Mechanistically, we also demonstrate that $K_V1.3$ blockers must cross the BBB to have benefit in reducing inflammation in ischemic stroke by comparing PAP-1 to another non-brain-penetrant peptidic $K_V1.3$ blocker, ShK-223. Here, ShK-223 was able to reduce inflammatory marker expression (likely produced from infiltrating peripheral immune cells), but failed to reduce infarct size and improve neurological function. Lastly, we showed that PAP-1, like senicapoc, does not interfere with tPA activity in-vitro. Overall, our work shows that PAP-1 has a wide therapeutic window and can be another potential immunomodulating therapeutic for ischemic stroke. Like with senicapoc, future studies should focus on elucidating PAP-1's effects on MCAO animals with comorbidities like diabetes, atherosclerosis, or hypertension in an effort to better mimic the human condition.

Future directions

In this body of work, we show that both $K_V1.3$ and $K_{Ca}3.1$ are attractive potential drug candidates for ischemic stroke, and we allude to what future research should focus on for each of the channels in the text above.

Comparing the two channels, sometimes I wonder which of the two may work better than the other in improving stroke outcomes. As of yet, the short answer is that it is still unclear. Senicapoc has an advantage having already shown safety in humans, but on the other hand, there is much more preclinical research specific to ischemic stroke for PAP-1. Also of note, all of the stroke work for both channels has been conducted in animal or in in-vitro models, despite senicapoc's tumultuous history as a failed clinical trial drug—so we might not be able to compare how they truly fare until we cross into the realm of clinical research. After all, our overarching goal is demonstrating our drugs improve stroke outcomes in humans, not rodents. Personally, I would like to see PAP-1 and senicapoc represent different treatment arms of a multi-arm acute stroke

randomized clinical trial so that we can assess their performance side-by-side. I would also like to see what effects a combination of both senicapoc and PAP-1, would have on ischemic stroke and how this combination compares to the drugs when given alone.

Mechanistically, it would also be beneficial to investigate further the contribution neuroinflammation (whether from the periphery or from the central nervous system) plays in patients who experience clinical deficits that are disproportionately severe relative to their infarct volumes, even after receiving standard of care therapies like EVT and tPA (Nogueira et al., 2018).

As new technologies and standards of care arise for ischemic stroke, preclinical research strategies, therapeutics, imaging modalities, and outcome assessments must adapt to the ever-shifting, rapidly evolving stroke "playing field." One prime example that our aforementioned K^+ channel blockers take advantage of—the introduction of EVT since it was first approved in 1995 (Smith & Furlan, 2016) has spurred the re-thinking of stroke therapeutics as an adjunct to reperfusion therapy (Savitz, Baron, Yenari, Sanossian, & Fisher, 2017). As human life expectancies continue to increase (Crimmins, 2015), ischemic strokes will likely become more prevalent, and I anticipate that there will probably be more EVT-capable centers available for providing endovascular interventions to meet this demand (Alberts et al., 2005). As a result, two possible domino effects include: a decrease in "door-to-knife" times, and subsequently, an increase in number of patients with reperfusion injury. Additional preclinical and clinical research focused on mitigating reperfusion injury is just one of many promising developments on the horizon that have the potential to significantly improve stroke prevention, diagnosis, and treatment.

References

Alberts, M. J., Latchaw, R. E., Selman, W. R., Shephard, T., Hadley, M. N., Brass, L. M., Koroshetz, W., Marler, J. R., Booss, J., Zorowitz, R. D., Croft, J. B., Magnis, E., Mulligan, D., Jagoda, A., O'Connor, R., Cawley, C. M., Connors, J. J., Rose-DeRenzy, J. A., Emr, M., Warren, M., & Walker, M. D. (2005). Recommendations for Comprehensive Stroke Centers. *Stroke, 36*(7), 1597-1616. doi:10.1161/01.STR.0000170622.07210.b4

Ataga, K. I., Reid, M., Ballas, S. K., Yasin, Z., Bigelow, C., James, L. S., Smith, W. R., Galacteros, F., Kutlar, A., Hull, J. H., Stocker, J. W., & Investigators, I.-.-S. (2011). Improvements in haemolysis and indicators of erythrocyte survival do not correlate with acute vaso-occlusive crises in patients with sickle cell disease: a phase III randomized, placebo-controlled, double-blind study of the Gardos channel blocker senicapoc (ICA-17043). *British Journal of Haematology, 153*(1), 92-104. doi:doi: 10.1111/j.1365-2141.2010.08520.x.

Bravata, D. M., Wells, C. K., Gulanski, B., Kernan, W. N., Brass, L. M., Long, J., & Concato, J. (2005). Racial Disparities in Stroke Risk Factors. *Stroke, 36*(7), 1507-1511. doi:10.1161/01.STR.0000170991.63594.b6

Brown, D. L., Boden-Albala, B., Langa, K. M., Lisabeth, L. D., Fair, M., Smith, M. A., Sacco, R. L., & Morgenstern, L. B. (2006). Projected costs of ischemic stroke in the United States. *Neurology, 67*(8), 1390-1395. doi:10.1212/01.wnl.0000237024.16438.20

Chen, Y., Nguyen, H., Maezawa, I., Jin, L., & Wulff, H. (2018). Inhibition of the potassium channel Kv1.3 reduces infarction and inflammation in ischemic stroke. *Ann Clin Transl Neurol, 5*, 147-161.

Chen, Y.-J., Nguyen, H. M., Maezawa, I., Grössinger, E. M., Garing, A. L., Köhler, R., Jin, L.-W., & Wulff, H. (2016). The potassium channel KCa3.1 constitutes a pharmacological target for neuroinflammation associated with ischemia/reperfusion stroke. *Journal of cerebral blood flow and metabolism : official journal of the International Society of Cerebral Blood Flow and Metabolism, 36*(12), 2146-2161. doi:doi: 10.1177/0271678X15611434

Chen, Y.-J., Raman, G., Bodendiek, S., O'Donnell, M. E., & Wulff, H. (2011). The KCa3.1 blocker TRAM-34 reduces infarction and neurological deficit in a rat model of ischemia/reperfusion stroke. *Journal of cerebral blood flow and metabolism : official journal of the International Society of Cerebral Blood Flow and Metabolism, 31*(12), 2363-2374. doi:doi: 10.1038/jcbfm.2011.101

Chen, Y. J., Cui, Y., Singh, L., & Wulff, H. (2021). The potassium channel Kv1.3 as a therapeutic target for immunocytoprotection after reperfusion. *Annals of Clinical and Translational Neurology, 8*(10), 2070-2082. doi:10.1002/acn3.51456

Crimmins, E. M. (2015). Lifespan and Healthspan: Past, Present, and Promise. *The Gerontologist, 55*(6), 901-911. doi:10.1093/geront/gnv130

Girotra, T., Lekoubou, A., Bishu, K., & Ovbiagele, B. (2019). Abstract 73: The True Cost of Stroke: Assessment of Direct and Indirect Cost of Stroke Among All Age Groups in United States of America From 2003 to 2014. *Stroke, 50*(Suppl_1). doi:10.1161/str.50.suppl_1.73

Go, A. S., Mozaffarian, D., Roger, V. L., Benjamin, E. J., Berry, J. D., Blaha, M. J., Dai, S., Ford, E. S., Fox, C. S., Franco, S., Fullerton, H. J., Gillespie, C., Hailpern, S. M., Heit, J. A., Howard, V. J., Huffman, M. D., Judd, S. E., Kissela, B. M., Kittner, S. J., Lackland, D. T., Lichtman, J. H., Lisabeth, L. D., Mackey, R. H., Magid, D. J., Marcus, G. M., Marelli, A., Matchar, D. B., McGuire, D. K., Mohler, E. R., Moy, C. S., Mussolino, M. E., Neumar, R. W., Nichol, G., Pandey, D. K., Paynter, N. P., Reeves, M. J., Sorlie, P. D., Stein, J., Towfighi, A., Turan, T. N., Virani, S. S., Wong, N. D., Woo, D., & Turner, M. B. (2014). Executive Summary: Heart Disease and Stroke Statistics—2014 Update. *Circulation, 129*(3), 399-410. doi:10.1161/01.cir.0000442015.53336.12

Ikeme, S., Kottenmeier, E., Uzochukwu, G., & Brinjikji, W. (2022). Evidence-Based Disparities in Stroke Care Metrics and Outcomes in the United States: A Systematic Review. *Stroke, 53*(3), 670-679. doi:10.1161/strokeaha.121.036263

Lee, R. D., Chen, Y.-J., Nguyen, H. M., Singh, L., Dietrich, C. J., Pyles, B. R., Cui, Y., Weinstein, J. R., & Wulff, H. (2023). Repurposing the KCa3.1 Blocker Senicapoc for Ischemic Stroke. *Translational Stroke Research*. doi:10.1007/s12975-023-01152-6

Nogueira, R. G., Jadhav, A. P., Haussen, D. C., Bonafe, A., Budzik, R. F., Bhuva, P., Yavagal, D. R., Ribo, M., Cognard, C., Hanel, R. A., Sila, C. A., Hassan, A. E., Millan, M., Levy, E. I., Mitchell, P., Chen, M., English, J. D., Shah, Q. A., Silver, F. L., Pereira, V. M., Mehta, B. P., Baxter, B. W., Abraham, M. G., Cardona, P., Veznedaroglu, E., Hellinger, F. R., Feng, L., Kirmani, J. F., Lopes, D. K., Jankowitz, B. T., Frankel, M. R., Costalat, V., Vora, N. A., Yoo, A. J., Malik, A. M., Furlan, A. J., Rubiera, M., Aghaebrahim, A., Olivot, J.-M., Tekle, W. G., Shields, R., Graves, T., Lewis, R. J., Smith, W. S., Liebeskind, D. S., Saver, J. L., & Jovin, T. G. (2018). Thrombectomy 6 to 24 Hours after Stroke with a Mismatch between Deficit and Infarct. *New England Journal of Medicine, 378*(1), 11-21. doi:10.1056/NEJMoa1706442

Pendlebury, S. T., Rothwell, P. M., Algra, A., Ariesen, M.-J., Bakac, G., Czlonkowska, A., Dachenhausen, A., Krespi, Y., Kõrv, J., Krolikowski, K., Kulesh, S., Michel, P., Thomassen, L., Bogousslavsky, J., & Brainin, M. (2004). Underfunding of Stroke Research. *Stroke, 35*(10), 2368-2371. doi:10.1161/01.STR.0000140632.83868.a2

Savitz, S. I., Baron, J.-C., Yenari, M. A., Sanossian, N., & Fisher, M. (2017). Reconsidering Neuroprotection in the Reperfusion Era. *Stroke, 48*, 3413-3419.

Smith, W. S., & Furlan, A. J. (2016). Brief History of Endovascular Acute Ischemic Stroke Treatment. *Stroke, 47*(2). doi:10.1161/strokeaha.115.010863

U.S. Census Bureau Population Projections. (2017). Retrieved from https://www.census.gov/programs-surveys/popproj.html